December 2020 Volume 3, Issue 2
www.pmf.ni.ac.rs/chemianaissensis

Chemia Naissensis

ISSN 2620-1895

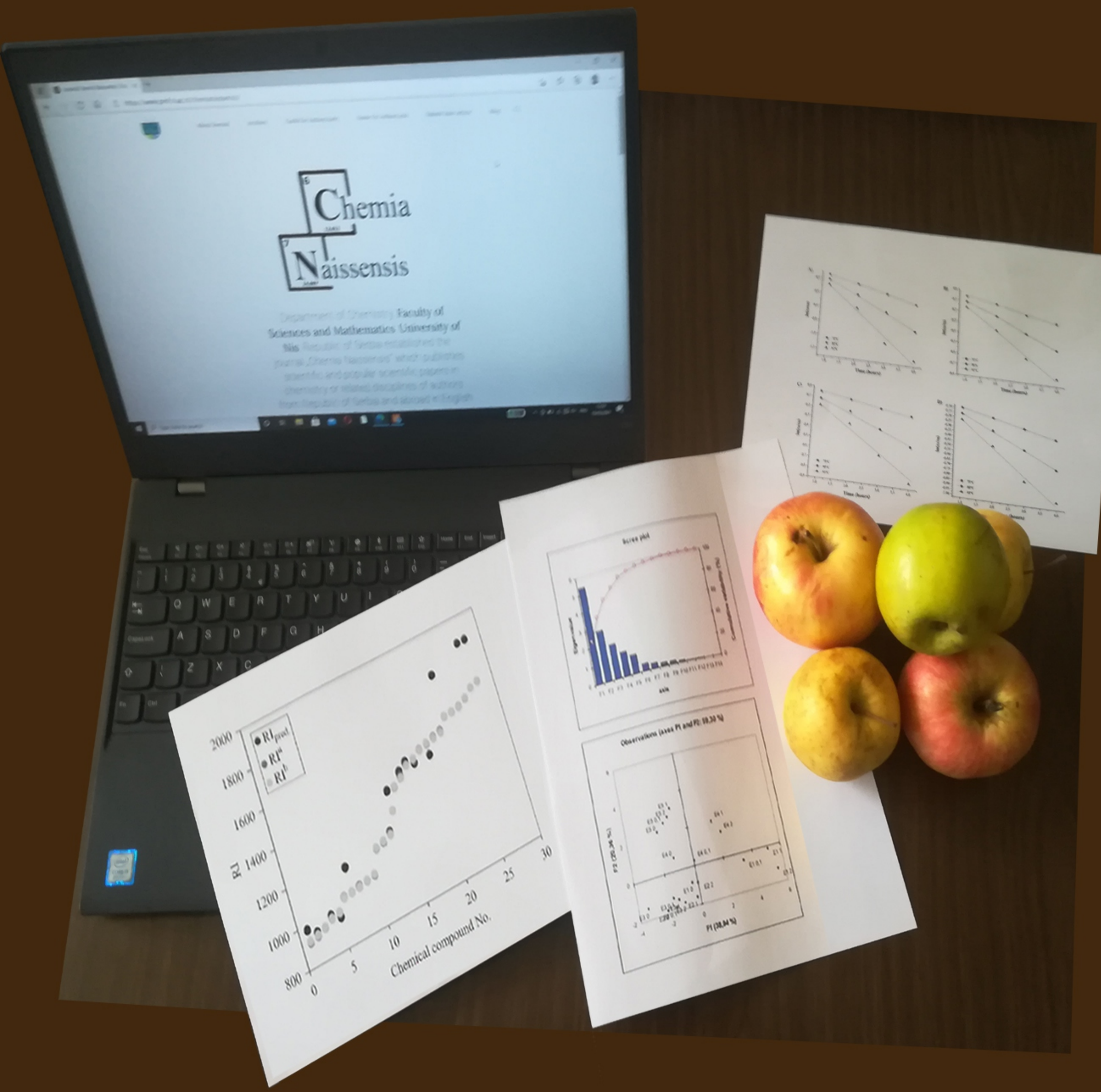

Idea for the cover image by Biljana Arsić

Technical support by Miloš Arsić

Chemia Naissensis

ISSN 2620-1895

Volume 3, Issue 2

December 2020

Category: M54

https://kobson.nb.rs/upload/documents/MNTR/Kategorizacija_casopisa/2019/MNTR2019_hemija.pdf

Publisher:

Faculty of Sciences and Mathematics, University of Niš

Chemical Education
Dr Vesna Stankov Jovanović, Department of Chemistry, Faculty of Sciences and Mathematics, University of Niš, Republic of Serbia

Language Editors:

1. **Dr Selena Stanković**, Department of French Language and Literature, Faculty of Philosophy, University of Niš, Republic of Serbia (French)
2. **Jovana Golubović** (French)
3. **Dr Velimir Ilić**, Department for Russian, Faculty of Philosophy, University of Niš, Republic of Serbia (Russian)
4. **Dr Nenad Blagojević,** Department for Russian, Faculty of Philosophy, University of Niš, Republic of Serbia (Russian)
5. **Dr Nikoleta Momčilović**, Department of German, Faculty of Philosophy, University of Niš, Republic of Serbia (German)
6. **Katarina Stamenković**, Department of German, Faculty of Philosophy, University of Niš, Republic of Serbia (German)
7. **Dr Nadežda Jović**, Department of Serbian language and literature, Faculty of Philosophy, University of Niš, Republic of Serbia (Serbian)
8. **Jelena Stošić**, Department of Serbian language and literature, Faculty of Philosophy, University of Niš, Republic of Serbia (Serbian)

PR Manager:

Dr Radomir Ljupković, Department of Chemistry, Faculty of Sciences and Mathematics, University of Niš, Republic of Serbia

Technical Secretary:

1. **Dr Jelena Nikolić**, Department of Chemistry, Faculty of Sciences and Mathematics, University of Niš, Republic of Serbia
2. **Milica Nikolić**, Department of Chemistry, Faculty of Sciences and Mathematics, University of Niš, Republic of Serbia

IT Support:

Predrag Nikolić, Haed of the Informational&Computional Center of Faculty of Science and Mathematics, University of Niš, Republic of Serbia

CONTENT

Research articles

Milan N. Mitić

Snežana S. Mitić, Branka T. Stojanović, Milan N. Mitić, Aleksandra N. Pavlović, Biljana Arsić, Vesna Stankov-Jovanović

Popular Scientific Article

Danijela Kostić, Nenad Krstić, Marina Blagojević

Chemia Naissensis, Vol 3, Issue 2, RESEARCH ARTICLE, 1-23

Elemental and morphological features of thermally modified clinoptilolite as an efficient sorbent for benzo(a)pyrene extraction from water preceding GC - MS analysis

Marija V. Dimitrijević[1], Dragoljub L. Miladinović[1], Slobodan A. Ćirić[2], Nenad S. Krstić[2], Jelena S. Nikolić[2], Violeta D. Mitić[2], Vesna P. Stankov Jovanović[2]

1- University of Niš, Faculty of Medicine, Boulevard of Dr Zorana Đinđića 81, 18000 Niš, Serbia

2- University of Niš, Faculty of Science and Mathematics, Department of Chemistry, Višegradska 33, 18000 Niš, Serbia

Marija V. Dimitrijević: marija.dimitrijevic@pmf.edu.rs
Dragoljub L. Miladinović: dragoljubm@gmail.com
Slobodan A. Ćirić: slobodan.ciric@pmf.edu.rs
Nenad S. Krstić: nenad.krstic@pmf.edu.rs
Jelena S. Nikolić: jelena.cvetkovic7@gmail.com
Violeta D. Mitić: violeta.mitic@pmf.edu.rs
Vesna P. Stankov Jovanović: vesna.stankov-jovanovic@pmf.edu.rs

ABSTRACT

Monitoring of benzo(a)pyrene (BaP) levels in water is of great importance because BaP is used as a marker for pollution by other polycyclic aromatic hydrocarbons (PAHs). The elemental and morphological features of clinoptilolite used as a sorbent in dispersive micro-solid phase extraction (D-μ-SPE) of BaP from water samples, before Gas Chromatography - Mass Spectrometry determination (GC - MS) is described.

SEM micrographs demonstrated agglomerated particles of Clinoptilolite with no changes in particles, but with increased porosity for Clinoptilolite modified at 300 and 400 ^{o}C. The content of elements is lower in thermally modified Clinoptilolite at higher temperatures (300 and 400 ^{o}C) than for clinoptilolite treated at 120 ^{o}C. After the extraction, EDX analysis of clinoptilolite adsorbed BaP, showed the increased percentage of carbon in the modification prepared at 300 ^{o}C, indicating the structure of the applied sorbent is more suitable compared to one treated at 400 ^{o}C. Recovery values of surrogate standards demonstrate good extraction efficiency for modification at 300 ^{o}C and 400 ^{o}C, but cheaper modification (prepared at 300 ^{o}C) was selected for BaP analysis.

Keywords: *SEM, EDX, GC – MS, PAH, Benzo(a)pyrene, Clinoptilolite*

Introduction

Biogenic and anthropogenic polycyclic aromatic hydrocarbons (PAHs), mainly derived from fossil fuel combustion, incineration, production of coke and asphalt, oil refining, aluminium manufacture, and burning of agricultural and forest biomass fuels, can reach water bodies and contaminate rivers due to storm water runoff and discharges of domestic sewage and industrial effluents (Lima et al., 2015).

Initially, concern about PAHs was only focused on their carcinogenic property (Rubin, 2001). Recently, however, searchlight has been beamed on their antagonism of hormonal functions and their potential effect on reproduction in humans, as well as their ability to depress immune function (Uppstad et al., 2011). These concerns have prompted both the World Health Organization (WHO) and the United States Environmental Protection Agency (USEPA). BaP is the only PAHs with enough toxicological evidence to allow the setting of a guideline (Muyela et al., 2012); according to that, BaP is often use as a marker for PAH pollution. At recent times, sorbent-based sample pretreatment techniques are techniques of choice for PAH analysis in water (Ćirić et al., 2018).

In general, usage of natural zeolites has increased for sorbent-based sample pretreatments (Faghihian et al., 2011; Ghazaghi et al., 2015). Most natural zeolites are formed as a result of volcanic activity.

Zeolites are aluminosilicate minerals with rigid anionic frameworks containing well-defined channels and cavities. These cavities contain metal cations, which are exchangeable, or they may also host neutral guest molecules that can also be removed and replaced. Cavities are

usually occupied by H_2O molecules. In the hydrated phases, dehydration occurs at temperatures mostly below about 400 °C and is largely reversible. The framework may be interrupted by (OH, F) groups; these occupy a tetrahedron apex that is not shared with adjacent tetrahedra (Coombs et al., 1997).

The majority of natural zeolites have a general formula, $M2/n:Al_2O_3: \times SiO_2:yH_2O$, where M stands for the extra-framework cation (Bogdanov et al., 2009). The mineral structure is based on AlO_4 and SiO_4 tetrahedra, which can share 1, 2, or 3 oxygen atoms, so there is a wide variety of possible structures as the network is extended in three dimensions. This structural feature determinates their microporous structure.

Based on the pore size and absorption properties, zeolites are among the most important inorganic cation exchangers and they are used in industrial applications for water and waste water treatments, catalysis, nuclear waste, agriculture, animal feed additives, and in biochemical applications (Bogdanov et al., 2009).

The mineral assemblies of the most common zeolite occurrences in nature are clinoptilolite and mordenite-containing tuffs, in which the zeolite clinoptilolite and mordenite content is high (80% and over). It may appear with the aluminium phyllosilicate clay smectite (bentonite) and accompanying phases present in lower percentages cristoballite, calcite, feldspar, and quartz. However, other types of zeolites (*e.g.*, phillipsite, chabazite) and clay minerals may dominate the mineral tuff assemblage, and properties of such materials may vary in the widest sense with respect to the final mineral content (Cejka et al., 2005).

Clinoptilolite belongs to the group heulandite (HEU), which possesses a two - dimensional structure (Roth et al., 2014). HEU tetrahedral framework is formed from tetrahedral

SiO_4 and AlO_4 units and contains three sets of intersecting channels. Two of the channels are parallel to the c-axis: A channels are formed by strongly compressed ten - membered rings (aperture 3.1 × 7.6 Å) and B channels are confined by eight-membered rings (aperture 3.6 × 4.6 Å). C channels are parallel to the a-axis and they are also formed by eight-membered rings (aperture 2.6 × 4.7 Å). Clinoptilolite unit cells are monoclinic with space group C2/m (Alberti, 1975; Armbrusteret al., 2001; Baerlocher et al., 2007). The general chemical formula is $(Na,K)_6Al_6Si_{30}O_{72}{\cdot}20H_2O$) (Armbrusteret al., 2001; Tsitsishvili et al., 1992) and the Si/Al ratio of clinoptilolite may vary from 4.0 to 5.3 (Kowalczyk et al., 2006).

Clinoptilolite shares a high structural similarity with the zeolite heulandite (they are 97% isostructural) and it is distinguished from helaundite by a higher silicon to aluminium ratio in favour to silicon, where Si / Al > 4.0 and (Na + K) > (Ca + Sr + Ba) (Boles, 1972). The thermal behaviour of clinoptilolite and heulandite is also different. The clinoptilolite structure is still not destroyed after 12 h of heating at 750°C, whereas the heulandite structure is destroyed after 12 h at 450°C (Ghiara et al., 2001).

Zeolites are of high interest to researchers working in the various fields such as energy recovery technology (Xu et al., 2019), water adsorption (Melkon et al., 2018), ion exchangers, adsorbents, catalysts (Auerbach, 2003; Gorshunova et al., 2016), acid-catalyzed dehydration of alcohols (Aleksei et al., 2015; Junko et al., 2005; Seonah et al., 2015) or dry reforming of methane (Alotaibi et al., 2015) and synthesis of zeolites with nonporous titania for corrosion resistance applications (Toshiyuki et al., 2015) as well for agriculture and food production (Nazife et al., 2017), where natural zeolites are used mainly as ion exchangers and in environment remediation (Marantos et al., 2011; Stocker et al., 2017). The majority of studies on clinoptilolite were done by using different, so-called activated materials to increase either the

surface area or to improve the clinoptilolite general adsorption or the ion - exchange capacity. Activation may be performed either through chemical treatment, *e.g.*, with an acid, by replacing stabilizing cations, or through mechanical modifications by means of different micronization methods, which may all increase the surface area and change the ion - exchange properties and adsorption capacity (Abdulkerim, 2012; Akimkhan, 2012; Canli et al., 2013b).

Table 1. Mineral Composition of Clinoptilolites from several countries

Composition	Serbia (Milovanović et al., 2015)	Japan (Kumar and Shigeo, 2009)	China (QiuJue et al., 2015)	Greece (Evangelos et al., 2016)	This study (Sekulic et al., 2013)
SiO_2	72.20	77.96	66.45	68.25	62.28
Al_2O_3	12.20	14.02	13.30	13.19	12.33
Fe_2O_3	5.70	1.30	1.49	1.41	3.20
TiO_2	0.90	-	0.19	0.17	/
MgO	1.0	0.46	0.92	1.14	1.18
CaO	5.0	1.23	3.97	0.75	6.65
Na_2O	0.50	1.15	1.02	4.12	1.46
K_2O	2.50	3.88	1.54	1.66	0.85

The chemical and thermal treatments are the most used techniques to modify the zeolite's characteristics. These treatments allow 1) the removal of impurities; 2) the enhancement of sorption properties, surface area, and porosity; and also 3) the determination of important crystallinity loss (Akkoca et al., 2013).

The aim of this work is the characterization of thermally modified clinoptilolite as an efficient sorbent in sample pretreatment preceding Gas Chromatography – Mass Spectrometry (GC – MS) determination of BaP. Prepared clinoptilolite modifications were applied in Dispersive micro-solid phase extraction (D-μ-SPE) to extract BaP from spiked water samples

and analyse its content. The elemental and morphological features of used sorbents before and after sample pretreatment are performed using SEM and SEM – EDX techniques.

Methods and materials

Chemicals and reagents

Hexane (HPLC grade), Acetonitrile (HPLC grade) - Sigma Aldrich; Surrogate standard mix: 2- chlorphenol-3,4,5,6-d_4, 2,4,6-tribromophenol, 2- fluorobiphenol - Supelco, Bellefonte, Pennsylvania; benzo(a)pyrene – Supelco; perylene d_{12} - Bellefonte, Pennsylvania; Deionized water specific conductivity - 0.05 μS cm^{-1}.

Standard solution preparation

As internal standard solution (ISs), was used perylene d_{12} prepared in dichloromethane (10 ppm). Surrogate standard mix solution in concentration of 0.75 ppm was added to every tested model sample in order to monitor extraction efficiency.

A series of standard solutions was prepared by diluting 0 - 200 μl of the standard solution containing BaP in hexane. Each standard solution contained 100 μl of internal standard solution and 100 μl of surrogate standard solution and was prepared in triplicate.

Preparation of model water samples

Deionized water, with verified absence of BaP, was used to prepare the model water samples which were spiked with BaP at two concentration levels 0.5 and 1.5 ppm. Surrogate standards mix was added in every model water samples in total concentration of 0.75 ppm. Blanks were prepared following the same procedure without adding BaP solution.

Sorbent preparation

Clinoptilolite (grain size 0.063 - 0.1 mm) containing over 90% clinoptilolite, obtained from the mine Zlatokop (South Serbia), was washed with deionized water to remove impurities,

dried and thermally modified in Annealing furnace for 3 h at temperatures of 120 °C , 300 °C, 400 °C (Ćirić et al., 2018). Elemental and morphological features were determined before and after the extraction procedure.

Dispersive micro-solid phase extraction (D-µ-SPE)

Dispersive micro - solid phase extraction (D-µ-SPE) was used to extract benzo(a)pyrene from model water samples. Hexane was used as the extractant and solvent mixture acetonitrile-water (1:4 v/v) a as disperser -. Model samples (400 µL) containing two levels of BaP concentration 0.5 and 1.5 and surrogate standard mix with total concentration of 0.75 were transferred into microextraction tubes, which contained 460 mg of the tested sorbent. After shaking (1 min) and centrifugation (5 min) water was removed *via* micropipette and 500 µL of extractant and 100 µL of disperser was added to the solid residue. After shaking for 5 min and centrifugation (15 min), 400 µL of extract was transferred to GC vial (Ćirić et al., 2018). Then, 200 µL of internal standard mix was added and extracts were analyzed by gas chromatography - mass spectrometry. All experiments were done in triplicate.

Gas Chromatography – mass spectrometry

All extracts were analyzed on a 7890/7000B GC-QQQ-MS system (Agilent Technologies, USA) in the selected ion monitoring (SIM) mode.

Chromatographic separations conditions: Column (HP-5 MS) - 5% Phenyl Methyl Siloxane column (30 m x 250 µm x 0.25 µm); Temperature program: 75 °C for 3 min, then 6 °C/min to 300 °C, keeping the final temperature for 10 min; Total run time*:* 50.5 min; Injection Volume/mode 2.5 µL of extracts was injected in splitless mode; Carrier gas; Helium with a flow of 1.0 mL/min.

Mass Spectrometry conditions: Ionization voltage: 70 eV**;** Acquisition mass range: 40-560**;** Scan time: 0.32 s.

Scanning Electronic Microscopy (SEM)

Morphological features thermally modified clinoptilolite were examined by scanning electronic microscopy (SEM), model: SEM - JSM 5300 JEOL instrument; Accelerating voltage was 0.5–30 kV, resolution 4.5 nm, magnification × 15–20.000.

Scanning Electron Microscopy with Energy Dispersive X-Ray Analysis (SEM-EDX)

Elemental compostition was performed using Scanning Electron Microscopy (SEM) with Energy Dispersive X-Ray Analysis (EDX) (Phenom-World, The Netherlands), and it was performed before and after extraction of PAHs from water.

Results and discussion

Characterization of clinoptilolite after heat treatment to 120 ^{o}C, 300 ^{o}C and 400 ^{o}C was done by SEM - EDX methods. The morphological structures of the clinoptilolite were determined by SEM (Figure 1).

From the micrographs, we can observe that the clinoptilolite particles are agglomerated, and there is no drastic changes in the particles shape where lamellar structure and heterogenicity were preserved after thermal modification. The lamellar and heterogenic structure of the modified clinoptilolite is noticed. If we narrow our focus to the samples thermally modified at different temperatures, we can see that clinoptilolite treated at 300 ^{o}C and 400 ^{o}C have the higher porosity and cavities than clinoptilolite treated at 120 ^{o}C. Increased porosity is a result of water loss due the heating.

Most zeolites can be dehydrated without a major change in the crystal structure, followed by their rehydration through water adsorption from the atmosphere or proximate liquid phase

(Cadar et al., 2020). Dehydration reaction affect the thermal expansion or contraction of samples. The high-temperature exposure does not always produce improvement in the surface area and porosity. Recent work (Wahono et al., 2019) has shown that high temperature, above 800 ^{o}C, leads to the loss of a porosity. It indicates that the material is converted from porous material into a solid or compact material which destructs the pore (Cobzaru, 2012; Wang and Zhu, 2006). For this reason, modifications were made in areas of lower temperatures.

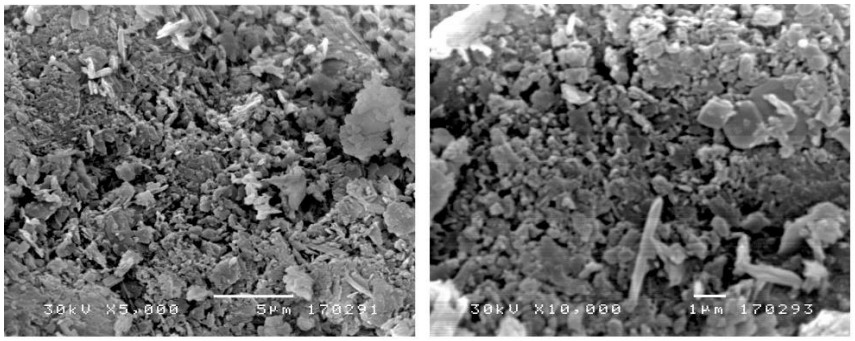

a)

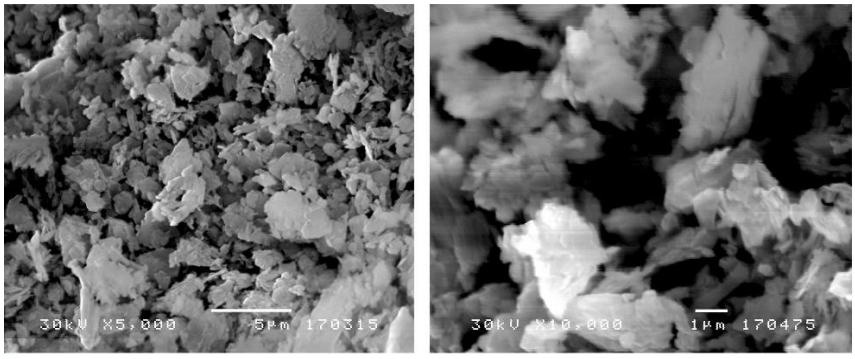

b)

c)

Figure 1. SEM morphology of clinoptilolite in various temperature treatments: (a) 120 ^{o}C; (b) 300 ^{o}C; (c) 400 ^{o}C

EDX analysis

EDX spectra specified the element composition of analyzed samples of clinoptilolite before the extraction procedure and results are presented in Figure 2. Weight (wt %) and atomic percentage (at %) of elements are included within the Figure 2.

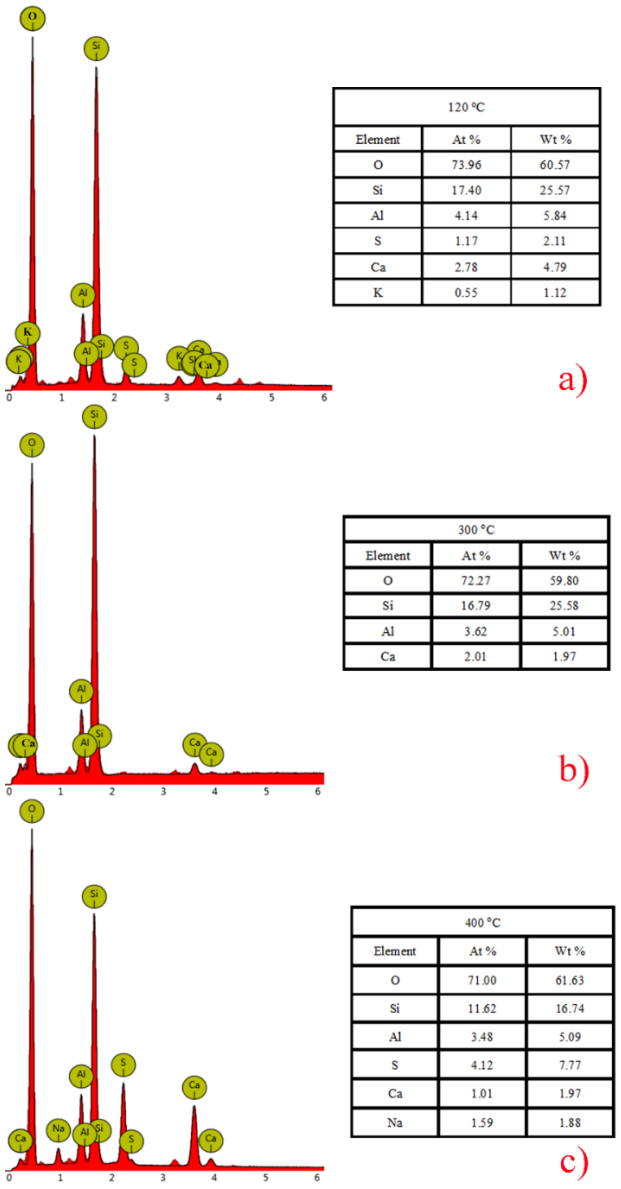

Figure 2. EDX spectra of clinoptilolite in various temperature treatments: (a) 120 ^{o}C; (b) 300 ^{o}C; (c) 400 ^{o}C

For all selected temperatures, the content of elements in clinoptilolite treated at lower temperatures is higher than for clinoptilolite treated at higher temperatures. This difference in the metal release could be attributed to the partial breakdown of the clinoptilolite structure at high temperatures, together with the intense dehydration, which can lead to cell volume reduction and to exchangeable cations trapping in the zeolite channels (Bish et al., 2001).

The dominant elements were oxygen, silicon, and aluminum. The percentage of these elements are not constant and changes depend on the thermal modification. There are no significant differences in the percentage of oxygen, which varies from 73.96 to 71%. The slight decrease of aluminum and silicon in thermally modified samples of clinoptilolite at higher temperatures (300 and 400 ^{o}C) is attributed to the removal of water molecules from the natural structure of clinoptilolite.

In addition to the mentioned elements, clinoptilolite also contains sodium, calcium, potassium, and sulfur, in smaller content which varies depending on the temperature.

The modification of clinoptilolite in various temperatures provides the similar Si/Al ratio. Si/Al ratio of clinoptilolite heated on 120 ^{o}C is 4.2. After the increase of the temperature on 300 ^{o}C, Si/Al ratio increases up to 4.64.

EDX analysis was carried out to examine the elemental distribution in the clinoptilolite framework after extraction procedure, and weight and atomic percentage of elements are presented in Table 2.

Table 2. Element compositions (at % and wt %) of the clinoptilolite thermally modified at 120 ^{o}C, 300 ^{o}C, and 400 ^{o}C after spike with surrogates' standards and benzo[*a*]pyrene

Element	120 °C		300 °C		400 °C	
	(at %)	(wt %)	(at %)	(wt %)	(at %)	(wt %)
C	/	/	47.82	19.49	43.87	21.26
O	65.99	48.49	12.10	6.57	33.44	21.59
Si	18.99	24.50	1.48	1.41	10.01	11.34
Ba					6.06	33.57
Fe	4.53	11.61	36.44	69.04	1.88	4.24
Al	4.40	5.45	/	/	1.73	1.89
Co	/	/	1.04	2.07	/	/
S	3.49	5.14	0.43	0.47	/	/
K	1.52	2.72	0.57	0.75	0.54	0.85
Ca	0.8	1.54	/	/	1.84	2.97
Ti	0.25	0.5	0.13	0.20	/	/

It can be seen that the ratio of elements has been changed. Major changes have occurred in the modification at 300 °C. The percentage of dominant elements has been changed drastically. The atomic percentage of oxygen, silicon and aluminum decreased from 72.27% to 12.10%, 16.74% to 1.48% and 3.62% to 0%, respectively. The EDX analysis revealed the highest percentage of carbon in the modification prepared at 300 °C. Carbon in this case originated from molecules of BaP. This fact indicates the suitability of this sorbent for bonding BaP. Also, a high atomic percentage of carbon can be observed in the modification achieved by preparing clinoptilolite modification at 400 °C, but the decrease in the percentage of dominant elements (oxygen, silicon and aluminum) is lower. Also, it could be expected that this modification will show great ability for sorption of BaP. Clinoptilolite prepared to 120 °C did not show significant changes in its composition after the treatment with the PAH surrogate standard.

Extraction efficiency

The characterized clinoptilolite modifications (at 300 and 400 °C) were used to evaluate the extraction efficiency of BaP from spiked water samples.

PAH surrogate standards are chemically similar to target BaP and they behave in similar manner throughout the sample preparation and analysis procedures. 2,4,6-tribromophenol, 2-fluorobiphenyl and 2-chlorphenol-3,4,5,6-d_4 was used as a surrogate standard in order to monitor extraction efficiency (Ćirić et al., 2018). The acceptable range of surrogate recoveries was set to contain within 50 and 120% (Wnorowski et al., 2006). Results of recoveries are presented in Table 3.

Table 3. Recovery values of surrogate standards and benzo[*a*]pyrene for sorbent modifications - clinoptilolite thermally treated at 120 °C, 300 °C and 400 °C

Modification	Spiking level (ppm)	2, 4, 6-Tribromophenol	2-Fluorobiphenyl	2-Chlorphenol-3, 4, 5, 6-d_4	Benzo[*a*]pyrene
Clinoptilolite modified at 120 °C	0.5	78.04±0.59	72.75±0.26	57.07±0.46	85.5±0.72
	1.5	135.93±3.35	81.40±0.95	76.05±2.28	104.91±0.84
Clinoptilolite modified at 300 °C	0.5	98.60±3.19	90.68±0.76	82.44±3.25	117.75±1.16
	1.5	80.84±5.94	78.44±1.15	76.05±1.67	93.05±2.01
Clinoptilolite modified at 400 °C	0.5	86.03±0.15	87.88±0.25	81.84±0.82	117.26±3.24
	1.5	82.63±1.75	61.68±0.46	78.64±4.76	105.03±1.8

Obtained values for three mentioned standards were in recommended range. The best values were for clinoptilolite modified at 300 °C, for all three surrogate standards, 80.84–98.60% for 2, 4, 6- Tribromophenol; 78.44–90.68% for 2-Fluorobiphenyl and 76.05–82.44% for 2-Chlorphenol-3, 4, 5, 6d_4. Also, the modification at 400 °C showed similar results. It can be noticed that modifications at 300 °C and 400 °C show a higher value of recovery for model water samples with lower concentrations of BaP. BaP is the only polycyclic aromatic hydrocarbon with enough toxicological evidence (Moret et al., 2005) and that can be used when designing experiments for PAHs analysis. Recovery values of BaP using clinoptilolite termally modified at

300 ^{o}C and 400 ^{o}C are higher for 0.5 ppm spiking level than for 1.5 ppm. In contrast, modification at 120 ^{o}C showed better recovery values for higher spiking level.

Conclusion

The use and application of mesoporous materials to encapsulate pollutant particles has attracted a particular interest. For this reason, clinoptilolite was the subject of this study. Elemental and morphological features of thermally modified clinoptilolite at 120 ^{o}C, 300 ^{o}C and 400 ^{o}C were performed using SEM-EDX. Mentioned sorbents were tested in a dispersive micro - solid phase extraction of BaP from water, using GC-MS.

SEM images indicate that there are no essential changes in the particles after thermal modification. EDX spectra show that the elemental composition of analyzed samples of clinoptilolite before and after extraction procedure is different. Before the extraction procedure, the content of elements is lower in thermally modified samples of clinoptilolite at higher temperatures (300 ^{o}C and 400 ^{o}C) than for clinoptilolite treated at 120 ^{o}C. After the extraction procedure EDX analysis showed the highest percentage of carbon in the modification prepared at 300 ^{o}C which indicates that the structure of the sorbent thus obtained is the most suitable for use in BaP studies. Based on recovery values for extraction efficiency, it can be concluded that modifications at 300 ^{o}C and 400 ^{o}C are more favorable for the analysis of BaP present in a lower concentration in the analyzed sample. However, the clinoptilolite sample that was thermally modified at 120 ^{o}C showed better recovery values for a higher spiking concentration of BaP, so it can be concluded that its usage would be favorable for samples with higher BaP concentrations.

Acknowledgment

The research was supported by the Ministry of Education, Science and Technological Development of the Republic of Serbia, Contract number 451-03-9/2021-14/200124.

Conflict-of-Interest Statement

No potential conflict of interest was reported by the authors.

References:

Abatal, M., Córdova Quiroz, A. V., Olguín, M. T., Vázquez-Olmos, A. R., Vargas, J., Anguebes-Franseschi, F., & Giácoman-Vallejos, G. (2019). Sorption of Pb(II) from Aqueous Solutions by Acid-Modified Clinoptilolite-Rich Tuffs with Different Si/Al Ratios. Applied Sciences, 9, 2415.

Abdulkerim Y. (2012). Influence of acid activation on the ion-exchange properties of manisa-gordes clinoptilolite. Physicochemical Problems of Mineral Processing, 48, 591–598.

Akimkhan, A. M. (2012). Ion Exchange Technologies. IntechOpen.

Akkoca, D. B., Yılgın, M., Ural, M., Akçin, H., & Mergen, A. (2013). Hydrothermal and thermal treatment of natural clinoptilolite zeolite from Bigadiç, Turkey: An experimental study. Geochemistry International, 51, 495–504.

Alberti, A. (1975). The crystal structure of two clinoptilolites. TMPM Tschermaks Mineralogische Und Petrographische Mitteilungen, 22, 25–37.

Alotaibi, R., Alenazey, F., Alotaibi, F., Wei, N., Al-Fatesh, A., & Fakeeha, A. (2015). Ni catalysts with different promoters supported on zeolite for dry reforming of methane. Applied Petrochemical Research, 5, 329–337.

Armbruster, T., & Gunter, M. E. (2001). Crystal Structures of Natural Zeolites. Reviews in Mineralogy and Geochemistry, 45, 1–67.

Auerbach, S. M., Carrado, K. A., & Dutta, P. K. (2003). Handbook of Zeolite Science and Technology. (1st ed.). CRC Press.

Baerlocher, C., McCusker, L. B., & Olson, D. H. (2007). C2/m. Atlas of Zeolite Framework Types, Amsterdam: Elsevier.

Bish, D.L., & Carey, J.W. (2001). Thermal behavior of natural zeolites. In Bish, D.L., Ming, D.W., (Ed.). Natural Zeolites: Occurrence, Properties, Applications (Reviews in Mineralogy and Geochemistry) (pp. 403–452). Washington: Mineralogical Society of America.

Bogdanov, B., Georgiev, D., Angelova, K., & Yaneva, K. Natural zeolites: Clinoptilolite Review, 730 International Science conference "Economics and Society Development on the Base of 731 Knowledge", Stara Zagora, Bulgaria, 2009.

Boles, J.R. (1972). Composition, optical properties, cell dimensions and thermal stability of some heulandite group zeolites. American Mineralogist, 57, 1463-1493.

Cadar, O., Senila, M., Hoaghia, M. A., Scurtu, D., Miu, I., & Levei, E. A. (2020). Effects of Thermal Treatment on Natural Clinoptilolite-Rich Zeolite Behavior in Simulated Biological Fluids. Molecules, 25, 2570.

Canli, M., Yuksel, A., & Ugur, S. B. (2013). Removal of methylene blue by natural and Ca and K-exchanged zeolite treated with hydrogen peroxide. Physicochemical Problems of Mineral Processing, 49, 481–496.

Cejka, J. (2005). Zeolites and Ordered Mesoporous Materials: Progress and Prospects. The 1st 746 FEZA School on Zeolites, Prague, Czech Republic, Gulf Professional Publishing.

Ćirić, S., Mitić, V., Jovanović, S., Ilić, M., Nikolić, J., Stojanović, G., & Stankov Jovanović, V. (2018). Dispersive micro-solid phase extraction of 16 priority polycyclic aromatic hydrocarbons

from water by using thermally treated clinoptilolite, and their quantification by GC-MS. Microchimica Acta, 185, 556.

Cobzaru, C. (2012). Handbook of Natural Zeolites.

Coombs, D.S., Alberti, A., Armbruster, T., Artioli, G., Colella, C., Galli, E., Grice, J. D., Liebau, F., Mandarino, J.A., Minato, H., Nickel, E.H., Passaglia, E., Peacor, D.R., Quartieri, S., Rinaldi, R., Ross, M., Sheppard, R.A., Tillmanns, E., & Vezzalini, G. (1997). Recommended Nomenclature for Zeolite Minerals: Report of The Subcommittee on Zeolites of the International Mineralogical Association, Commission on New Minerals and Mineral Names. The Canadian Mineralogist, 35, 1571–1606.

Ćirić, S., Mitić, V., Nikolić, J., Dimitrijević, M., Ilić, M., Dimitrijević M., Simonović, S., & Stankov Jovanović, V. (2018). Recent developments in sorbent-based water samples treatments prior GC-MS analysis of polycyclic aromatic hydrocarbons. Chemia Naissensis, 1, 93-123.

Eroglu, N., Emekci, M., & Athanassiou, C. G. (2017). Applications of natural zeolites on agriculture and food production. Journal of the Science of Food and Agriculture, 97, 3487–3499.

Faghihian, H., & Kabiri-Tadi, M. (2010). A novel solid-phase extraction method for separation and preconcentration of zirconium. Microchimica Acta, 168, 147–152.

Favvas, E. P., Tsanaktsidis, C. G., Sapalidis, A. A., Tzilantonis, G. T., Papageorgiou, S. K., & Mitropoulos, A. C. (2016). Clinoptilolite, a natural zeolite material: Structural characterization and performance evaluation on its dehydration properties of hydrocarbon-based fuels. Microporous and Mesoporous Materials, 225, 385–391.

Ghazaghi M., Shirkhanloo H., Mousavi H. Z., & Rashidi A. M. (2015). Ultrasound-assisted dispersive solid phase extraction of cadmium(II) and lead(II) using a hybrid nanoadsorbent composed of graphene and the zeolite clinoptilolite. Microchimica Acta, 1, 1263–1272.

Ghiara M. R., Petti C., Franco E., Lonis R., Luxoro S., & Gnazzo L. (1999). Occurrence of 766 clinoptilolite and modernite in tertiary calc-alkaline pyroclastites from Sardinia (Italy). Clays and Clay Minerals, 47, 319-328.

Gorshunova, K. K., Travkina, O. S., Kustov, L. M., & Kutepov, B. I. (2016). Synthesis and adsorption properties of the cation exchange forms of OFF-type zeolite. Russian Journal of Physical Chemistry A, 90, 652–657.

Jha, V. K., & Hayashi, S. (2009). Modification on natural clinoptilolite zeolite for its NH4+ retention capacity. Journal of Hazardous Materials, 169, 29–35.

Kim, S., Robichaud, D. J., Beckham, G. T., Paton, R. S., & Nimlos, M. R. (2015). Ethanol Dehydration in HZSM-5 Studied by Density Functional Theory: Evidence for a Concerted Process. The Journal of Physical Chemistry A, 119, 3604–3614.

Kondo, J. N., Ito, K., Yoda, E., Wakabayashi, F., & Domen, K. (2005). An Ethoxy Intermediate in Ethanol Dehydration on Brønsted Acid Sites in Zeolite. The Journal of Physical Chemistry B, 109, 10969–10972.

Kowalczyk, P., Sprynskyy, M., Terzyk, A. P., Lebedynets, M., Namieśnik, J., & Buszewski, B. (2006). Porous structure of natural and modified clinoptilolites. Journal of Colloid and Interface Science, 297, 77–85.

Lima, A., Heleno, F., Afonso, R., & Coutrim, M. (2015). Determination of PAHs in Surface Waters from the Doce and Piracicaba Rivers in Brazil. Journal of Water Resource and Protection, 7, 422-429.

Marantos, I., Christidis, G.E., & Ulmanu, M. (2011). Zeolite formation and deposits. In Inglezakis, V.J., Zorpas, A.A. (Ed.) Natural Zeolites Handbook (pp. 19–36). Bentham Science Publishers Ltd.

Milovanovic, J., Stensrød, R., Myhrvold, E., Tschentscher, R., Stöcker, M., Lazarevic, S., & Rajic, N. (2015). Modification of natural clinoptilolite and ZSM-5 with different oxides and studying of the obtained products in lignin pyrolysis. Journal of the Serbian Chemical Society, 80, 717–729.

Moret, S., Purcaro, G., & Conte, L. S. (2005). Polycyclic aromatic hydrocarbons in vegetable oils from canned foods. European Journal of Lipid Science and Technology, 107, 488–496.

Muyela B., Shitandi A., & Ngure, R. (2012). Determination of benzo [*a*] pyrene levels in smoked and oil fried *Lates niloticus*. International Food Research Journal, 19, 1595–1600.

Roth, W. J., Nachtigall, P., Morris, R. E., & Čejka, J. (2014). Two-Dimensional Zeolites: Current Status and Perspectives. Chemical Reviews, 114, 4807–4837.

Rubin, H. (2001). Synergistic mechanisms in carcinogenesis by polycyclic aromatic hydrocarbons and by tobacco smoke: a bio-historical perspective with updates. Carcinogenesis, 22, 1903–1930.

Wahono, S. K., Prasetyo, D. J., Jatmiko, T. H., Suwanto, A., Pratiwi, Hernawan, D., & Vasilev, K. (2019). Transformation of Mordenite-Clinoptilolite Natural Zeolite at Different Calcination

Temperatures, The 2nd International Conference on Natural Products and Bioresource Sciences - IOP Conference Series: Earth and Environmental Science, 251, 120–129.

Sekulic, Z., Dakovic, A., Kragovic, M., Markovic, M., Ivosevic, B., & Kolonja, B. (2013). Quality of zeolit from Vranjska banja deposit according to size classes. Hemijska Industrija, 67, 663–669.

Stocker, K., Ellersdorfer, M., Lehner, M., & Raith, J. G. (2017). Characterization and Utilization of Natural Zeolites in Technical Applications. BHM Berg- Und Hüttenmännische Monatshefte, 162, 142–147.

Tsitsishvili, G.V., Andronikashvli, T.G., Kirov, G.R., & Filizova, L.D. (1992). Natural Zeolites, Ellis Horwood.

U.S. EPA. National Primary Drinking Water Standards, 2003.

Uppstad, H., Osnes, G. H., Cole, K. J., Phillips, D. H., Haugen, A., & Mollerup, S. (2011). Sex differences in susceptibility to PAHs is an intrinsic property of human lung adenocarcinoma cells. Lung Cancer, 71, 264–270.

Vjunov, A., Derewinski, M. A., Fulton, J. L., Camaioni, D. M., & Lercher, J. A. (2015). Impact of Zeolite Aging in Hot Liquid Water on Activity for Acid-Catalyzed Dehydration of Alcohols. Journal of the American Chemical Society, 137, 10374–10382.

Wang, S., & Zhu, Z. (2006). Characterisation and environmental application of an Australian natural zeolite for basic dye removal from aqueous solution. Journal of Hazardous Materials, 136, 946–952.

WHO, Guidelines for Drinking Water Quality, WHO, Geneva, Switzerland, 3rd edition, 2006.

Wnorowski, A., Tardif, M., Harnish, D., Poole, G., & Chiu, C. H. (2006). Correction of analytical results for recovery: determination of PAHs in ambient air, soil, and diesel emission control samples by isotope dilution gas chromatography-mass spectrometry. Polycyclic Aromatic Compounds, 26, 313–329.

Wu, Q. J., Wang, Q. Y., Wang, T., & Zhou, Y. M. (2015). Effects of clinoptilolite (zeolite) on attenuation of lipopolysaccharide-induced stress, growth and immune response in broiler chickens. Annals of Animal Science, 15, 681–697.

Xu, S. Z., Wang, R. Z., Wang, L. W., & Zhu, J. (2019). Performance characterizations and thermodynamic analysis of magnesium sulfate-impregnated zeolite 13X and activated alumina composite sorbents for thermal energy storage. Energy, 167, 889–901.

Yokoi, T., Mochizuki, H., Namba, S., Kondo, J. N., & Tatsumi, T. (2015). Control of the Al Distribution in the Framework of ZSM-5 Zeolite and Its Evaluation by Solid-State NMR Technique and Catalytic Properties. The Journal of Physical Chemistry C, 119, 15303–15315.

Elementne i morfološke osobine termički modifikovanog klinoptilolita kao efikasnog sorbenta za ekstrakciju benzo(a)pirena iz vode pre GC - MS analize

Marija V. Dimitrijević[1], Dragoljub L. Miladinović[1], Slobodan A. Ćirić[2], Nenad S.Krstić[2], Jelena S. Nikolić[2], Violeta D. Mitić[2], Vesna P. Stankov Jovanović[2]

1- Univerzitet u Nišu, Medicinski fakultet, Bulevar dr Zorana Đinđića 81, 18000 Niš, Srbija

2- Univerzitet u Nišu, Prirodno-matematički fakultet, Odeljenje za hemiju, Višegradska 33, 18000 Niš, Srbija

SAŽETAK

Praćenje sadržaja benzo (a) pirena (BaP) u vodi je od velike važnosti, jer se BaP koristi kao pokazatelj zagađenja drugim policikličnim aromatičnim ugljovodonicima (PAH). Opisane su elementne i morfološke osobine klinoptilolita koji se koristi kao sorbent u disperzivnoj ekstrakciji mikro-čvrstom fazom (D-μ-SPE) BaP iz uzoraka vode, pre određivanja gasnom hromatografijom - masenom spektrometrijom (GC - MS).

SEM mikrografije pokazale su aglomerisane čestice klinoptilolita bez promena na česticama, ali sa povećanom poroznošću za klinoptilolit modifikovan na 300 i 400 ^{o}C. Sadržaj elemenata je niži u termički modifikovanom klinoptilolitu na višim temperaturama (300 i 400 ^{o}C) nego u klinoptilolitu tretiranom na 120 ^{o}C. Nakon ekstrakcije, EDX analiza klinoptilolita koji je adsorbovao BaP, pokazala je povećani procenat ugljenika u modifikaciji pripremljenoj na 300 ^{o}C, ukazujući na to da je struktura primenjenog sorbenta pogodnija u poređenju sa onim tretiranim na 400 ^{o}C. Efikasnost ekstrakcije surogat-standarda je dobra za modifikaciju na 300 ^{o}C i 400 ^{o}C, ali je za BaP analizu izabrana jeftinija modifikacija (pripremljena na 300 ^{o}C).

Ključne reči: SEM, EDX, GC - MS, PAH, klinoptilolit

Caractéristiques élémentaires et morphologiques de la clinoptilolite thermiquement modifiée comme sorbant efficace pour l'extraction du benzo(a)pyrène à partir de l'eau avant l'analyse GC-MS

Marija V. Dimitrijević[1], Dragoljub L. Miladinović[1], Slobodan A. Ćirić[2], Nenad S. Krstić[2], Jelena S. Nikolić[2], Violeta D. Mitić[2], Vesna P. Stankov Jovanović[2]

1- Université de Niš, Faculté de médecine, Boulevard du Dr Zorana Đinđića 81, 18000 Niš, Serbie

2- Université de Nis, Faculté des sciences naturelles et des mathématiques, Département de chimie, Višegradska 33, 18000 Niš, Serbie

RÉSUMÉ

La surveillance des niveaux de benzo(a)pyrene (BaP) dans l'eau, a d'une grande importance parce que le BaP est utilisé comme marqueur de pollution par d'autres hydrocarbures aromatiques polycycliques (HAP). Les caractéristiques élémentaires et morphologiques de la clinoptilolite utilisée comme sorbant dans l'extraction en phase micro-solide dispersive (D-µ-SPE) de BaP à partir d'échantillons d'eau, avant l'détermination par chromatographie gazeuse - spectrométrie de masse (GC-MS) sont décrites.

Les micrographies SEM ont montré des particules agglomérées de Clinoptilolite sans changement de particules, mais avec une porosité accrue pour la Clinoptilolite modifiée à 300 et 400 ^{o}C. La teneur en éléments est plus faible dans la clinoptilolite thermiquement modifiée à des températures plus élevées (300 et 400 ^{o}C) que dans la clinoptilolite traitée à 120 ^{o}C. Après l'extraction, l'analyse EDX du BaP adsorbé par clinoptilolite a montré l'augmentation du pourcentage de carbone dans la modification préparée à 300 ^{o}C, indiquant que la structure du sorbant appliqué est plus appropriée que celle traitée à 400 ^{o}C. Les valeurs de récupération des étalons de substitution démontrent une bonne efficacité d'extraction pour la modification à 300 ^{o}C et 400 ^{o}C, mais une modification moins chère (préparée à 300 ^{o}C) a été sélectionnée pour l'analyse BaP.

Mots clés : SEM, EDX, GC - MS, HAP, Benzo(a)pyrène, Clinoptilolite

Элементные и морфологические особенности термомодифицированного клиноптилолита как эффективного сорбента для экстракции бензо(а) пирена из воды перед ГХ-МС-анализом

Мария В. Димитриевич[1], Драголюб Л. Миладинович[1], Слободан А. Чирич[2], Ненад С. Крстич[2], Елена С. Николич[2], Виолета Д. Митич[2], Весна П. Станков Йованович[2]

1- Университет в Нише, Медицинский факультет, Бульвар доктора Зорана Джинджича 81, 18000 Ниш, Сербия

2-Университет в Нише, Естественно-математический факультет, Кафедра химии, Вишеградска 33, 18000 Ниш, Сербия

Аннотация

Мониторинг уровней бензо(а)пирена (БаП) в воде имеет большое значение, поскольку BaP используется в качестве маркера загрязнения другими полициклическими ароматическими углеводородами (ПАУ). Описаны элементные и морфологические особенности клиноптилолита, используемого в качестве сорбента при дисперсионной микро-твердофазной экстракции (D-μ-SPE) BaП из проб воды перед газ-хроматографическим масс-спектрометрическим определением (ГХ-МС).

СЭМ-микрографии продемонстрировали агломерированные частицы клиноптилолита без изменений в составе частиц, но с повышенной пористостью для клиноптилолита, модифицированного при 300 и 400 ºC. Содержание элементов в термически модифицированном клиноптилолите при более высоких температурах (300 и 400 ºC) ниже, чем в клиноптилолите, обработанном при 120 ºC. После экстракции, EDX-анализ клиноптилолита, на котором адсорбирован БаП, показал повышенное процентное содержание углерода в модификации, полученной при 300 ºC, что указывает на то, что структура нанесенного сорбента более подходящая по сравнению с сорбентом, обработанным при 400 ºC. Значения утилизации суррогатных стандартов демонстрируют хорошую эффективность экстракции для модификации при 300 ºC и 400 ºC, но для анализа БаП была выбрана более дешевая модификация (приготовленная при 300 ºC).

Ключевые слова: СЭМ, EDX, ГХ - МС, ПАУ, бензо(а)пирен, клиноптилолит

Elementare und morphologische Merkmale von thermisch modifiziertem Klinoptilolith als wirksames Sorptionsmittel für die Benzo (a) pyren-Extraktion aus Wasser vor der GC-MS-Analyse

Marija V. Dimitrijević[1], Dragoljub L. Miladinović[1], Slobodan A. Ćirić[2], Nenad S.Krstić[2], Jelena S. Nikolić[2], Violeta D. Mitić[2], Vesna P. Stankov Jovanović[2]

1- Universität Niš, Medizinische Fakultät, Boulevard von Dr. Zoran Đinđić 81, 18000 Niš, Serbien

2- Universität Niš, Fakultät für Naturwissenschaften und Mathematik, Fachbereich Chemie, Višegradska 33, 18000 Niš, Serbien

ABSTRAKT

Die Überwachung des Benzo (a) pyren (BaP) -Gehalts in Wasser ist von großer Bedeutung, da BaP als Marker für die Verschmutzung durch andere polycyclische aromatische Kohlenwasserstoffe (PAK) verwendet wird. Die elementaren und morphologischen Merkmale von Klinoptilolith, das als Sorptionsmittel bei der dispersiven Mikro-Festphasenextraktion (D-μ-SPE) von BaP aus Wasserproben vor der Bestimmung der Gaschromatographie - Massenspektrometrie (GC - MS) verwendet wird, werden beschrieben.

REM-Aufnahmen zeigten agglomerierte Partikel von Clinoptilolite ohne Partikelveränderungen, jedoch mit erhöhter Porosität für Clinoptilolite, modifiziert bei 300 ˚C und 400 ˚C. Der Gehalt an Elementen ist in thermisch modifiziertem Clinoptilolith bei höheren Temperaturen (300 ˚C und 400°C) geringer als bei 120 °C behandeltem Clinoptilolith. Nach der Extraktion zeigte die EDX-Analyse von Clinoptilolith-adsorbiertem BaP den erhöhten Prozentsatz an Kohlenstoff in der bei 300 °C hergestellten Modifikation, was darauf hinweist, dass die Struktur des verwendeten Sorbents im Vergleich zu einer bei 400 °C behandelten besser geeignet ist. Die Wiederfindungswerte von Ersatzstandards zeigen eine gute Extraktionseffizienz für die Modifikation bei 300 °C und 400 °C, aber eine billigere Modifikation (hergestellt bei 300 °C) wurde für die BaP-Analyse ausgewählt.

Schlüsselwörter: SEM, EDX, GC-MS, PAH, Benzo(a)pyren, Klinoptilolith

Intra- and intermolecular H-bonding of benzotriazole UV stabilizers evidenced using 1D nuclear Overhauser effect experiments

Jonathan Hobley,[1#*] Vincenzo Malatesta[2]

1- OndaLabs R&D Consultancy, Deca Homes, Clark Free-Port, Mabalacat, Angeles, the Philippines 20102

 # Current address National Cheng Kung University, Department of Bioengineering, University Road, Tainan City, Taiwan, ROC, 70101

2- Universita Degli Studi di Milano-Bicocca, Department of Materials, Milano, Italia.

[*]corresponding author: Jonathan Hobley: jonathan.hobley@gmail.com

ABSTRACT

The UV absorber protection mechanism of 2-hydroxyphenylbenzotriazoles is based upon energy dissipation *via* an excited state proton transfer from the phenolic OH group to the triazole nitrogen(s). Using ^{1}H-NMR NOE experiments we have established that 2-(2'hydroxy-5'-methylphenyl)-benzotriazole (**UVA1**) exists in chloroform as an intramolecularly H-bonded form whereas in DMSO this bond is disrupted by the formation of intermolecular H-bonding to the solvent. Conversely, for compounds 2-(2'-hydroxy-3',5'-di(1,1-dimethyl propane))-benzotriazole (**UVA2**), and 3'-methylene-hydantoin-2-(2'-hydroxy-5'-methylphenyl)-benzotriazole (**UVA3**) having bulky substituents ortho to the phenolic OH group ^{1}H-NMR NOE experiments indicate that upon changing solvent from DMSO to chloroform the strength of the intramolecular H-bond is not appreciably affected. The implication of the H-bond strength upon the UV stabilizing effectiveness is discussed.

Keywords: benzotriazole,UV stabilizer,nuclear Overhauser effect NOE, spin diffusion

Introduction

The plastics industry represents a huge portion of the greater petrochemicals industry, making various products that are often structural, yet exposed to severe elements of nature, such as sunlight and heat. In the field of polymer chemistry photo-oxidation is the degradation of a polymer surface due to the action of light and oxygen (Zweifel, 1996). Photodegradation is the most important process in the weathering of plastics in the field (Feldman, 2002). Photo-oxidation causes polymer chain scission, resulting in the polymer becoming more brittle, and in discoloration and crack formation. This leads to mechanical failure and to the formation of microplastics, which is currently a key global concern. UV stabilizers prevent the degradation that plastics suffer under the effects of sunlight, UV rays, heat and reactions with oxygen. Therefore, UV stabilizers are essential in the prevention of photo-induced decomposition of plastics that are continuously subjected to sunlight or other sources of UV irradiation. One class of compounds that have been shown to be particularly effective light stabilizers are the substituted benzotriazoles (Bocian, 1983; Catalan, 1990, 1992, 1997; Durr, 2006; Flom, 1983; Huston, 1982; McGarry, 1997; Werner, 1979; Woessner, 1984, 1985 ,). These compounds are sold under the generic tradename Tinuvin^{Tm}. Their mechanism of UV protection comes from the fact that when they absorb energetic UV photons which would normally destroy a polymer over a period of prolonged irradiation, they dissipate the excess of energy *via* a mechanism involving excited state intramolecular proton transfer (ESIPT) (Bocian, 1983; Durr, 2006; Flom, 1983; Huston, 1982; 3, McGarry, 1997)

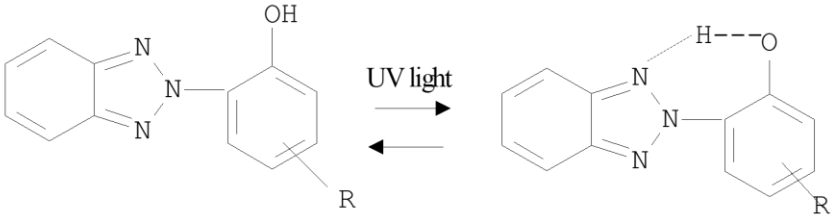

Scheme 1. ESIPT reaction of benzotriazole

In the process of ESIPT photoexcited molecules relax their excess energy through tautomerization by proton transfer. Some molecules have different minimum-energy tautomers in their ground and excited electronic states. This means that in an excited electronic state for molecules like Tinuvin^{Tm} the structure of the minimum-energy tautomer has a proton-transferred geometry between neighboring atoms and proton transfer in the excited state spontaneously occurs rapidly after

photoexcitation. The tautomerization is similar to the well-known keto-enol tautomerism (Benassi, 1996).

ESIPT is often implied to be occurring when anomalous red emission is observed with a very large Stokes shift from the maximum of the absorption spectrum. This is because the lower energy of the proton-transferred tautomer adds to the usual Stokes shift. Based on the characteristic that molecules usually have extraordinarily larger Stokes shift when ESIPT occurs, various applications have been developed using red-shifted fluorescence (Sheng, 2019). However, in the current work the application of interest is UV stabilization of plastics.

The effectiveness of this proton transfer mechanism depends upon the presence of a hydrogen bond between the phenyl hydrogen and the non-bridging nitrogen atoms on the benzotriazole ring (Catalan, 1992;McGarry, 1997). McGarry et al. (1997) have convincingly demonstrated that in DMSO competitive disruption of this bond allows photoinduced proton abstraction by the solvent leading to irreversible photochemistry and a reduction in the working lifetime of the benzotriazole. It has long been proposed that some equilibrium exists between UVA1 in an intermolecular hydrogen bonded form and in an intramolecular hydrogen bonded form (Durr, 2006). Here, we present ^{1}NMR and NOE data which support this hypothesis and further derive estimates of internuclear distance ratios between the phenyl proton and its closest neighbors in DMSO and chloroform. The effect of a bulky group ortho to the phenyl OH-group is also investigated.

Experimental

Materials

2-(2'-hydroxy-5'-methylphenyl)-benzotriazole (UVA1) 2-(2'-hydroxy-3',5'-di(1,1-dimethyl propane))-benzotriazole (UVA2) and 3'-methylene-hydantoin-2-(2'-hydroxy-5'-methylphenyl)-benzotriazole (UVA3) (Scheme 2) were supplied by Great Lakes Chemical Italia and used as received. Approximately 10 mg of each was respectively dissolved in non-polar, poorly H-bonding chloroform-d 99.96% atom % D, stored over silver, Merck,) and polar, H-bonding DMSO-d (99.96% atom % D, Aldrich) using sonication.

UVA1 **UVA2**

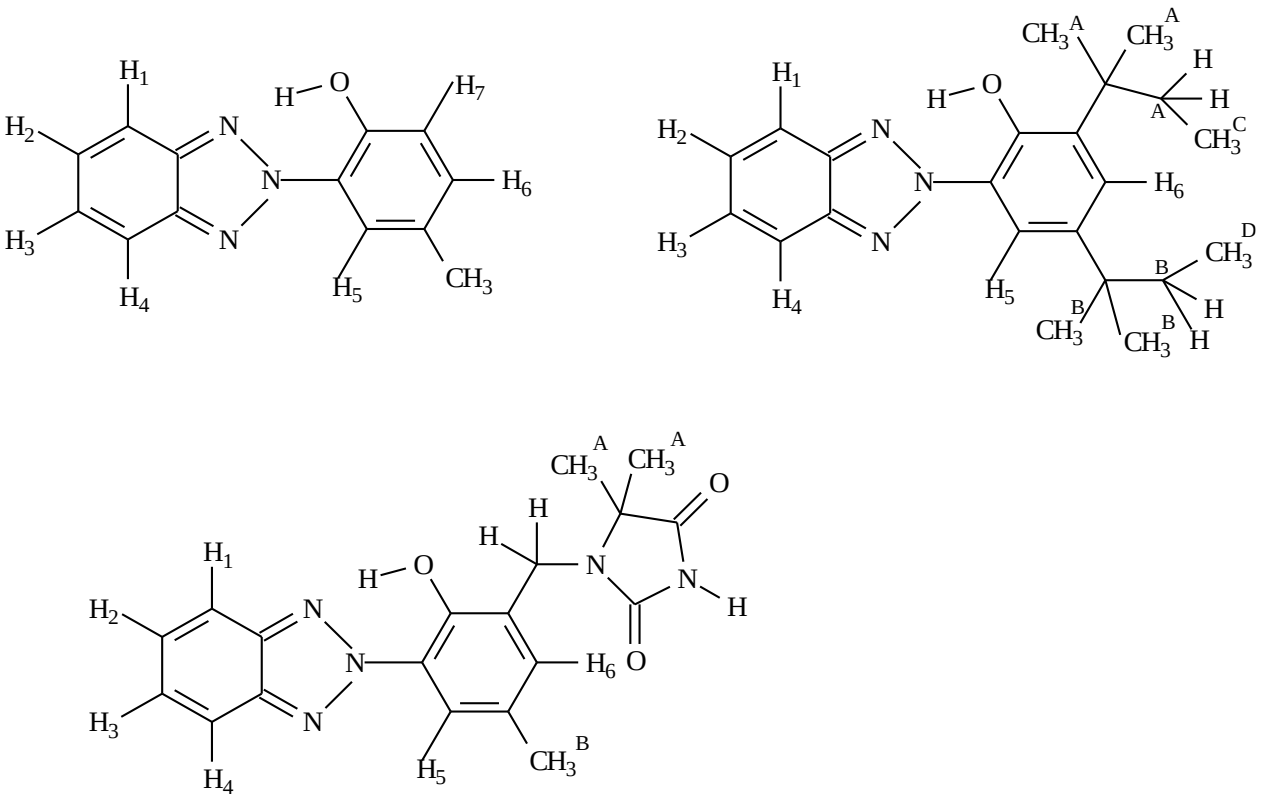

UVA3

Scheme 2. Benzotriazoles used in the investigation.

Instrumentation

^{1}H NMR and two dimensional ^{1}H-^{1}H -NOESY

^{1}H NMR and two dimensional ^{1}H-^{1}H -NOESY spectroscopic studies were done on a Varian VXR 400 spectrometer in phase sensitive mode using the hypercomplex method to achieve quadrature in F1. The data were collected with a slit width of 4081.6 Hz in both dimensions with 2K data points in the F2 domain and 100 increments in the F1 domain. An optimized 2s mixing time was used. ^{1}H-TOE (truncated or driven NOE (Saunders, 1988)), ^{1}H-NOE, ^{1}H-NMR and T1 inversion recovery ^{1}H-NMR experiments were done on a Bruker AF 200NR 200 MHz spectrometer in the deuterated solvents described in the materials section.

Truncated NOE

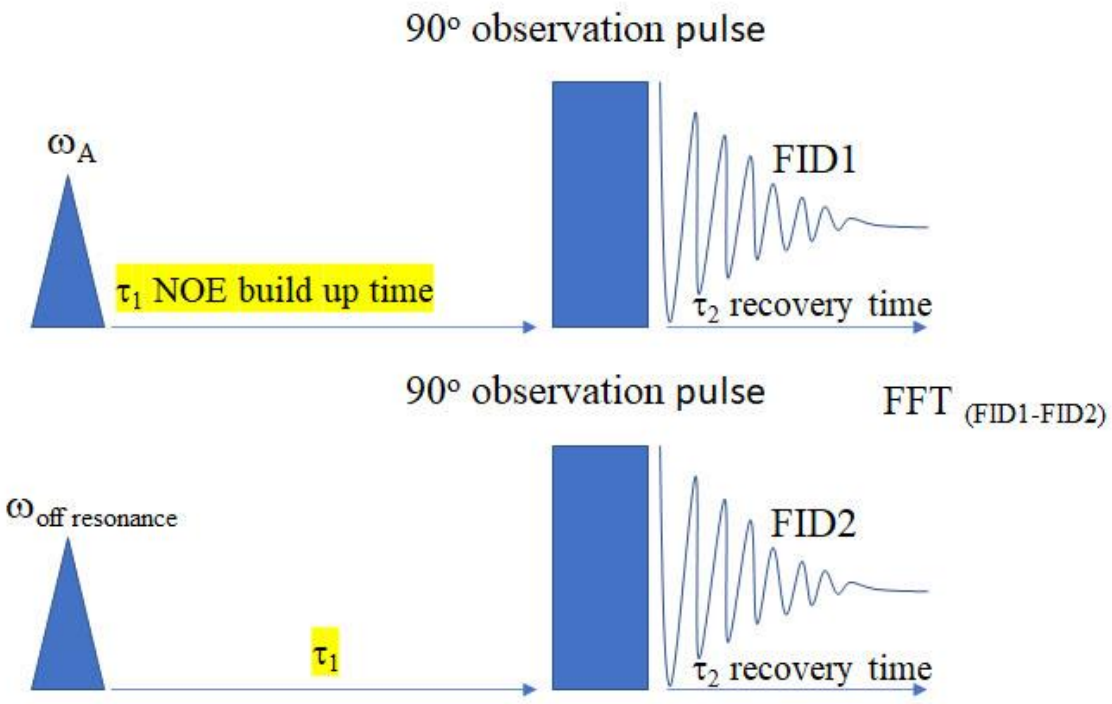

Figure 1 The pulse sequence for the truncated NOE experiment

The pulse sequence for the truncated NOE experiment is shown in Figure 1 and summarized below.

(ω_A)- delay τ_1- 90° observation pulse - recovery time τ_2

τ_I($\omega_{off\text{-}resonance}$) - delay τ_1 -90° observation pulse - recovery time τ_2)$_n$

The experiment starts with a selective low power pulse applied to resonance of interest, Spin A. This low power pulse is set to a power and duration that is insufficient to fully saturate Spin A. An observation pulse then follows, after a waiting time, τ_1 during which the NOEs are built up. A reference spectrum with an off resonance applied frequency without NOE is recorded after a waiting period τ_2 during which the spin system is allowed to recover. This is done to counter any shifts induced by the applied field ω. The on-and off resonance free inductive decays are then subtracted, one from the other to determine the NOE at each of the variable mixing times τ_1. The process is repeated n-times for acquiring sufficient signal to noise ratio, for a range of τ_1 values.

T_1 (spin-lattice) inversion relaxation.

Inversion relaxation or recovery experiments (Figure 2) monitor the longitudinal relaxation (parallel to the external B_0 field) of magnetized nuclei following inversion along the z-axis using a 180° RF pulse. The degree of longitudinal relaxation is monitored as a function of time using a second 90° pulse to rotate any z-axis magnetization into the xy-plane where its intensity can be monitored by the NMRs detector coils. The z-axis magnetization decays from a maximum negative (fully inverted) value through zero (null) magnetization and back to a maximum positive (fully recovered) value. The time when zero magnetization is observed is referred to as the null time (Neuhaus, 1996). Long null times correspond to systems with long T_1s caused by less efficient longitudinal relaxation. The time dependence of the inversion recovery is obtained using a variable delay between the 180° pulse and the 90° pulse.

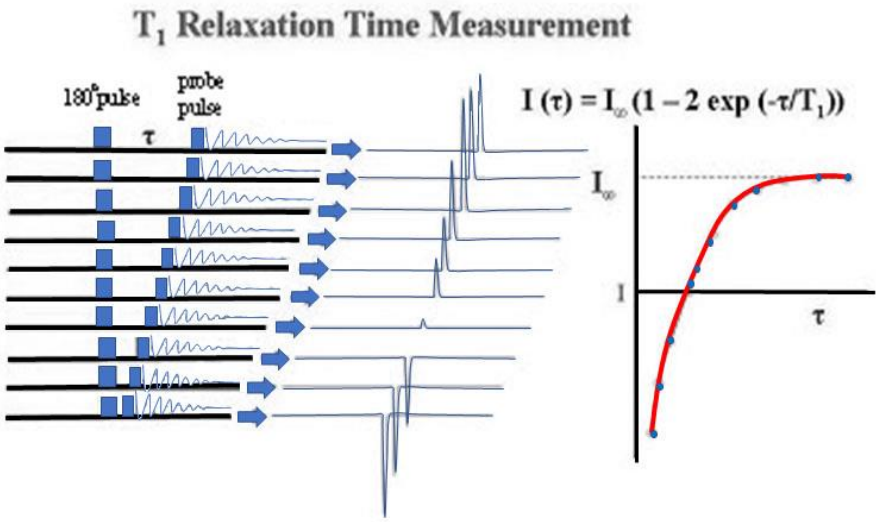

Figure 2. The T1 recovery experiment

Results and Discussion

^{1}H-NMR assignments were assisted with one dimensional ^{1}H-NOE experiments and two dimensional ^{1}H-^{1}H-NOESY experiments.

UVA1: DMSO-*d_6* (δ, ppm): OH 10.35, H1 and H4 8.0, H5 7.66, H2 and H3 7.5, H6 7.22, H7 7.06, CH_3 2.3

$CDCl_3$ (δ, ppm): OH 11.11, H1 and H4 7.9, H5 8.16, H2 and H3 7.45, H6 7.13, H7 7.06, CH_3 2.39

UVA2: DMSO-d_6 (δ, ppm) : OH 11.24, H1 and H4 8.10, H5 8.0, H2 and H3 7.58, H6 7.28, CH_2^A 1.94, CH_2^B 1.65, CH_3^A 1.42, CH_3^B 1.3 $CH_3^{C/D}$ 0.65.

$CDCl_3$ (δ, ppm): OH 11.74, H5 8.22, H1 and H4 7.93, H2 and H3 7.46, H6 7.23, CH_2^A 1.99, CH_2^B 1.69, CH_3^A 1.45, CH_3^B 1.35 $CH_3^{C/D}$ 0.70.

UVA3: DMSO-d_6 (δ, ppm) : NH 11.0, OH 10.84, H1 and H4 8.07, H5 7.87, H2 and H3 7.58, H6 7.26, CH_2 4.53, CH_3^B 2.34, CH_3^A 1.28.

$CDCl_3$ (δ, ppm): OH 11.61, NH 8.59, H5 8.16, H1 and H4 7.93, H2 and H3 7.48, H6 7.30, CH_2 4.72, CH_3^B 2.38, CH_3^A 1.38.

Table 1. Null times in the inversion recovery of **UVA1**

Solvent	OH	H5	H1, H4	H2, H3	H6	H7	CH_3
DMSO-d_6	1	1.5	1.5	1	1	1	0.5
$CDCl_3$	3.25	2.5	2	1.5	2	2	1.25

Table 2. Null times in the inversion recovery of **UVA3**

Solvent	OH	NH	H5	H1, H4	H2, H3	H6	CH_2	CH_3^A	CH_3^B
DMSO-d_6	1.25	0.5	1	1	0.63	0.5	0.15	0.18	0.3
$CDCl_3$	1.75	0.6	1.5	1.25	0.9	1	0.25	0.25	0.5

Table 3. Null times in the inversion recovery of **UVA2**

Solvent	OH	H5	H1, H4	H2, H3	H6	CH_3^A	CH_3^B	$CH_3^{C/D}$	CH_2^A	CH_2^B
DMSO-d_6	1.5	0.6	1	0.7	0.2	0.14	0.18	0.4	0.13	0.15
$CDCl_3$	2	1.25	1.5	1.3	0.5	0.35	0.4	0.7	0.4	0.4

The null times for **UVA1**, **UVA2** and **UVA3** from inversion recovery experiments are given in Tables 1-3. Longitudinal, or spin-lattice relaxation occurs due to loss of magnetism (against the B_0 field) *via* transfer of thermal energy to the lattice *via* (magnetic) dipole-dipole interactions. These dipole-dipole interactions occur due to fluctuations in the local magnetic field of a proton caused by the motions of neighboring protons or electrons. The energy transfer is optimal when the relative rate of motion of the dipoles matches the Larmor frequency ν_0 (the precession rate of the

magnetism in the B_0 field). However, generally Figure 3 shows how T_1 will change with parameters such as viscosity and molecular size for small molecules at moderate viscosity as in the present case. The null times of all protons were always shorter in DMSO-d_6 than in deuterated chloroform for all three compounds. This is expected because T_1 is inversely proportional to correlation time (τ_c) for small molecules at relatively low field strength and moderate viscosity. τc is the time that it takes for a particle to rotate by 1 radian and thus τ_c is obviously slower with higher solvent viscosity (Neuhaus 1996). Even in DMSO-d_6 τ_c should be ps-timescale.

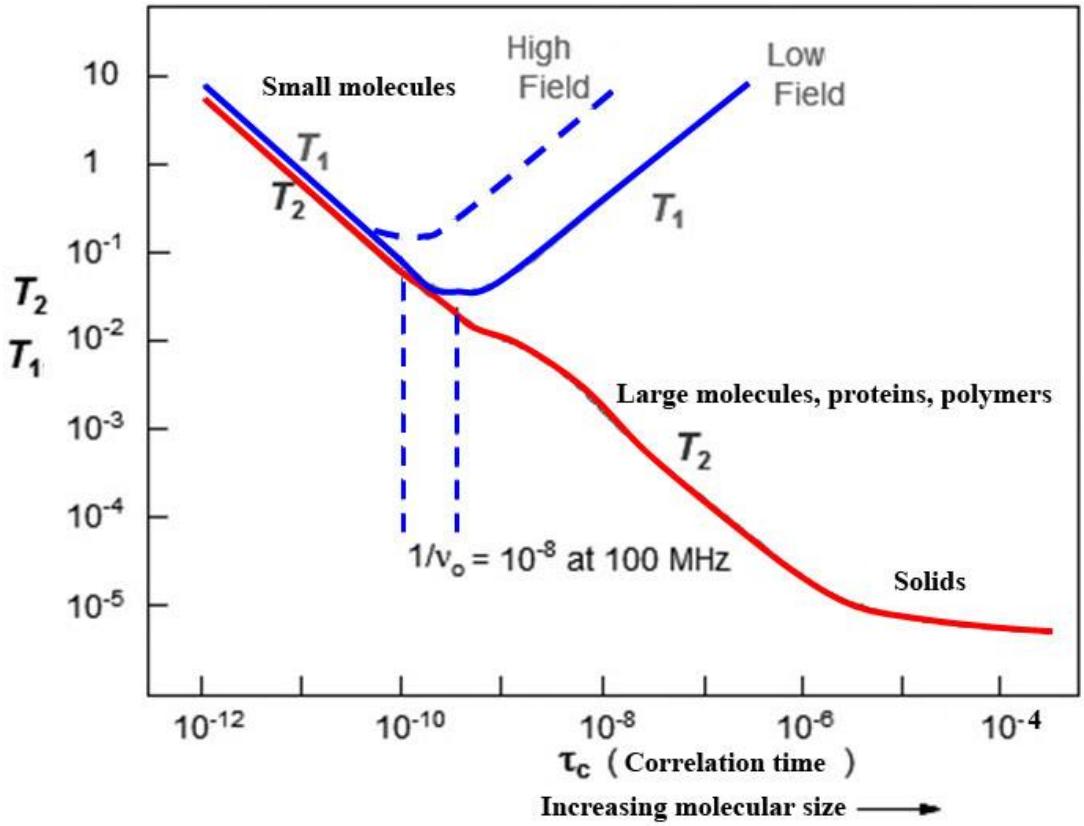

Figure 3. T1 and T2 with τ_c (molecular size and viscosity) (adapted from N. Bloembergen, E.M. Purcell, R.V. Pound "Relaxation Effects in Nuclear Magnetic Resonance Absorption" Physical Review 1948, 73, 679-746)

The protons bonded to sp^3 carbons (CH_n) on all three compounds relax as expected with groups having free motion nearby neighboring magnetic dipoles (protons) relaxing faster than those with less free motion and fewer dipolar neighbours. Protons bonded to sp^2 carbons relaxed more slowly (Neuhaus, 1996).

$$\tau_c = 4\pi\eta r^3/3kT \qquad (1)$$

where **η** is the viscosity, **r** is the effective hydrodynamic radius, and **kT** are Boltzmann's constant and temperature.

It is interesting to note the null times of the phenyl protons of the three compounds studied in deuterated chloroform and DMSO-*d*$_6$. From Tables 1-3 it is apparent that the solvent dependence of the T1 recovery of the phenyl proton of **UVA1** is relatively higher than the solvent dependence of this proton's recovery in the other two compounds. This suggests that in **UVA2** and **UVA3** the mobility of the phenyl protons is more restricted and/or the proton is always directed into H-bonding with the nitrogen atoms on the triazole ring irrespective of solvent. This is consistent with the concept that the bulky substituents on these compounds push the phenyl proton into an H-bonding configuration even in solvents like DMSO.

It is likely that, for **UVA1**, the phenyl proton is more isolated from its nearest neighbours in deuterated chloroform than it is in DMSO-*d*$_6$ due to the presence of an intramolecular H-bond in deuterated chloroform between the phenyl hydrogen and the non-bridging nitrogen atoms on the benzotriazole ring. In deuterated chloroform this bond holds the phenyl proton away from its nearest neighbours making intramolecular longitudinal relaxation less efficient. This bond is disrupted in DMSO-*d*$_6$ and the phenyl proton can get closer to H7 and longitudinally relax more quickly.

^{1}H-TOE

The TOE experiment monitors the build-up of the NOE as a function of time. From such experiments the initial build-up rate of the NOE can be estimated, and this value of initial rate can be used to estimate relative internuclear distances. For the initial NOE build up rate the following relationship is used (Neuhaus, 1996):

$$\sigma_{IS}.t = f_I(S) \text{ at time t.} \qquad (2)$$

Where σ_{IS} is the initial cross relaxation rate of spins I and S, $f_I(S)$ is the fractional enhancement of S upon saturating I and t is the NOE build-up time.

$$\sigma_{IS} = \zeta r_{IS}^{-6} \quad (3)$$

Where ζ is a variable dependent upon the correlation time and r_{IS} is the internuclear distance between spins I and S. When comparing distances, by using a reference distance, the ratios of cross relaxation rates can be used to estimate relative distances. In many cases differences in τ_c can be ignored with little error. Values of σ_{IS} are obtained from the initial slope of the NOE build-up curve.

The NOE build-up curves shown in Figure 4 have been obtained for the H1, H4 protons and the H7 proton for **UVA1** and H1, H4 and the CH_2 (methylene bridge) protons for **UVA3** in DMSO-d_6 and in deuterated chloroform upon irradiation of the phenyl proton.

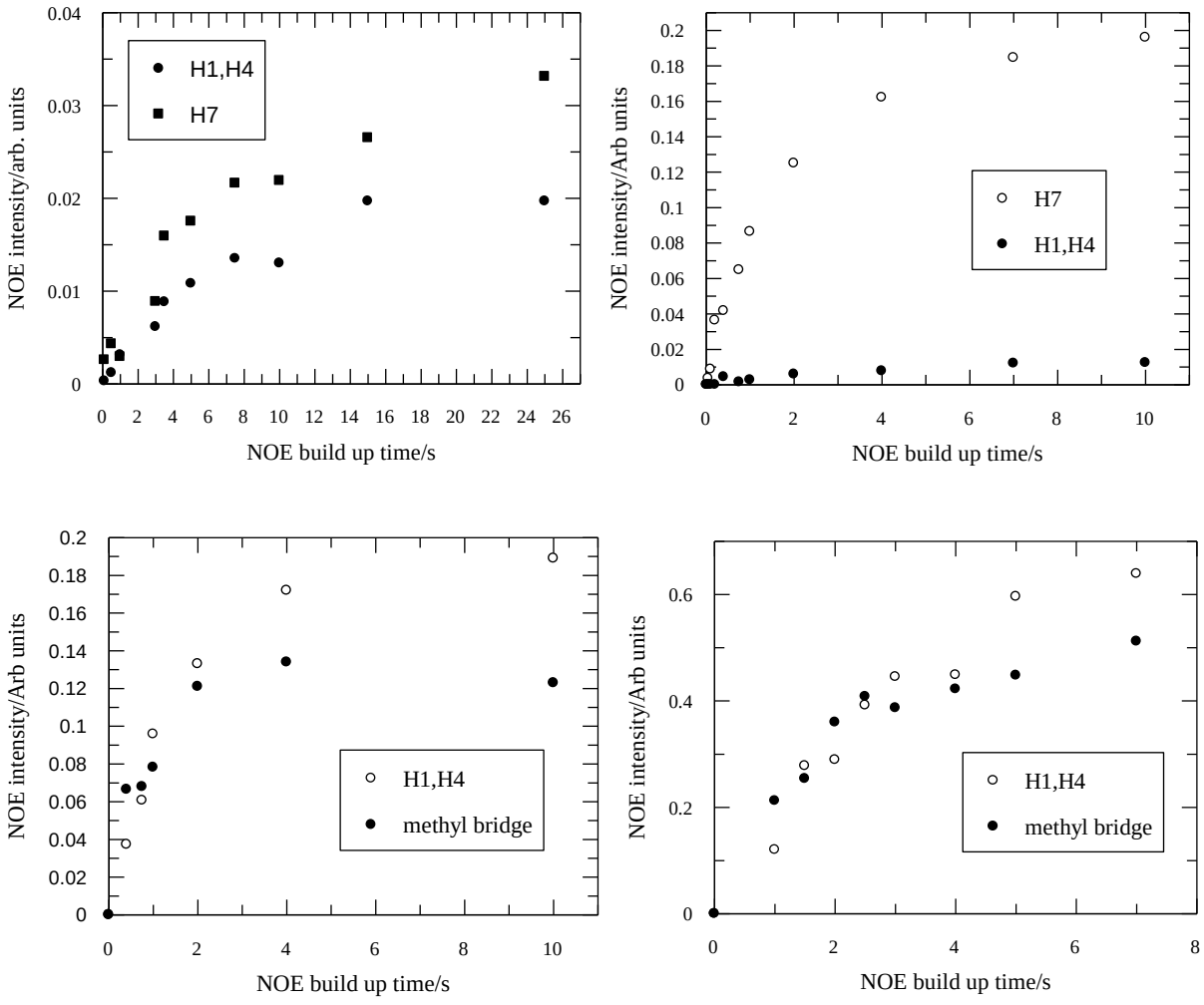

Figure 4. Top left, NOE build-up curves for H7, H1 and H4 on **UVA1** in deuterated chloroform. **Top right**, NOE build-up curve for H7, H1 and H4 on **UVA1** in DMSO-d_6. **Bottom left**, NOE build-up curve for H1, H4 and the methylene bridge protons of' **UVA3** in deuterated chloroform, **Bottom right**, NOE build-up curve for H1, H4 and the methylene bridge protons of **UVA3** in DMSO-d_6.

In these curves the absolute NOE intensity is plotted and not the fractional enhancement. From these NOE build-up curves it is immediately apparent that, for **UVA1** the phenolic OH group proton must be closer to H7 than it is to H1 and H4 in both DMSO-d_6 and deuterated chloroform. However, in DMSO-d_6 the phenolic OH group proton must be positioned relatively much closer to H7 than it is in deuterated chloroform. This fully supports the view that any intramolecular H-bonding that occurs in deuterated chloroform is disrupted in DMSO-d_6 and the phenyl OH-group proton can swing out of plane and towards H7.

Quantification of this statement using the initial rate of NOE build-up suggests that in deuterated chloroform the ratio $r_{(H7\text{-}HO)}$:$r_{(OH\text{-}H1,H4)}$ is 0.89, whereas in DMSO-d_6 this ratio is reduced to 0.56. Note that H1 and H4 are in fact equivalent upon the 200 MHz NMR time scale due to rotation about the bridging C-N bond; however, only one of these protons at a time will be spatially close to the phenyl proton and receive an NOE. Also note that, since a simple comparison is being made between build-up times for different spins on the same molecular sample, under exactly the same experimental conditions, this method is internally referenced.

Similar build-up curves obtained for **UVA3** demonstrate that the relative NOE build up rates for this compound in DMSO-d_6 and deuterated chloroform are very similar and, therefore, the internuclear distance are, also more similar in these two solvents. This result indicates that the 3´-methylene-hydantoinyl group forces the phenyl proton into a position suitable for intramolecular H-bond formation even in strongly H-bonding media.

^{1}H-^{1}H-NOESY

Using ^{1}H-NOESY on **UVA2** it was observed that the cross peak intensity for the OH proton and H1, H4 and the ortho iso-butyl protons is relatively unchanged upon changing solvent from deuterated chloroform to DMSO-d_6. This again supports the view that substitution with a bulky group ortho to the phenolic OH group encourages intramolecular H-bonding even in competition

with strongly H-bonding solvents. However, to be clear, the more appropriate methodology for accurately evaluating relative internuclear distances is the 1-dimensional truncated NOE experiment, rather than, often more popular, ^{1}H-NOESY. This is because the entire sequence of the ^{1}H-NOESY experiment takes so long that usually only a single mixing time τ_1 is used, which for small molecules is usually between 1-3 s. However, in the 1D version it is possible to vary τ_1 over a wide range of 1s to 10s of seconds in the same total accumulation time as for a single ^{1}H-NOESY experiment with a single mixing time τ_1. For structural determinations, the 2D ^{1}H-NOESY is unrivalled, but for determination of relative internuclear distances the 1D NOE experiment has many advantages.

Conclusion

The present work provides firm evidence that for **UVA1** in non-H-bonding solvents there is an intramolecular H-bond between the phenolic OH-group and the non-bridging nitrogen atoms on the benzotriazole ring. This bond is disrupted by hydrogen bonding solvents due to competitive intermolecular H-bonding. In compounds such as the **UVA3** the presence of the bulky group ortho to the phenolic OH-group promotes the intramolecular H-bond even in strongly H-bonding solvents such as DMSO. Since the geometry of the Frank-Condon excited state is the same as the ground state, this enhanced intramolecular H-bonding should increase the efficiency of excited state intramolecular proton transfer relative to intermolecular proton transfer to groups in hydrogen bonding dispersive media which can lead to irreversible photochemistry. This in turn should give compounds such as **UVA3** a greater stability and longer working lifetime compared to **UVA1**.

Conflict of Interests.

There are no conflicts of interest related to this publication.

References

Benassi, R. (1996) Furans and their benzo derivatives: Structure, in Comprehensive heterocyclic chemistry, 2, 259-295 Pergamon

Bloembergen, N., Purcell, E. M. & Pound, R. V. (1948) "Relaxation Effects in Nuclear Magnetic Resonance Absorption" Physical Review, 73, 679-746

Bocian, D. F., Huston, A. L., & Scott, G. W. (1983) Low temperature spectroscopy of internally hydrogen-bonded 2-(2′-hydroxy-5′-methylphenyl)-benzotriazole in a mixed crystal J. Chem. Phys., 76(12), 5802-5807.

Catalan, J., Fabero, F., Guijarro, M. S., Charamunt, R. M., Santa Maria, M. D., de la Concepcion Foces-Foces, M., Cano, F. H., Elguero, J., & R. Sastre. (1990) Photoinduced intramolecular proton transfer as the mechanism of ultraviolet stabilizers: a reappraisal, J. Am. Chem. Soc., 112, 747-759.

Catalan, J., Perez, P., Fabero, F., Wilshire, J. F. K. Claramunt, R. M. & Elguero, J. (1992) Photophysical properties of some 2-(2'-hydroxyaryl)benzotriazoles: dramatic effect of an ortho-located bulky tert-butyl group, J. Am. Chem. Soc., 114, 964-966.

Catalan, J., de Paz, L. G., Torres, M. R. & Tornero. J. D. (1997) Molecular structure of a unique UV stabilizer: Tinuvin P, J. Chem. Soc., Farad. Trans., 93(9), 1691-1696

Durr, H., Bouas-Laurent, H. & Kramer, H. E. A. (1990) Photochromism Molecules and Systems (1st Ed.). - Elsevier Ch. 16, 654-684.

Feldman, D., (2002) Polymer Weathering: Photo-Oxidation. Journal of Polymers and the Environment. 10 (4): 163–173.

Flom, S. R. & Barbara, P. F. (1983) The photodynamics of 2-(2′-hydroxy-5′-methylphenyl)-benzotriazole in low-temperature organic glasses, Chem. Phys. Lett., 94(5), 488-493.

Huston, A. L. Scott, G. W. & Gupta, A. (1982) Mechanism and kinetics of excited-state relaxation in internally hydrogen-bonded molecules: 2-(2′-hydroxy-5′-methylphenyl)-benzotriazole in solution J. Chem. Phys. 76(10), 4978-4985.

McGarry, P. F., Jockusch, S., Fujiwara, Y., Kaprindis, N. A., & Turro, N. J. (1997) DMSO Solvent Induced Photochemistry in Highly Photostable Compounds. The Role ofIntermolecular Hydrogen Bonding J. Phys. Chem. A, 101, 764-767.

Neuhaus, D., & Williamson, M. P. (1996) The Nuclear Overhauser Effect In Structural And Conformational Analysis, (1st Ed.). VCH Publishers Inc. New York, Ch. 4, 103-140.

Saunders, J. K. M. & Hunter, B. K. (1988) Modern NMR Spectroscopy, (A Guide For Chemists), (1st Ed.). Oxford University Press, Oxford, pp173.

Sheng, H., Hu, Y., Zhou, Y., Fan, S., Cao, Y., Zhoa, X. & Yang, W. (2019) A highly selective ESIPT-based fluorescent probe with a large Stokes shift for the turn-on detection of cysteine and its application in living cells, Dyes and Pigments, 160, 48-57

Werner, T. (1979) Triplet deactivation in benzotriazole-type ultraviolet stabilizers J. Phys. Chem., 83(3), 320-325.

Woessner, G., Goeller, G., Kollat, P., Stezowski, J. J., Hauser, M., Klein, U. K. A. & Kramer H. E. A. (1984) Photophysical and photochemical deactivation processes of ultraviolet stabilizers of the (2-hydroxyphenyl)benzotriazole class, J. Phys. Chem., 88, 5544-5550.

Woessner, G., Goeller, G., Reiker, J., Hoier, H., Stezowski, J. J., Daltrozzo, E., Neureiter, M. & Kramer, H. E. A. (1985) Ultraviolet stabilizers of the 2-hydroxyphenylbenzotriazole class - influence of the solvent on the absorption spectra and photochemical deactivation mechanism J. Phys. Chem., **89**, 3629-3636.

H. Zweifel, R. D. Maier, M. Schiller, (2009). Plastics additives handbook (6th ed.). Munich: Hanser.

Intra- i intermolekularno H-vezivanje benzotriazol UV stabilizatora dokazano korišćenjem 1D eksperimenata nuklearnog Overhauserovog efekta

Džonathan Hobli, [1#], Vinćenco Malatesta[2]

1- OndaLabs R&D Konsultantske usluge, Deca Homes, Clark Free-Port, Mabalacat, Angeles, Filipini 20102

 # Nacionalni Čeng Kung Univerzitet, Departman za bioinženjering, University Road, Tainan Citi, Taivan, ROC, 70101

2- Univerzitet Milano-Bikoka, Departman za materijale, Milano, Italija.

SAŽETAK

Zaštitni mehanizam 2-hidroksifenilbenzotriazola od UV apsorpcije je zasnovan na rasipanju energije preko pobuđenog stanja transfera protona sa fenolne OH grupe na azot(e) trizola. Korišćenjem ^{1}H-NMR NOE eksperimenata, utvrdili smo da 2-(2'-hidroksi-5'-metilfenil)-benzotriazol (**UVA1**) postoji u hloroformu u formi sa intramolekulskom vodoničnom vezom, dok je u DMSO ova veza prekinuta zbog formiranja intermolekulske vodonične veze sa rastvaračem. Obrnuto, za jedinjenja 2-(2'-hidroksi-3',5'-di(1,1-dimetilpropil))-benzotriazol (**UVA2**), i 3'-metilen-hidantoin-2-(2'-hidroksi-5'-metilfenil)-benzotriazol (**UVA3**) koja imaju voluminozne orto supsituente u odnosu na fenolnu OH grupu, ^{1}H-NMR NOE eksperimenti su pokazali da promena rastvarača (DMSO umesto hloroforma) ne utiče značajno na jačinu intramolekulske vodonične veze. Diskutovan je uticaj jačine vodonične veze na efikasnost UV stabilizacije.

***Ključne reči*: benzotriazol, UV stabilizator, nuklearni Overhauser efekat NOE, difuzija spina**

Liaison H intra- et intermoléculaire des stabilisants UV benzotriazole mise en évidence à l'aide d'expériences sur l'effet Overhauser nucléaire 1D.

Jonathan Hobley, [1 #] Vincenzo Malatesta[2]

1-OndaLabs R&D Consultancy, Deca Homes, Clark Free-Port, Mabalacat, Angeles, Philippines 20102

 # Adresse actuelle Université nationale Cheng Kung, Département de bio-ingénierie, University Road, Tainan City, Taiwan, ROC, 70101

2- Université de Milan-Bicocca, Département des matériaux, Milan, Italie.

Résumé

Le mécanisme de protection de l'absorbeur UV des 2-hydroxyphénylbenzotriazoles est basé sur la dissipation d'énergie via un transfert de protons à l'état excité du groupe OH phénolique au(x) azote(s) triazole(s). En utilisant des expériences de H-NMR NOE, nous avons établi que le 2-(2'hydroxy-5'-méthylphényl) -benzotriazole (**UVA1**) existe dans le chloroforme sous forme de liaison intramoléculaire H alors que dans le DMSO, cette liaison est interrompue par la formation de H intermoléculaire -adhérence au solvant. Inversement, pour les composés 2-(2'-hydroxy-3', 5'-di (1,1-diméthyl propane)) -benzotriazole (**UVA2**) et 3'-méthylène-hydantoïne-2- (2'hydroxy-5 '-méthylphényl) -benzotriazole (**UVA3**) ayant des substituants volumineux ortho au groupe OH phénolique, les expériences de RMN 1H NOE indiquent que lors du changement de solvant du DMSO au chloroforme, la force de la liaison H intramoléculaire n'est pas sensiblement affectée. L'implication de la force de liaison H sur l'efficacité de stabilisation UV est discutée.

Mots-clés : benzotriazole, stabilisant UV, NOE effet Overhauser nucléaire, diffusion de spin.

Подтверждение внутри- и межмолекулярных водородных связей бензотриазольных УФ-стабилизаторов путем одномерных экспериментов с ядерным эффектом Оверхаузера

Джонатан Хобли, [1#] Винченцо Малатеста[2]

1- OndaLabs R&D Consultancy, Deca Homes, Кларк Фри-Порт, Мабалакат, Анхелес, Филиппины, 20102

 # Текущий адрес Национальный университет Ченг Кунг, факультет биоинженерии, Юниверсити Роуд, город Тайнань, Тайвань, Китай, 70101

2- Миланский университет Бикокка, Отдел материаловедения, Милан, Италия.

Аннотация

Механизм защиты 2-гидроксифенилбензотриазолов УФ-поглотителем основан на диссипации энергии за счет переноса протона в возбужденном состоянии от фенольной группы OH к триазольному азоту (ам). Используя 1H-ЯМР-эксперименты с NOE, мы установили, что 2- (2'-гидрокси-5'-метилфенил) -бензотриазол (УФА1) существует в хлороформе в виде внутримолекулярной H-связанной формы, тогда как в ДМСО эта связь разрывается с образованием межмолекулярной H -связи с растворителем. И наоборот, для соединений 2- (2'-гидрокси-3', 5'-ди (1,1-диметилпропан)) бензотриазол (УФА2) и 3'-метилен-гидантоин-2- (2'-гидрокси-5'-метилфенил) -бензотриазол (УФА3), имеющий объемные заместители орто относительно фенольной OH-группы. Эксперименты 1H-ЯМР NOE показывают, что при замене растворителя с ДМСО на хлороформ на прочность внутримолекулярной H-связи существенно не влияет. Обсуждается влияние прочности водородных связей на эффективность УФ-стабилизации.

Ключевые слова: бензотриазол, УФ-стабилизатор, ядерный эффект Оверхаузера, NOE, спиновая диффузия.

Intra- und intermolekulare H-Bindungen von Benzotriazol-UV-Stabilisatoren wurden durch 1D Kern-Overhauser-Effekt-Experimente nachgewiesen.

Jonathan Hobley,[1#] Vincenzo Malatesta[2]

1- OndaLabs R&D Consultancy, Deca Homes, Clark Free-Port, Mabalacat, Angeles, Philippinen 20102

 # Die aktuelle Adresse Nationale Cheng Kung Universität, Lehrstuhl für Bioingenieurswesen, Universität Road, Tainan City, Taiwan, ROC, 70101

2- Universität Degli Studi di Milano-Bicocca, Lehrstuhl für Materialien, Milano, Italien.

ABSTRACT

Der UV-Absorber-Schutzmechanismus von 2-Hydroxyphenylbenzotriazolen basiert auf der Energiedissipation durch einen Protonentransfer im angeregten Zustand von der phenolischen OH-Gruppe auf den/die Triazol-Stickstoff(e). Mit Hilfe von 1H-NMR NOE-Experimenten haben wir festgestellt, dass 2-(2'Hydroxy-5'-methylphenyl)-benzotriazol (**UVA1**) in Chloroform als intramolekular H-gebundene Form vorliegt, während diese Bindung in DMSO durch die Bildung von intermolekularen H-Bindungen mit dem Lösungsmittel unterbrochen wird. Umgekehrt gilt für die Verbindungen 2-(2'-Hydroxy-3',5'-di(1,1-dimethylpropan))-benzotriazol (**UVA2**), und 3'-Methylen-Hydantoin-2-(2'-Hydroxy-5'-methylphenyl)-benzotriazol (**UVA3**), dass sie sperrige Substituenten in Ortho-Stellung zur phenolischen OH-Gruppe aufweisen, zeigen 1H-NMR NOE-Experimente, dass der Wechsel des Lösungsmittels von DMSO zu Chloroform die Stärke der intramolekularen H-Bindung nicht nennenswert beeinflusst. Die Auswirkung der H-Bindungsstärke auf die UV-stabilisierende Wirksamkeit wurde diskutiert.

Schlüsselwörter: Benzotriazol, UV-Stabilisator, Kern-Overhauser-Effekt NOE, Spin-Diffusion

Kinetic and Thermodynamic Characteristics of Thermal Degradation of Anthocyanins from Strawberry and Blueberry Commercial Juices

Milan N. Mitić[1*]

1- University of Niš, Faculty of Sciences and Mathematics, Department of Chemistry, Višegradska 33, 18000 Niš, Serbia

Milan. N. Mitić: milamitic83@yahoo.com

ABSTRACT

Thermal stabilities of anthocyanins in strawberry and blueberry commercial juices were studied over the temperatures 75, 85 and 95 ^{o}C. Results indicated that the thermal degradation of anthocyanins followed the first-order reaction kinetics. The temperature-dependent degradation was adequately modeled on the Arrhenius equation. During heating, anthocyanins in the strawberry juice degraded faster than in blueberry juice, with the activation energies of 74.16 kJ/mol and 65.75 kJ/mol, respectively. Cyanidin-3-glucoside (cyd-3-glu) was more susceptible to the thermal treatment than pelargonidin glycosides in strawberry juice. Delphinidin glycosides were more susceptible to the thermal treatment than cyanidin glycosides in blueberry juice. However, cyd-3-glu in strawberry juice was more sensitive to the thermal treatment than in blueberry juice. Obtained results for activation enthalpies indicated that the degradation process was endothermic and Gibbs free energy of activation indicated that they were not spontaneous.

Keywords: *Thermal degradation, anthocyanins, degradation kinetics, blueberry juice, strawberry juice*

Introduction

Anthocyanins are a group of naturally occurring phenolic compounds, which are responsible for the attractive colors of many flowers, fruits (particularly in berries), vegetables and related products derived from them (Wang and Xu, 2007). Except as colorants, anthocyanins have multiple biological roles, *e.g.*, antioxidant activity, anti-inflammatory action, inhibition of blood platelet aggregation and antimicrobial activity, treatment of diabetic retinopathy and prevention of cholesterol-inducted atherosclerosis (Clifford, 2000; Espin et al., 2000). Nevertheless, anthocyanins easily degrade during food processing and storage, being highly sensitive to factors such as light, pH, temperature, presence of oxygen and enzymes (Mercali, 2013).

Food processing generally includes heat treatments that effectively preserve foodstuffs and also provide desirable sensory properties. However, current knowledge indicates that heat processing, particularly under severe conditions, may affect anthocyanin levels in fruit products and vegetables (Hou et al., 2013; Jimenez et al., 2010). The thermal degradation of anthocyanins has been studied in grape juice (Dalisman et al., 2015), blackberries (Wang and Xu, 2007), blueberry juice (Kechinski et al., 2010), elderberry juices (Casati et al., 2015), and sour cherry juice (Szaloki-Darko et al., 2015). Reported results show that rate constants for anthocyanin degradation with respect to the temperature can always be assumed to follow a first-order reaction, and the Arrhenius model can be used to describe this dependence between temperature and anthocyanin degradation. The kinetics degradation of anthocyanins can also be evaluated from a thermodynamic perspective based on activation functions such as free energy, ΔG, enthalpy, ΔH, entropy, ΔS, and activation energy, E_a. These functions can be estimated for reactions that occur in foods and may provide valuable information concerning thermal degradation kinetics (Cassati et al., 2015).

The objective of the present study was to comparatively evaluate the effect of heating on the degradation kinetics of individual anthocyanins in strawberry and blueberry juices at temperatures ranging from 75 to 95°C.

Experimental

Chemical and reagents

Cyanidin-3-glucoside, pelargonidin-3-glucoside and delphinidin-3-glucoside were purchased from Merck (Darmstadt, Germany). Other anthocyanin-glycosides were purchased from Extrasynthese S.A.S (Ganay, France). Formic acid and acetonitrile (HPLC grade) were purchased from Merck (Darmstadt, Germany). Deionized water was used for the preparation of all solutions, and it was produced using MicroMed high purity water systems (TKA Wasseraufbereitungssystem GmbH).

Degradation studies of juice samples

Commercial strawberry and blueberry juices were purchased from local market. The thermal stability of strawberry and blueberry juices anthocyanins was studied at 75, 85 and 95°C. Juice aliquots (20 ml) were put into glass tubes which were well capped for avoiding evaporation of the samples. Tubes were put in preheated water bath at desired temperature. At predetermined time intervals, the samples were removed and rapidly cooled in the ice bath. Immediately, the anthocyanin content was analysed. All measurements were done in triplicate in each case.

HPLC analysis of anthocyanins

Quantification of individual anthocyanin compounds was determined using reversed phase HPLC method. The analysis was performed by HPLC-DAD (Agilent 1200 series, Agilent Technology, USA) system, equipped with four solvent delivery unit G1354A, UV-Vis detector G1315D and HP Chemstation chromatography workstation. Chromatographic analyses were performed on 150 mm x 4.6 mm i.d., Zorbax Eclipse XDB C18 column (Agilent Technologies, USA). The column was thermostated at 30°C. The flow rate was 0.8 ml/min and the injection volume was 5 µL. The mobile phase consisted of A: H_2O+5% HCOOH and B: 80% ACN+5% HCOOH+H_2O. The gradient procedure was: 0-10 min with 0% B, 10-28 min gradually increases 0-25% B, from 28 to 30 min 25% B, from 30 to 35 min gradually increases 25-

50% B, from 35 to 40 min gradually increases 50-80% B, and finally for the last 5 min gradually decreases 80-0% B. Individual cyanidin, delphinidin, peonidin, petunidin and pelargonidin glycosides were quantified as corresponding equivalents of the five anthocyanin glucosides using external calibration curves of authentic standards ranging from 5 to 125 μg/ml. Total anthocyanins were calculated as the sum of individual anthocyanin glycosides with results expressed as mg per 1L of juice.

Kinetic models

A first-order reaction model has been applied for the description of degradation of anthocyanins from various sources (Szaloki-Darko et al., 2015; Verbeyst et al., 2011; Zhao et al., 2012). The model is expressed as:

$$\ln\left(\frac{c_t}{c_o}\right) = -k \cdot t \qquad (1)$$

where c_0 is the initial anthocyanin content and c_t is the anthocyanin content after treatment time (min) at the given temperature, k is the rate constant (1/min), and the half-life $t_{1/2}$ is the time needed for 50% degradation of anthocyanin, which is calculated by the following equation:

$$t_{1/2} = \frac{\ln(0.5)}{k} = \frac{0.693}{k} \qquad (2)$$

Thermodynamic analysis

The activation energy was calculated using the Arrhenius equation, which was used to describe the temperature dependence of the first-order degradation rate constant. It is expressed as Eq. (3), and can be rearranged as a linear Eq. (4) (Liu et al., 2014):

$$k = k_0 \cdot e^{-E_a/RT} \qquad (3)$$

$$\ln k = \ln k_0 + \left(\frac{-E_a}{R}\right)\frac{1}{T} \qquad (4)$$

where: k_0-frequency factor (1/min); E_a-activation energy (kJ/mol); R-universal gas constant (8.314 J/mol·K) and T-absolute temperature (K).

The coefficient Q_{10} (temperature coefficient) is another way to characterize the effect of the temperature on the rate of a reaction, which represents the change in the degradation when the temperature increases by 10°C, is calculated as follows (Kechinski et al., 2010):

$$Q_{10} = \left(\frac{k_{T_2}}{k_{T_1}}\right)^{10/T_2 - T_1} \quad (5)$$

All of the activation parameters: activation enthalpy change, ΔH^* (kJ/mol), activation entropy change, ΔS^* (J/K·mol), and activation Gibbs free energy change, ΔG^* (kJ/mol), were used to investigate the thermodynamic changes in the transition state of the degradation reaction. ΔH^* and ΔS^* were calculated using the Eq. (6) and Eyring equation shown in Eq. (7), while the activation Gibbs free energy change was determined using Eq. (8) (Park and Kim, 2017):

$$\Delta H^* = E_a - RT \quad (6)$$

$$\frac{\ln k}{T} = \ln \frac{k_B}{h} + \frac{\Delta S^*}{R} - \frac{\Delta H^*}{RT} \quad (7)$$

$$\Delta G^* = \Delta H^* - T\Delta S^* \quad (8)$$

The rate constant (k) was obtained using the Eq. (1), k_B is the Boltzman constant (1.3807 x 10^{-23} J/K) and h is the Planck constant (6.6261 x 10^{-34} J·s).

Results and Discussion

HPLC-DAD analysis of juices

Monomeric anthocyanins existing in red fruit juices were derivatives of cyanidin, delphinidin, pelargonidin, malvidin and peonidin. So, it is evident that juices produced with different red fruits, such as strawberry, raspberry, blueberry, black currant and grapes, differ in the quantity and the type of anthocyanins.

The results of HPLC-DAD analysis of the commercial strawberry and blueberry juices are shown in Table 1.

Table 1. Concentrations of anthocyanins in commercial juices (mg/L) determined by HPLC-DAD method and the percentage distribution of anthocyanins

Anthocyanins	Sample	Concentration (mg/L)	Total anthocyanins (%)
Cyanidin-3-glucoside (cyd-3-glu)	Strawberry juice	67.5±0.34	50.5
Pelargonidin-3-glucoside (pgd-3-glu)		62.4±0.42	46.7
Pelargonidin-3-rutinoside (pgd-3-rut)		2.84±0.42	2.8
Total anthocyanins (TA)		**133±0.29**	**100**
Delphinidin-3-galactoside (dpd-3-gal)	Blueberry juice	11.2±0.25	9.30
Delphinidin-3-glucoside (dpd-3-glu)		7.13±0.22	5.95
Delphinidin-3-arabinoside (dpd-3-ara)		53.9±0.87	44.9
Cyanidin-3-galactoside (cyd-3-gal)		10.3±0.37	8.6
Cyanidin-3-glucoside (cyd-3-glu)		9.45±0.18	7.88
Cyanidin-3-arabinoside (cyd-3-ara)		6.91±0.15	5.76
Petunidin-3-galactoside (ptd-3-gal)		10.9±0.24	9.15
Peonidin-3-galactoside (pnd-3-gal)		10.1±0.20	8.44
Total anthocyanins (TA)		**120±0.31**	**100**

The major anthocyanins in strawberry commercial juice were cyanidin-3-glucoside (50.5%), followed by pelargonidin-3-glucoside (46.7%), whereas the concentration of pelargonidin-3-rutinoside were relatively low (2.8%). Da Silva et al. (2007), Jakobek et al. (2007) and Stój et al. (2006) determined the existence of cyanidin 3-glucoside, pelargonidin 3-glucoside, and pelargonidin 3 rutinoside in strawberry juice, where the major anthocyanin was pelargonidin 3-glucoside.

Blueberry commercial juice contained a mixture of three delphinidin-3-glycosides (galactoside, glucoside and arabinoside), three cyanidin-3-glycosides (galactoside, glucoside and arabinoside), petunidin-3-galactoside and peonidin-3-galactoside, where the delphinidin-3-arabinoside being the most abundant (44.9%). These data are in accordance with those found in literature (Obon et al., 2011; Prior et al., 2001; Wu and Prior, 2005).

Thermal degradation kinetics of anthocyanins

Previous studies showed that thermal degradation of anthocyanins followed a first-order reaction. To verify the applicability of a first-order kinetic model, $\ln(c_t/c_0)$ is plotted against time (Figures 1 and 2).

It is clear from Figures 1 and 2 that the thermal degradation of strawberry and blueberry anthocyanins followed first order reaction kinetics.

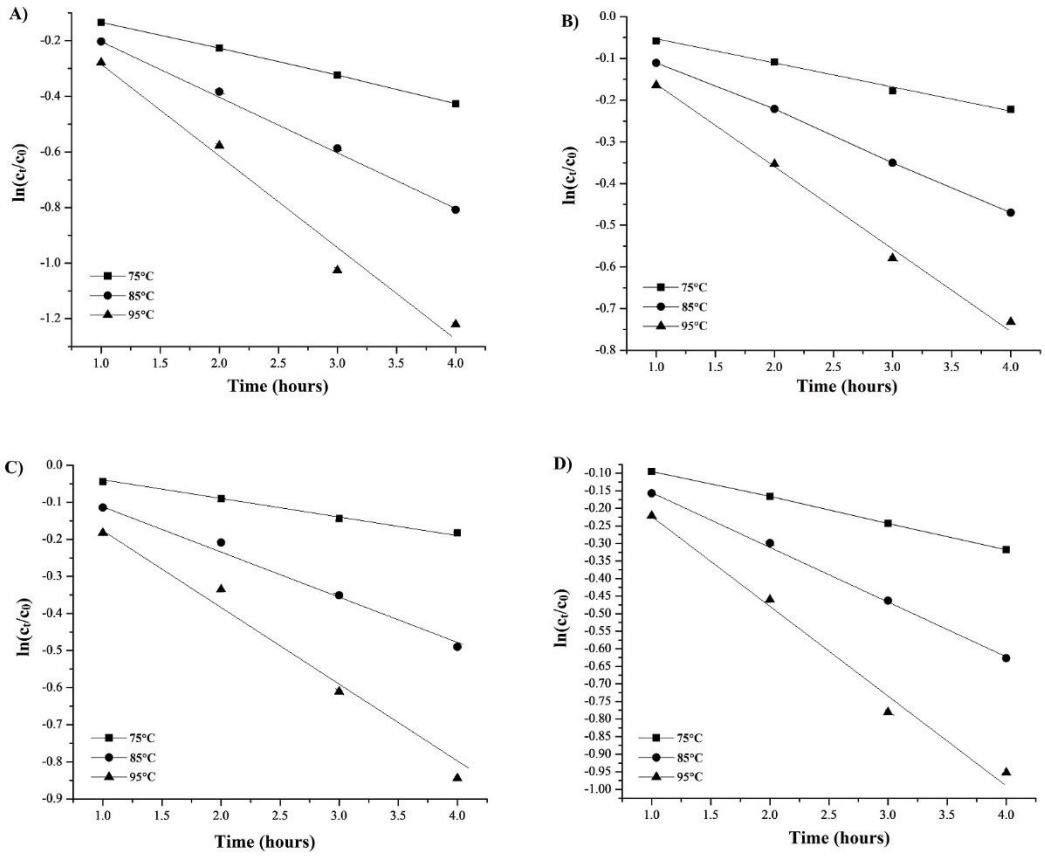

Figure 1. Degradation of anthocyanins in strawberry juice during heating: **A**) cyd-3-glu, **B**) pgd-3-glu, **C**) pgd-3-rut, **D**) total anthocyanins.

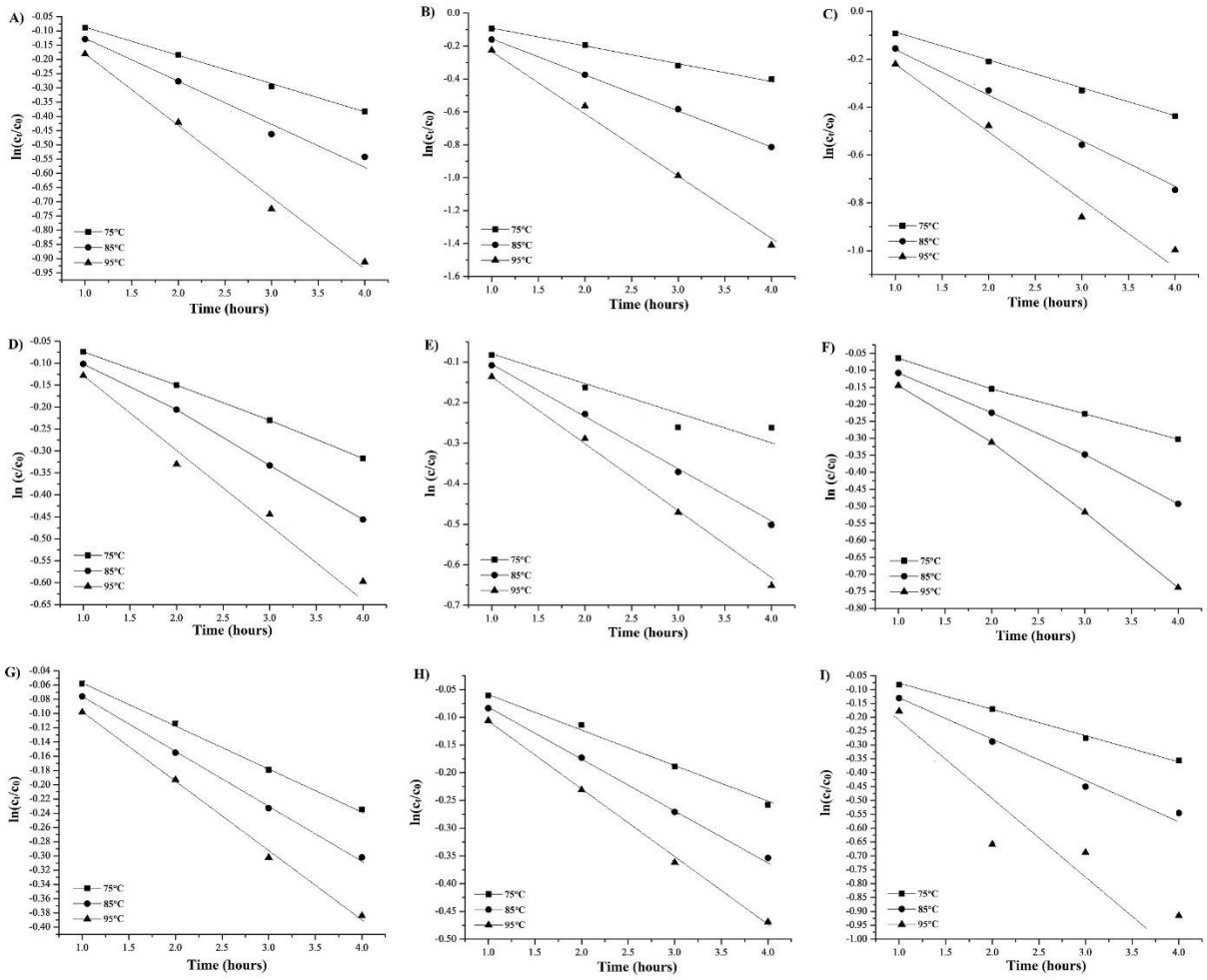

Figure 2. Degradation of anthocyanins in blueberry juice during heating: **A**) dpd-3-gal, **B**) dpd-3-glu, **C**) dpd-3-ara, **D**) cyd-3-gal, **E**) cyd-3-glu, **F**) cyd-3-ara, **G**) ptd-3-gal, **H**) pnd-3-gal, **I**) total anthocyanins.

The kinetic parameters of individual anthocyanins and total anthocyanins in juices are shown in Table 2. It is clear that the degradation of strawberry and blueberry anthocyanins increased with increasing heating temperature and time.

For the cyd-3-glu as a predominant anthocyanin in strawberry juice, the degradation rate constant (k) increased from 1.58 to $6.22 \cdot 10^{-3}$ 1/min with the temperature increase from 75 to 95°C. For the pgd-3-rut, the degradation rate also showed similar trend, with k increasing from 0.84 to $3.57 \cdot 10^{-3}$ 1/min as a result of temperature increase. Increasing the temperature for 20°C (from 75 to 95°C), k is increased by

approximately 3.8 to 4.3 fold. For dpd-3-ara as a predominant anthocyanin in blueberry juice, for the same temperature increase (20°C), the degradation rate constant (k) increased from 1.88 to $6.35 \cdot 10^{-3}$ 1/min. In this case, increasing the temperature for 20 °C (from 75 to 95 °C), k increased by approximately 1.7 to 3.4 fold.

Table 2. Effect of heating temperature on the degradation of strawberry and blueberry juices anthocyanins

	Temperature (°C)	$k \cdot 10^3$ (1/min)	$t_{1/2}$ (h)		Temperature (°C)	$k \cdot 10^3$ (1/min)	$t_{1/2}$ (h)
Strawberry juice							
	75	1.58±0.02	7.04		75	0.92±0.01	12.6
cyd-3-glu	85	3.2±0.1	3.61	pgd-3-glu	85	1.98±0.01	5.83
	95	6.22±0.02	1.86		95	3.45±0.02	3.35
	75	0.84±0.01	13.8		75	1.23±0.01	9.39
pgd-3-rut	85	1.97±0.01	5.86	**TA**	85	2.55±0.02	4.53
	95	3.57±0.02	3.23		95	4.66±0.02	2.48
Blueberry juice							
	75	1.72±0.02	6.72		75	2.02±0.01	5.72
dpd-3-gal	85	2.78±0.01	4.15	dpd-3-glu	85	3.35±0.02	3.44
	95	5.43±0.03	2.13		95	5.32±0.03	2.17
	75	1.88±0.01	6.14		75	1.29±0.01	8.95
dpd-3-ara	85	3.52±0.02	3.26	cyd-3-gal	85	1.92±0.02	6.02
	95	6.35±0.02	1.82		95	2.63±0.04	4.39
	75	1.36±0.01	8.49		75	1.48±0.02	7.80
cyd-3-glu	85	1.99±0.01	5.80	cyd-3-ara	85	2.19±0.03	5.27
	95	3.1±0.1	3.72		95	2.79±0.02	4.14
	75	1.01±0.01	11.4		75	1.06±0.01	10.9
ptd-3-gal	85	1.31±0.02	8.82	pnd-3-gal	85	1.55±0.01	7.45
	95	1.69±0.02	5.42		95	2.13±0.03	5.42
	75	1.61±0.01	7.22				
TA	85	2.67±0.02	4.32				
	95	4.25±0.02	2.72				

The $t_{1/2}$ values of anthocyanins are expressed in Eq. 2 and presented in Table 2. The $t_{1/2}$ values varied from 13.8 to 1.86 h and 11.4 to 1.82 h for strawberry and blueberry juices, respectively. The half-life at 95°C of cyd-3-glu (in strawberry juice) and dpd-3-ara (in blueberry juice) was 1.86 and 1.82 h, respectively. The half-life values of anthocyanin degradation in blackberry juice at 60-90°C were from 16.7 to 2.9 h (Wang and Xu, 2007) and in plum juice at 50-120°C were from 6.27 to 0.40 h (Turturica et al., 2018).

Cemeroglu et al. (1994) reported that $t_{1/2}$ value of anthocyanin degradation at 80°C in sour cherry juice and concentrate was 8.1 and 2.8 h, respectively. These results for $t_{1/2}$ values of anthocyanin degradation were considerably higher, compared to the juices analyzed in the present study. Sugar and ascorbic acid present in juices can also increase or decrease the anthocyanin degradation depending on their concentration (Gerard et al., 2019; Svensson, 2010). Different food matrix and chemical structure of anthocyanin-conjugated sugar (the type and place of glycosylation, the presence of hydroxyl groups) probably affect its thermal stability (Dai et al., 2009).

The activation energy E_a was calculated based on a linear regression of ln k and 1/T using Eq. (4). Table 3 presents activation energy values for both juices during heating process. The compared activation energy values for total anthocyanins were: 74.16 kJ/mol and 65.75 kJ/mol, for strawberry and blueberry juice, respectively. High activation energy implies that the degradation of anthocyanins in strawberry juice are more susceptible to temperature elevations that those in blueberry juice. The high activation energy value indicates strong temperature dependence which means that the reaction runs very slowly at low temperature, but relatively fast at high temperatures.

Table 3. The activation energy E_a and temperature coefficient Q_{10} obtained for anthocyanin degradation during heating

	E_a (kJ/mol)	R^2	Q_{10} 75-85°C	Q_{10} 85-95°C
Strawberry juice				
cyd-3-glu	75.99	0.9935	2.02	1.94
pgd-3-glu	73.27	0.9856	2.15	1.42
TA	74.16	0.9912	2.07	1.83
Blueberry juice				
dpd-3-ara	71.50	0.9954	1.62	1.95
dpd-3-gal	63.68	0.9932	1.87	1.80
TA	65.75	0.9948	1.67	1.59

The obtained results are similar to the previously reported E_a for grape juice (64.89 kJ/mol) at 70-90°C (Dalisman et al., 2015), Bordo grape anthocyanins (72.74 kJ/mol) at 70-90°C (Hillman et al., 2011), Cornelian cherry juices (58.09 kJ/mol) at 2-75°C (Moldovan and David, 2020) and blackberry anthocyanins

(58.95 kJ/mol) at 60-90°C (Wang and Xu, 2007). Morever, Kechinski et al. (2010) reported a higher value (80.4 kJ/mol) for the degradation blueberry anthocyanins at 40-80°C.

Table 3 presents the values of Q_{10} for the temperatures used in this study. The higher value is obtained for the cyd-3-glu and pgd-3-glu in strawberry juice within the range 75-85°C, indicating that in this range the degradation kinetics was strongly affected by the temperature. Similar behavior can be observed for the dpd-3-ara and dpd-3-gal in blueberry juice within the range 85-95°C, but to a minor extent. In the range of 85-95°C for pgd-3-glu in strawberry juice and in the range of 75-85°C for dpd-3-ara in blueberry juice Q_{10} values were lower indicating that within those 2 ranges the degradation kinetics are barely affected by the temperature change. According to Kechinski et al. (2010) the relatively low values of Q_{10} suggest the significance of molecular association that could decrease the rate of anthocyanin degradation. Al-Zubaidy and Khalil (2007) also mentioned that this effect can be confirmed by determining the activation energies and other related thermodynamic functions of this degradation process.

Estimation of thermodynamic parameters may also provide valuable information regarding thermal degradation kinetics of anthocyanins. The equilibrium state between an activated complex and reactant is called the transition state. When an activated complex passes the transition state, products are formed (Park and Kim, 2017). Calculated thermodynamic parameters: Gibbs free activation energy ΔG^*, the activation enthalpy ΔH^* and the activation entropy ΔS^*, at all temperatures evaluated during heating are presented in Table 4.

Table 4. Activation thermodynamic parameters obtained for anthocyanin degradation during heating

	Temperature (°C)	ΔH^* (kJ/mol)	ΔS^* (J/mol·K)	ΔG^* (kJ/mol)
Strawberry juice				
cyd-3-glu	75	73.1	-89.7	104.3
	85	73	-90.2	105.3
	95	72.9	-90.6	106.3
pgd-3-glu	75	70.4	-102.1	105.9
	85	70.3	-101.8	106.7
	95	70.2	-102.9	108.1

TA	75	71.3	-97.1	105.1
	85	71.2	-97.2	106
	95	71.1	-99.6	107.8
		Blueberry juice		
dpd-3-ara	75	68.6	-108.9	106.5
	85	68.5	-109.4	108.8
.	95	68.4	-109.7	108.8
dpd-3-gal	75	60.8	-124.4	104.1
	85	60.7	-125.7	105.7
	95	60.6	-125.2	106.7
TA	75	62.9	-119.1	104.4
	85	62.8	-120.3	105.8
	95	62.7	-121.6	107.5

According to the obtained results, the positive values of the activation enthalpies indicated the process was endothermic and that external source energy was required to raise the energy level of anthocyanins contributing to degradation yield to their state transition. Negative values of activation entropy may arise as a result of association mechanism; degrees of freedom were lost due to this activation complex formation, which meant that reacting species joined themselves from state transition during degradation process (Borsato et al., 2014). The Gibbs free energy of that activation was used to determine the spontaneity of the degradation process for all temperature tested. Positive value of ΔG^* indicated that the degradation process was not spontaneous. The obtained results are similar to the previously reported thermodynamic parameters for anthocyanins in acerola pulp (ΔH^* 71.91 to 71.79 kJ/mol; ΔS^*, -82.23 to -82.63 J/mol·K; ΔG^*, 100.53 to 101.78 kJ/mol) at 75-90°C and for blood orange, blackberry and roselle anthocyanins (ΔH^*, 34.24 to 63.11 kJ/mol; ΔS^*, -149 to - 233 J/mol·K;) at 35-90°C (Cisse et al., 2009).

Conclusion

The present study analyzed the thermal degradation of individual and total anthocyanins determined by HPLC-DAD method in strawberry and blueberry commercial juices. The results show that the degradation of strawberry and blueberry anthocyanins follows a first-order reaction kinetics and that the variation in the degradation rate constants according to the temperature obey the Arrhenius relationship.

The strawberry and blueberry anthocyanins, during heating, degraded more quickly with temperature increasing. Obtained results for activation enthalpies indicated that the thermal degradation processes were endothermic, and Gibbs free energy of activation indicated that they were nonspontaneous.

Acknowledgment

The work was supported by the Ministry of Education, Science and Technological Development of the Republic of Serbia (contract number 451-03-68/2020-14/200124).

Conflict-of-Interest Statement

None.

References

Al-Zubaidy, M.M.I., & Khalil, R.A. (2007). Kinetic and prediction studies of ascorbic acid degradation in normal and concentrate local lemon juice during storage. Food Chemistry, 101, 254-259.

Borsato, D., Galvan, D., Pereira, J.L., Orives, J.R., Angilelli, K.G., & Coppo, R.L. (2014). Kinetic and thermodynamic parameters of biodiesel oxidation with synthetic antioxidants: simplex centroid mixture design. Journal of the Brazilian Chemical Society, 25, 1984-1992.

Casati, C.B., Baeza, R., Sanchez, V., Catalano, A., Lopez, P., & Zamora, M.C. (2015). Thermal degradation kinetics of monomeric anthocyanins, colour changes and storage effect in elderberry juices. Journal of Berry Research, 5, 29-39.

Cemeroglu, B., Velioglu, S., & Isik, S. (1994). Degradation kinetics of anthocyanins in sour cherry juice and concentrate. Journal of Food Science, 59, 1216-1218.

Cisse, M., Vaillant, F., Acosta, O., Dhuique-Mayer, C., & Dornier, M. (2009). Thermal degradation kinetics of anthocyanins from blood orange, blackberry and roselle using Arrhenius, eyring and ball models. Journal of Agricultural and Food Chemistry, 57, 6285-6291.

Clifford, M.N. (2000). Anthocyanins nature, occurrence and dietary burden. Journal of the Science of the Food and Agriculture, 80, 1063-1072.

Da Silva, F.L., Escribano-Bailón, M.T., Alonso, J.J.P., Rivas-Gonzalo, J.C., & Buelga, S.C. (2007). Anthocyanin pigments in strawberry. LWT-Food Science and Technology, 40, 374-382.

Dai, J., Gupte, A., Gates, L., & Mumper, R.J. (2009). A comprehensive study of anthocyanin-containing extracts from selected blackberry cultivars: Extraction methods, stability, anticancer properties and mechanisms. Food Chemical Toxicology, 47, 837-847.

Dalisman, G., Arslan, E., & Toklucu, A.K. (2015). Kinetic analysis of anthocyanin degradation and polymeric colour formation in grape juice during heating. Czech Journal of Food Science, 33, 103-108.

Espin, J.C., Soler-Rivas, C., Wichers, H., & Garcia-Viguera, C. (2000). Anthocyanin-based natural colorants: a new source of antiradical activity for food stuff. Journal of Agricultural and Food Chemistry, 48, 1588-1592.

Gerard, V., Ay, E., Morlet-Savary, F., Graff, B., Galopin, C., Orgen, T., Mulilangi, W., & Valevee, J. (2019). Thermal and photochemical stability anthocyanins from black carrot, grape juice, and purple sweet potato in model beverages in the presence of ascorbic acid. Journal of Agricultural and Food Chemistry, 67, 5647-5660.

Hillmann, M.C.R., Burin, V.M., & Bordignon-Luiz, M.T. (2011). Thermal degradation kinetics of anthocyanins in grape juice and concentrate. International Journal of Food Science and Technology, 46, 1997-2000.

Hou, Z., Qin, P., Zhang, Y., Cui, S., & Ren, G. (2013). Identification of anthocyanins isolated from black rice (*Oryza sativa* L.) and their degradation kinetics. Food Research International, 50, 691-697.

Jakobek, L., Serugi, M., Medvidovic-Kosanovic, M., & Novak, I. (2007). Anthocyanin content and antioxidante activity of various red fruit juices. Deutsche Lebensmitlel-Rundschau, 2, 58-64.

Jimenez, N., Bohuon, P., Lima, J., Dornier, M., Vaillant, F., & Perez, A.M. (2010). Kinetics of anthocyanins degradation and browning in reconstituted blackberry juice treated at high temperatures (100-180°C). Journal of Agricultural and Food Chemistry, 58, 2314-2322.

Kechinski, C.P., Guimaraes, P.V.R., Norena, C.P.Z., Tessaro, I.C., & Marczak, L.D.F. (2010). Degradation kinetics of anthocyanin in blueberry juice during thermal treatment. Journal of Food Science, 75, C173-176.

Liu, J., Dong, N., Wang, Q., Li, J., Qian, G., Fan, H., & Zhao, G. (2014). Thermal degradation kinetics of anthocyanins from Chinese red radish (*Raphanus sativus* L.) in various juice beverages. European Food Research Technology, 238, 177-184.

Mercali, G.D., Jaeschke, D.P., Tessaro, I.C., & Marczak, L.D.F. (2013). Degradation kinetics of anthocyanins in acerola pulp: Comparison between ohmic and conventional heat treatment. Food Chemistry, 136, 853-857.

Moldovan, B., & David, L. (2020). Influence of different sweeteners on the stability of anthocyanins from cornelian cherry juice. Foods, 9, 1266, doi:10.3390/foods9091266.

Obón, J.M., Díaz-García, M.C., & Castellar, M.R. (2011). Red fruit juice quality and authenticity control by HPLC. Journal of Food Composition and Analysis, 24, 760-771.

Park, J.N., & Kim, J.H. (2017). Kinetic and thermodynamic characteristics of fractional precipitation of (+)-dihydromyricetin. Process Biochemistry, 53, 224-231.

Prior, R.L., Lazarus, S.A., Cao, G., Muccitelli, H., & Hammerstone, J.F. (2001). Identification of procyanidins and anthocyanins in blueberry and cranberries (*Vaccinium* spp.) using high performance liquid chromatography/mass spectrometry. Journal of Agricultural and Food Chemistry, 49, 1270-1276.

Stój, A., Malik, A., & Targónski, Z. (2006). Comparative analysis of anthocyanin composition of juices obtained from selected species of berry fruits. Polish Journal of Food and Nutrition Science, 15, 401-407.

Svensson, D. (2010). Effects of heat treatment and additives on the anthocyanin content in blackcurrants and its relation to colour and texture. MSc Thesis. Chalmers University of Technology.

Szaloki-Darko, L., Vegvari, G., Ladanyi, M., Ficzek, G., & Steger-Mate, M. (2015). Degradation of anthocyanin content in sour cherry juice during heat treatment. Food Technology and Biotechnology, 53, 354-360.

Turturica, M., Stanciuc, N., Muresan, C., Rapeanu, G., & Croitoru, C. (2018). Thermal degradation of plum anthocyanins: comparison of kinetics from simple to natural systems. Journal of Food Quality, 2018, Article ID 1598756, https://doi.org/10.1155/2018/1598756.

Verbeyst, L., Van Crombruggen, K., Van der Plancken, I., Hendrickx, M., & Van Loey, A. (2011). Anthocyanin degradation kinetics during thermal and high pressure treatments of raspberries. Journal of Food Engineering, 105, 513-521.

Wang, W.D., & Xu, S.Y. (2007). Degradation kinetics of anthocyanins in blackberry juice and concentrate. Journal of Food Engineering, 82, 271.

Wu, X., & Prior, R. (2005). Systematic identification and characterization of anthocyanins by HPLC–ESI-MS/MS in common fruits in the United States: Fruits and berries. Journal of Agricultural and Food Chemistry, 53, 2589-2599.

Zhao, M., Li, Y., Xu, X., Wu, J., Liao, X., & Chen, F. (2012). Degradation kinetics of malvidin-3-glucoside and malvidin-3,5-diglucoside exposed to microwave treatment. Journal of Agricultural and Food Chemistry, 61, 373-378.

Kinetičke i termodinamičke karakteristike termičke degradacije antocijanina iz komercijalnih sokova jagoda i borovnica

Milan N. Mitić[1]

1- Univerzitet u Nišu, Prirodno-matematički fakultet, Departman za hemiju, Višegradska 33, 18000 Niš, Srbija

SAŽETAK

Proučavane su termičke stabilnosti antocijana u komercijalnim sokovima jagode i borovnice u temperaturnom opsegu od 75 do 95ºC. Rezultati su pokazali da termička degradacija antocijana sledi kinetiku reakcije prvog reda. Degradacija zavisna od temperature je adekvatno modelovana prema Arrhenius-ovoj jednačini. U toku zagrevanja, antocijani u soku od jagode se brže degradiraju nego u soku od borovnice, sa energijama aktivacije od 75.99 kJ/mol i 73.27 kJ/mol. Cijanidin-3-glukozid (cyd-3-glu) je više osetljiv na termički tretman of pelargonidin-glikozida u soku od jagode. Delfinidin-glikozidi su više osetljivi na termički tretman od cijanidin-glikozida u soku od borovnice. Međutim, cyd-3-glu u soku od jagode je više osetljiv na termički tretman nego u soku od borovnice. Dobijeni rezultati za aktivacione entalpije pokazuju da je degradacioni proces endoterman, a Gibbs-ove slobodne energije aktivacije ukazuju da nije spontan.

Ključne reči: *Termička degradacija, antocijani, kinetika degradacije, sok od borovnice, sok od jagode*

Caractéristiques cinétiques et thermodynamiques de la dégradation thermique des anthocyanes des jus commerciaux de fraise et de myrtille

Milan N. Mitić[1]

1-Université de Niš, Faculté des sciences naturelles et des mathématiques, Département de chimie, Višegradska 33, 18000 Niš, Serbie

Résumé

Les stabilités thermiques des anthocyanes dans les jus commerciaux de fraises et de myrtille ont été étudiées à la température de 75° à 95°C. Les résultats ont indiqué que la dégradation thermique des anthocyanes suivait une cinétique de réaction de premier ordre. La dégradation dépendant de la température a été correctement modélisée sur l'équation d'Arrhenius. Lors du chauffage, les anthocyanes dans le jus de fraise se dégradaient plus rapidement que dans le jus de myrtille, avec des énergies d'activation de 75,99 kJ/mol et 73,27 kJ/mol, respectivement. Le cyanidine-3-glucoside (cyd-3-glu) était plus sensible au traitement thermique que les glycosides de pélargonidine dans le jus de fraise. Les glycosides de delphinidine étaient plus sensibles au traitement thermique que les glycosides de cyanidine dans le jus de myrtille. Cependant, le cyd-3-glu dans le jus de fraise était plus sensible au traitement thermique que dans le jus de myrtille. Les résultats obtenus pour les enthalpies d'activation ont indiqué que le processus de dégradation était endothermique et l'énergie d'activation libre de Gibbs a indiqué qu'elles n'étaient pas spontanées.

Mots-clés : dégradation thermique, anthocyanes, cinétique de dégradation, jus de myrtille, jus de fraise.

Кинетические и термодинамические характеристики термодеструкции антоцианов из коммерческих соков из клубники и черники

Милан Н. Митич[1]

1-Университет в Нише, Естественно-математический факультет, Кафедра химии, Вишеградска 33, 18000 Ниш, Сербия

Аннотация

Термическая стабильность антоцианов в коммерческих соках из клубники и черники исследована в диапазоне температур от 75 до 95 ° C. Результаты показали, что термическое разложение антоцианов следует кинетике реакции первого порядка. Зависимая от температуры деградация адекватно моделировалась согласно уравнению Аррениуса. Во время нагревания антоцианы в клубничном соке разлагаются быстрее, чем в черничном соке, с энергиями активации 75,99 кДж / моль и 73,27 кДж / моль. Цианидин-3-глюкозид (cyd-3-glu) более подвержен термической обработке, чем гликозиды пеларгонидина в клубничном соке. Гликозиды дельфинидина были более чувствительными к термической обработке, чем гликозиды цианидина в черничном соке. Однако cyd-3-glu в клубничном соке был более чувствительным к термической обработке, чем в черничном соке. Полученные результаты по энтальпии активаций показали, что процесс разложения был эндотермическим, а свободные энергии активации Гиббса указали, что он не произошел спонтанно.

Ключевые слова: термическое разложение, антоцианы, кинетика разложения, черничный сок, клубничный сок.

Kinetische und thermodynamische Eigenschaften des thermischen Abbaus von Anthocyanen aus kommerziellen Erdbeer- und Heidelbeersäften

Milan N. Mitić[1]

1-Universität in Niš, Fakultät für Naturwissenschaften und Mathematik, Lehrstuhl für Chemie, Višegradska 33, 18000 Niš, Serbien

Abstract

Die thermischen Stabilitäten von Anthocyanen in handelsüblichen Erdbeer- und Heidelbeersäften wurden im Temperaturbereich von 75 bis 95°C untersucht. Die Ergebnisse zeigten, dass der thermische Abbau von Anthocyanen der Reaktionskinetik erster Ordnung folgte. Der temperaturabhängige Abbau wurde anhand der Arrhenius-Gleichung angemessen modelliert. Während des Erhitzens wurden die Anthocyane im Erdbeersaft schneller abgebaut als die im Heidelbeersaft, wobei die Aktivierungsenergien 75,99 kJ/mol bzw. 73,27 kJ/mol betrugen. Cyanidin-3-glucosid (cyd-3-glu) war anfälliger für die Wärmebehandlung als Pelargonidin-Glykoside im Erdbeersaft. Delphinidin-Glykoside waren gegenüber der Wärmebehandlung empfindlicher als Cyanidin-Glykoside im Heidelbeersaft. Cyd-3-glu im Erdbeersaft war jedoch empfindlicher gegenüber der Wärmebehandlung als im Heidelbeersaft. Die erhaltenen Ergebnisse für die Aktivierungsenthalpien zeigen, dass der Abbauprozess endotherm war, und Gibbs freie Aktivierungsenergie zeigte, dass er nicht spontan waren.

Schlüsselwörter: Thermische Abbau, Anthocyane, Abbaukinetik, Heidelbeersaft, Erdbeersaft

Multi-element analysis of methanol apple peel extracts by inductively coupled plasma-optical emission spectrometry

Snežana S. Mitić[1*], Branka T. Stojanović[1], Milan N. Mitić[1], Aleksandra N. Pavlović[1], Biljana Arsić[1], Vesna Stankov-Jovanović[1]

1- University of Niš, Faculty of Sciences and Mathematics, Department of Chemistry, Višegradska 33, 18000 Niš, Serbia

Snežana S. Mitić*: mitich_s@yahoo.com (corresponding author)
Branka T. Stojanović: brankastojanovic81@gmail.com
Milan N. Mitić: milanmitic83@yahoo.com
Aleksandra N. Pavlović: petra1974@yahoo.com
Biljana Arsić**:** ba432@ymail.com
Vesna Stankov-Jovanović: sjvesna@pmf.ni.ac.rs

ABSTRACT

Apples are among the most popular fruits in the world. They are rich in phenolic compounds, pectin, sugars, and a vast number of inorganics beneficial for the human health. In this study, variations of macroelements and microelements contents of five different apple cultivars peel's methanol extracts from Serbia were investigated, using inductively coupled plasma-optical emission spectrometry and principal component analysis (PCA). Regarding macro-elements, K, Na, Ca and Mg are with the highest contents. The most abundant essential element is Fe. Among toxic and potentially toxic elements, only the presence of Al and Sr is registered. The analyzed samples are classified into five groups by PCA.

Keywords: macroelements, microelements, methanol extract, apple cultivars

Introduction

Fruit and fruit juices are a highly appreciated, tasty food and usually have exceptional nutritional qualities. However, they can be a potential source of toxic elements, some of them having an accumulative effect or leading to nutritional problems due to the low concentrations of essential elements, justifying the control of mineral composition in fruit and fruit juice (Hague et al., 2008; Tormen et al., 2011).

Trace metals are present in foods in amounts below 50 ppm and have some toxicological or nutritional significance. The elements such as Na, K, Ca, and P are essential for people, while metals like Pb, Cd, Hg, and As, are found to cause deleterious effects even at low levels of 10–50 ppm. However, Fe, Cu, and Zn are found to be necessary in certain quantities in foods, but these elements can cause ill effects when ingested in high amounts. Other non-toxic metals which are not harmful when present in amounts not exceeding 100 ppm include Al, B, Cr, Ni and Sn. The non-nutritive toxic metals which are known to have deleterious effects even in small quantities (below 100 ppm) are As, Sb, Cd, F, Pb, Hg, and Se. For this reason, the determination of both major and trace levels of metal contents in food is important for both food safety and nutritional considerations (Dehelean and Magdas, 2013).

The trace element levels of fruits and fruit juices may be expected to be influenced by the nature of the fruit, the mineral composition of the soil coming from, the composition of the irrigation water, the weather conditions, the agricultural practices such as the types and amounts of fertilizers used, and other factors (Beattie and Quoc, 2000).

The determination of minerals in fruit and their juices has been carried out using several analytical techniques, each with its advantages and disadvantages. Several methods for the determination of trace metals have been commonly conducted by flame atomic absorption spectrometry (FAAS) (Bakkali et al., 2009), graphite furnace atomic absorption spectrometry (GFAAS) (Ekinci and Koklu, 2000), inductively coupled plasma-atomic/optical emission spectroscopy (ICP-AES/OES) (Mitic et al., 2012) or inductively coupled plasma mass spectrometry. Inductively coupled plasma-optical emission spectrometry (ICP-OES) has proved to be a rapid and accurate technique for the determination of minor and major element contents in fruits (Mitić et al., 2019). ICP-OES is attractive for trace analysis, owing to the satisfactory sensitivity coupled with the advantage of simultaneous determinations of several metals at different spectral lines. ICP-OES and exploratory analysis were used for the determination of metals in apple peel, apples and apple juice (Froes et al., 2009; Stojanović et al., 2014).

The extraction of organic compounds is widely studied (Carreraetal., 2012; Kitanovic et al., 2008), while the extraction of minerals is rarely investigated (Milić et al., 2014). Various extraction techniques have been employed for recovering extractive substances from plants. Today, novel extraction

techniques such as ultrasound assisted solvent extraction are recommended because they have a greater separation efficiency of bioactive compounds in a shorter time and require a less amount of extracting solvent than the traditional ones (Wang and Weller, 2006).

Therefore, the objectives of this research were: a) to determine the mineral profile of peel of five different apple cultivars, and to examine the efficiency of different HCl concentrations in methanol for the ultrasound-assisted extraction of minerals, and b) to apply principal component analysis (PCA) to obtained results to characterize and differentiate the studied apple's cultivars.

Experimental

Fruit material

Five red apple cultivars (Pink Lady, Red Delicious, Idared, Braeburn and Modi) were purchased from local markets in Niš. All analyzed apple cultivars are frequently consumed in Serbia.

Chemicals

Ultra-scientific ICP multi-standard solutions of about 20.00±0.10 mg/L were used as a stock solution for calibration. Hydrochloric acid and methanol (Merck, Darmstadt, Germany) were both of the analytical grade.

Samples preparation

All apple samples were washed thoroughly and separately. Running tap water was employed to remove the dust and adhered particles and then the fruits were peeled off with a ceramic knife. The samples (apple peel) were later rinsed thrice with deionized water and subsequently dried in the oven at 60-80 ˚C and homogenized in a blender. Prior to ICP-OES analysis, 10 g of homogenized apple peel samples were transferred to an Erlenmeyer flask with 20 ml of solvent. After 1 h in an ultrasound bath (Bandelin SONOREX Digital 10 P, Sigma, USA), the solvent was decanted, fresh solvent added, and the process repeated five times. The extracts were combined, filtered using Whatman Filter Paper 3 Quantitative (pore size 6 μm) and made up to 50 ml with the solvent. Extracts were kept in the fridge until analysis (Stojanović et al., 2017).

The following solvents were used: methanol (%), methanol with 0.1% HCl, methanol with 1.0% HCl and methanol with 2.0% HCl for apple peel.

Instrumentation

The iCAP 6000 inductively coupled plasma-optical emission spectrometer which combines an Echelle optical design, and a change injection device (CID) solid state detector (Thermo Scientific, Cambridge, United Kingdom) was used for the analysis of the mineral contents. The blank sample involving the addition of all used reagents except sample was also processed to make corrections during calculation of elemental concentration. iTEVA operating software series was used to control all functions of the instrument. Under the optimal operating conditions for the instrument (working frequency power – 1150 W; analysis pump rate – 50 rpm; flush pump rate – 100 rpm; nebulizer gas flow – 0.7 L/min; coolant gas flow – 12 L/min and auxiliary gas flow – 0.5 L/min), analytical emission lines for each of the element were selected based on the tables of known interferences, baseline shifts and the background correction (the highest signal-to-background ratio) which was manually selected for the quantitative measurements.

Analyses were made in triplicates and the mean values are reported.

Analytical balance Mettler Toledo (Switzerland) was used to measure the mass. High purity water (conductivity 0.05 μS/cm) was obtained using MicroMed high purity water system, Thermo Electron LED GmbH (Germany).

Statistical analysis

Principal component analysis (PCA) was used as a statistical tool, and it was performed using the statistical application available for Microsoft Excel® (XLSTAT 2014.2.03, Addinsoft SARL, Paris, France).

Results and Discussion

The contents of the 17 minerals were determined in the apple peel extracts. The results, given as mean ± standard deviation, expressed as mg/dm^3 or μg/dm^{3}of extract. The determined elements were classified according to the criteria of the World Health Organization into the following groups: essential

macroelements (Na, K, Mg, Ca, and P), essential trace elements and trace elements that are probably essential (Cu, Fe, Mn, Ni, Zn, B, V), and toxic and potentially toxic elements - some possibly with essential functions at low levels (Sr, Al, Pb, As, Cd).

The present study confirmed the presence of Na, K, P, Ca and Mg in the extracts obtained from apple peels by methanol solution with different concentrations of HCl. Table 1 shows how the macroelements content change in methanol solution at different acidity. Higher values of macro-elements were detected in the methanol extract with 2% HCl. Content of minerals increased with increasing HCl concentration because of better solubility of the minerals in acidic medium.

The order is as follows: K>P>Ca>Mg>Na. The results of ICP-OES analysis show that the content of K, Mg and P varies depending on the cultivars of apple while the contents Na and Ca show the smallest differences between the different cultivars. The higher Mg, P and Ca content was found in peel of Pink Lady, while higher amounts of K and Na were detected in the peel of Braeburn.

Potassium is the element with a major content in all samples, which average concentration is 22.329 mg/dm^3 in Pink Lady, 18.197 mg/dm^3 in Red Delicious, 8.258 mg/dm^3 in Idared, 23.042 mg/dm^3 in Braeburn and 7.518 mg/dm^3 in Modi, respectively. It plays a role in the maintenance of the balance of the physical fluid system and assisting nerve functions through its role in the transmittance of nerve impulses. It is also related to the heart activity muscle contraction (Ko et al., 2008; Lambert et al., 2008; Martinez-Ballesta et al., 2010). The recommended intake for K is 3500 mg per day (Martinez-Ballesta et al., 2010). Foods of plant origin contain potassium (K) from 20 to 730 mg/100 g fresh weight, although some plants such as 'Idaho' potatoes (*S. tuberosum*), banana (*Musa* spp.) and avocado (*Persea americana*) may all present high K contents (>700 mg/100 g fresh weight) (Martinez-Ballesta et al., 2010).

Mean value of phosphorus of the five cultivars in methanol with 2% HCl is 3.031 mg/dm^3. Phosphorus (P) is present in vegetables in the range of 16.2–437 mg/100 g. The lowest content of P is shown in fruits, which are in the range 9.9–94.3 mg/100 g (Szefer and Grembecka, 2007). Phosphorus is closely related to Ca homeostasis and related to the bone and teeth formation and most of the metabolic actions in the body, including kidney functioning, cell growth and the contraction of the heart muscle (Renkemaet al., 2008; Szefer and Grembecka, 2007). The phosphorus daily recommended intake is 800–1300 mg (Martinez-Ballesta et al., 2010).

Calcium concentration ranged from 1.744 to 2.153 mg/dm^3. The concentration of calcium (Ca) in foods of plant origin shows a wide range of variation. The lower values belong to apples (*Malus domestica*), green pepper (*Capsicum annuum*) and potatoes (*Solanum tuberosum*) (<8.7 mg/100 g) and higher values are present in broccoli (*Brassica oleracea* L. var. italica) (100 mg/100 g) and spinach (*Spinacia oleracea*) (600 mg/100 g) (Martinez-Ballesta et al., 2010). Calcium is an essential mineral for

human health, participating in the biological functions of several tissues (musculoskeletal, nervous and cardiac system, bones and teeth, and parathyroid gland). In addition, Ca may act as a cofactor in enzyme reactions (fatty acid oxidation, mitochondrial carrier for ATP, *etc.*) and it is involved in the maintenance of the mineral homeostasis and physiological performance in general (Morgan, 2008; Williams, 2008). Recommended Daily Allowance (RDA) for these nutrients is set out in the wide range of 800–1300 mg/day (Martinez-Ballesta et al., 2010).

The concentration of sodium ranged from 0.813 mg/dm^3 (Idared, solvent-pure methanol) to 1.399 mg/dm^3 (Braeburn, solvent methanol with 1.0 HCl). Raw vegetables and fruit juices contain relatively low levels of sodium (Na) in the range from 2.28 to 94.0 mg/100 g and from 0.04 to 277 mg/100 g, respectively (Szefer and Grembecka, 2007). The role of Na in human physiology is related to the maintenance of the balance of physiological fluids (blood pressure, kidney function, nerve and muscle functions) (Hall, 2003; Sobotka et al., 2008).

It was found that the average contents of Mg found in five varieties of the apple peel samples were 1.860, 1.540, 0.415, 1.072, 0.559 mg/dm^3, respectively. Magnesium (Mg) has a strong presence in vegetable foods and also shows a critical role in the maintenance of human health through the diet. Vegetables and fruits contain, in general, Mg^{2+} in the range of 5.5–191 mg/100 g fresh weight, and the recommended daily intake is 200-400 mg (Martinez-Ballesta et al., 2010). This essential mineral acts as a Ca antagonist on vascular smooth muscle tone and on post-receptor insulin signaling. It has also been related to energy metabolism, release of neurotransmitters and endothelial cell functions (Bo and Pisu, 2008).

There is no literature available for the comparison with the current report as there are no studies on the evaluation of mineral content in methanol extract of apple peels. Nevertheless, several studies have evaluated the mineral composition of apple juice and the methanol extracts of plants. High contributions of K, Mg, and Na were observed in the infusions obtained from *Melissa officinalis* (852.3, 80.0, and 16.2 mg/L, respectively) (Petenatti et al., 2011). Also, high contribution of K, Mg, Ca, Na and P was observed in the methanol extracts of *Semecarpus anacardium* leaf (587.7, 44.5, 8.7, 47.0 and 10.4, respectively) (Pednekar and Raman, 2013). In apple juice the concentration ranges are the following for the major elements: 1.12–196.11 mg/L for Na, 13.07–140.42 mg/L for Mg, 52.52–642.34 mg/L for K and 21.54–338.35 mg/L for Ca (Dehelean and Magdas, 2013). The low contents of mineral in methanol extracts of apple peels are results of the low solubility of minerals in methanol.

Table 1. The content of essential macroelements (mean±SD[a] (mg/dm^3)) in apple peel extracts

Sample/ % HCl	K	Mg	Na	P	Ca
E1, 0.0	6.990±0.062	0.552±0.016	1.124±0.027	1.303±0.020	1.996±0.022
E1, 0.1	26.476±0.221	2.284±0.030	1.150±0.015	3.252±0.047	2.070±0.023
E1, 1.0	27.173±0.077	2.313±0.049	1.129±0.023	3.344±0.039	2.145±0.022
E1, 2.0	28.677±0.188	2.291±0.056	1.132±0.014	4.928±0.075	2.153±0.027
E2, 0.0	16.609±0.108	1.272±0.025	0.973±0.025	1.195±0.028	1.744±0.021
E2, 0.1	18.427±0.140	1.628±0.028	1.075±0.019	1.266±0.018	1.751±0.032
E2, 1.0	18.583±0.153	1.616±0.032	1.147±0.06	2.044±0.039	1.766±0.021
E2, 2.0	19.169±0.100	1.645±0.024	1.219±0.027	2.193±0.036	1.774±0.025
E3, 0.0	5.269±0.076	0.325±0.008	0.813±0.033	1.181±0.003	1.896±0.026
E3, 0.1	6.428±0.063	0.421±0.012	0.863±0.005	2.806±0.003	1.910±0.039
E3, 1.0	10.525±0.093	0.438±0.005	0.851±0.004	2.810±0.008	1.930±0.042
E3, 2.0	10.811±0.106	0.475±0.003	0.863±0.004	3.052±0.013	1.932±0.037
E4, 0,0	20.083±0.144	0.604±0.019	1.257±0.003	1.072±0.002	1.974±0.024
E4, 0.1	20.448±0.376	0.688±0.021	1.214±0.013	1.668±0.006	1.992±0.033
E4, 1.0	23.724±0.305	1.285±0.022	1.399±0.006	1.967±0.009	2.069±0.034
E4, 2,0	27.911±0.426	1.710±0.043	1.393±0.006	2.093±0.035	2.055±0.017
E5, 0.0	4.347±0.065	0.353±0.004	1.049±0.005	2.030±0.010	1.850±0.021
E5, 0.1	7.738±0.094	0.431±0.008	1.232±0.005	1.167±0.010	1.853±0.024
E5, 1.0	9.233±0.057	0.671±0.008	1.231±0.008	2.147±0.018	1.935±0.025
E5, 2.0	8.754±0.081	0.782±0.011	1.255±0.005	2.889±0.010	1.949±0.007

[a]SD-standard deviation for triplicate determination; E1 - Pink Lady; E2 - Red Delicious; E3 - Idared; E4 - Braeburn; E5 – Modi

The results of microelements are shown in Table 2. No significant variations were found for Zn, Ni, B, V and Cu, while Mn and Fe ranged from 3.2 to 43.6 μg/dm^3, 31.6 to 87.6 μg/dm^3 in methanol extracts with different HCl concentrations. In this study it was determined the lower contents for Fe, Mn, Cu, Zn and Ni compared to the apple juice (Dehelean and Magdas, 2013). The literature data showed the low extraction coefficients of these minerals in methanol solution (Micić et al., 2013).

The major microelements found in the methanol extract of apple peel were Fe (Table 2) with mean concentration of 60.8 μg/dm^3 in Pink Lady, 71.3 μg/dm^3 in Red Delicious, 72.5 μg/dm^3 in Idared, 67.5 μg/dm^3 in Braeburn and 83.2 μg/dm^3 in Modi, followed by Mn (34.65, 10.7, 18.4, 22.3, 17.4 μg/dm^3, respectively) and V (6.9, 5.9, 8.9, 7.6, 9.2 μg/dm^3, respectively). The other essential microelements determined (Ni, Zn, B, Cu) exist in much lower concentrations. Iron (Fe) contents in vegetables and fruits are low, varying from 0.13 to 3.01 mg/100 g. The iron in foods of plant origin is mostly present in the form of insoluble complexes of Fe^{3+} with phytic acid, phosphates, oxalates and carbonates. However, the bioavailability of the Fe present in foods is less than 8%. The major function of Fe is related to the synthesis of hemoglobin and myoglobin (Huskisson et al., 2007). The recommended intake of iron is 8–18 mg/day (Martinez-Ballesta et al., 2010). Fruits and vegetables are also characterized by a low content of manganese (Mn). Vegetables contain Mn in the range 0.01–0.078 mg/100 g and fruits 0.01–0.66 mg/100 g (Szefer and Grembecka, 2007). The recommended intake of Mn is 2 mg/day (Martinez-Ballesta et al., 2010), and its main physiological function is being an enzyme cofactor involved in antioxidant reactions related to the glucose metabolism (metabolism of carbohydrates and gluconeogenesis) (Huskisson et al., 2007).

Table 2. The content of essential trace elements (mean±SD[a] (μg/dm^3)) in apple peel extracts

Sample/ % HCl	Mn	Ni	V	Zn	B	Cu	Fe
E1, 0.0	16.8±0.9	0.8±0.0	6.2±0.4	1.6±0.0	0.4±0.0	1.6±0.0	31.6±1.5
E1, 0.1	37.6±2.2	0.4±0.0	7.0±0.4	1.6±0.0	0.4±0.0	1.8±0.0	52.6±1.3
E1, 1.0	40.6±2.0	0.2±0.0	7.2±0.4	1.8±0.0	0.6±0.0	1.8±0.0	79.8±0.8
E1, 2.0	43.6±2.1	2.0±0.0	7.2±0.4	1.8±0.0	0.6±0.0	1.8±0.0	79.2±0.6
E2, 0.0	4.8±0.4	1.6±0.0	5.6±0.4	1.4±0.0	0.4±0.0	1.4±0.0	57.0±1.0
E2, 0.1	8.8±0.6	1.6±0.0	5.8±0.6	1.4±0.0	0.4±0.0	1.4±0.0	57.8±2.0
E2, 1.0	14.6±0.4	1.8±0.0	5.8±0.4	1.6±0.0	0.4±0.0	1.4±0.0	82.8±1.8
E2, 2.0	14.6±0.2	1.4±0.0	6.4±0.6	1.6±0.0	0.4±0.0	1.4±0.0	87.6±1.4
E3, 0.0	3.2±0.2	1.4±0.0	8.6±0.8	1.4±0.0	0.2±0.0	1.2±0.0	63.8±1.6
E3, 0.1	23.4±2.0	1.6±0.0	9.2±0.6	1.4±0.0	0.4±0.0	1.4±0.0	70.8±2.0
E3, 1.0	23.2±2.0	1.6±0.0	9.4±0.6	1.4±0.0	0.4±0.0	1.4±0.0	77.2±2.0
E3, 2.0	24.0±0.6	1.4±0.0	8.4±0.4	1.4±0.0	0.4±0.0	1.4±0.0	78.2±1.6
E4, 0,0	16.2±0.4	1.4±0.0	7.4±0.4	1.4±0.0	0.4±0.0	1.4±0.0	67.2±1.9
E4, 0.1	23.6±0.2	1.4±0.0	7.6±0.6	1.4±0.0	0.6±0.0	1.4±0.0	51.2±1.8
E4, 1.0	24.6±0.4	1.2±0.0	8.0±0.6	1.4±0.0	0.6±0.0	1.6±0.0	77.4±0.6

E4, 2,0	25.0±0.6	1.4±0.0	7.6±0.4	1.4±0.0	0.6±0.0	1.6±0.0	74.4±0.6
E5, 0.0	13.8±0.4	1.0±0.0	8.8±0.8	1.4±0.0	0.4±0.0	1.6±0.0	79.0±0.6
E5, 0.1	15.8±0.6	1.2±0.0	9.6±0.8	1.4±0.0	0.4±0.0	1.6±0.0	75.8±0.6
E5, 1.0	20.0±0.4	1.2±0.0	9.2±0.8	1.4±0.0	0.4±0.0	1.8±0.0	81.0±0.6
E5, 2.0	20.0±0.4	1.0±0.0	9.4±0.6	1.4±0.0	0.4±0.0	1.6±0.0	97.2±0.6

E1 -Pink Lady; E2 -Red Delicious; E3 -Idared; E4 -Braeburn; E5 – Modi

The most toxic heavy metal loadings (Pb, As and Cd) of the samples are not detected, which suggest the absence of these pollutants in the vegetation zone.

According to Lopez et al. (2002) concentration range of Al in fruit juices was 49.3 to 1144 μg/dm^3. Also, a high level of aluminum was reported by Savić et al. (2015) who detected the aluminum content in the range of 0.29−2.1 mg/L in orange juice. In this study, the recorded amount of aluminum was in the range of 0.8 - 1.2 μ/L (Table 3). Aluminum is known as an extremely pro-inflammatory, pathological and genotoxic element which is particularly deleterious to the normal homeostatic operation of brain cells. But fortunately, aluminum insolubility at biological pH and highly effective epithelial, gastrointestinal and blood–brain barriers prevent this ubiquitous neurotoxin from accessing human biological compartments where it appears to contribute to inflammatory degeneration and pathogenic gene expression programs highly characteristic of the Alzheimer's disease (AD) (Savić et al., 2015; Velimirović et al., 2013).

Strontium belongs to the group of trace minerals and it has a similar biochemical pathway as Ca in the vertebrate body. Strontium has the role in increasing bone deposition, as well as in reducing bone resorption. In our study, the detected amount of strontium was in the range of 6.6 – 9.2 μg/L (Table 3). The obtained concentration of strontium was lower when compared to the results reported by Savić et al. (2015) where the content of strontium in the range of 0.05 – 0.46 mg/L was recorded in orange juices.

Table 3. The content of toxic and potentially toxic elements (mean±SD^a (μg/dm^3 w.w.)) in the apple peel

Sample/% HCl	**Sr**	**Al**	**Pb**	**As**	**Cd**
E1, 0.0	8.6±0.0	1.0±0.0	nd	nd	nd
E1, 0.1	8.4±0.2	1.0±0.0	nd	nd	nd
E1, 1.0	8.8±0.2	1.0±0.0	nd	nd	nd
E1, 2.0	9.2±0.4	1.0±0.0	nd	nd	nd
E2, 0.0	7.6±0.2	0.8±0.0	nd	nd	nd

E2, 0.1	7.8±0.4	0.8±0.0	nd	nd	nd
E2, 1.0	8.6±0.4	1.0±0.0	nd	nd	nd
E2, 2.0	8.4±0.4	1.0±0.0	nd	nd	nd
E3, 0.0	8.2±0.8	0.8±0.0	nd	nd	nd
E3, 0.1	8.4±0.6	0.8±0.0	nd	nd	nd
E3, 1.0	8.8±0.8	0.8±0.0	nd	nd	nd
E3, 2.0	9.0±0.4	0.8±0.0	nd	nd	nd
E4, 0,0	7.0±0.6	1.0±0.0	nd	nd	nd
E4, 0.1	7.4±0.4	1.2±0.0	nd	nd	nd
E4, 1.0	7.6±0.6	1.2±0.0	nd	nd	nd
E4, 2,0	8.0±0.2	1.2±0.0	nd	nd	nd
E5, 0.0	6.6±0.2	1.2±0.0	nd	nd	nd
E5, 0.1	6.8±0.6	1.2±0.0	nd	nd	nd
E5, 1.0	7.4±0.4	1.2±0.0	nd	nd	nd
E5, 2.0	7.2±0.06	1.2±0.0	nd	nd	nd

E1 -Pink Lady; E2 -Red Delicious; E3 -Idared; E4 -Braeburn; E5 – Modi

For better illustration, PCA was conducted to evaluate the metal content in the extract of apple peel samples.

Based on the data obtained from the determination of the selected elements in the extract of the apple peels (Tables 1, 2 and 3), PCA was used for the possible similarities/differences of apple peel samples. PCA is a useful tool, because one of its advantages is a reduction of the number of variables of the experimental data and extraction of a small number of latent factors (principal components, PCAs) for analyzing relationships among the observed variables (Horel, 1981; Horel, 1984). According to such plot, it is possible to classify samples by their element distribution. The starting point for the PCA calculations was a matrix of data with dimensions n x p, where n is number of cases (rows) and p is the number of variables (columns). In matrix, methanol extracts of apple peel samples (Pink Lady, Red Delicious, Idared, Braeburn and Modi) with different acid concentrations were used as rows. Columns were the results of selected elements analysis of apple samples. As a result of PCA analysis, 14 new variables were obtained which were characterized by Eigenvalues.

Performed statistics with Pearson correlation matrix on apple peel samples based on selected elements content shows that there is a high positive correlation between the quantity of potassium and magnesium (0.868), zinc and magnesium (0.722), phosphorus and manganese (0.755), calcium and

manganese (0.733), and aluminum and sodium (0.760); medium positive correlation between the quantity of potassium and manganese (0.648), sodium and potassium (0.552), zinc and potassium (0.523), boron and potassium (0.695), calcium and potassium (0.493), manganese and potassium (0.569), phosphorus and magnesium (0.468), boron and magnesium (0.477), copper and magnesium (0.490), strontium and manganese (0.545), zinc and manganese (0.643), boron and manganese (0.615), copper and manganese (0.480), boron and sodium (0.511), copper and sodium (0.525), strontium and phosphorus (0.568), zinc and phosphorus (0.612), calcium and phosphorus (0.558), copper and phosphorus (0.570), zinc and strontium (0.616), copper and zinc (0.513), aluminum and copper (0.634), calcium and boron (0.696), and copper and calcium (0.631); medium negative correlation between the quantity of vanadium and potassium (-0.525), vanadium and magnesium (-0.600), copper and nickel (-0.533), and aluminum and strontium (-0.528).

The number of factors represents the total number of variables used in the dataset. Eigenvalues for the first five factors are higher (5.451, 2.851, 1.912, 1.360 and 1.066, respectively) compared to values for the rest of factors. So, five factors must be used to explain the obtained variabilities (38.94 %, 20.36 %, 13.66 %, 9.72 % and 7.61 %) (Figure 1).

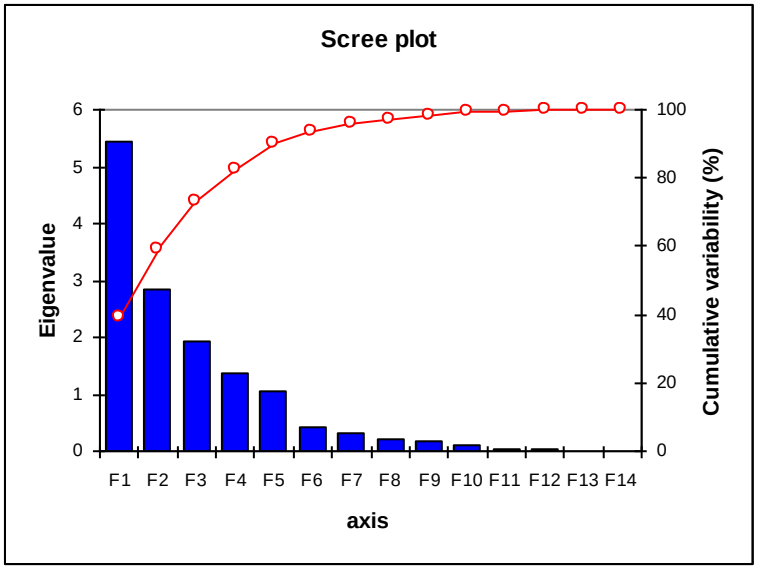

Figure 1. The importance of factors and values of cumulative variabilities

Observation plots based on the content of selected elements are represented in Figure 2.

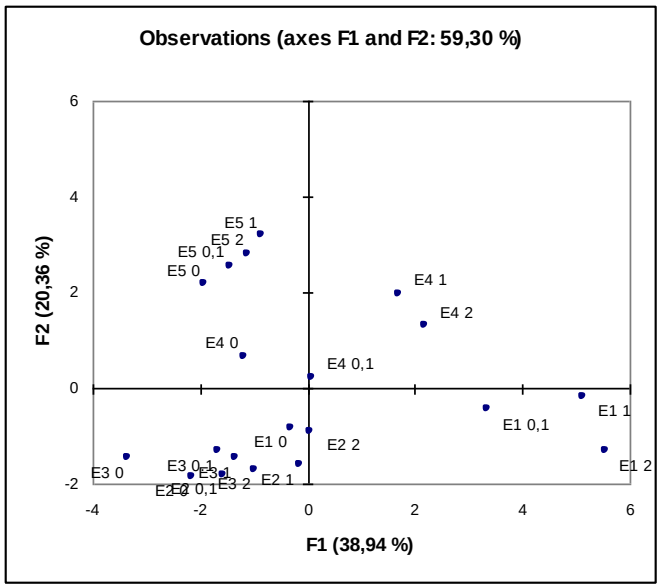
Observations (axes F1 and F2: 59,30 %)
F2 (20,36 %)
F1 (38,94 %)
E5 1
E5 2
E5 0,1
E5 0
E4 1
E4 2
E4 0
E4 0,1
E1 1
E1 0,1
E1 0
E2 2
E1 2
E3 0
E3 0,1
E2 1
E3 2

a)

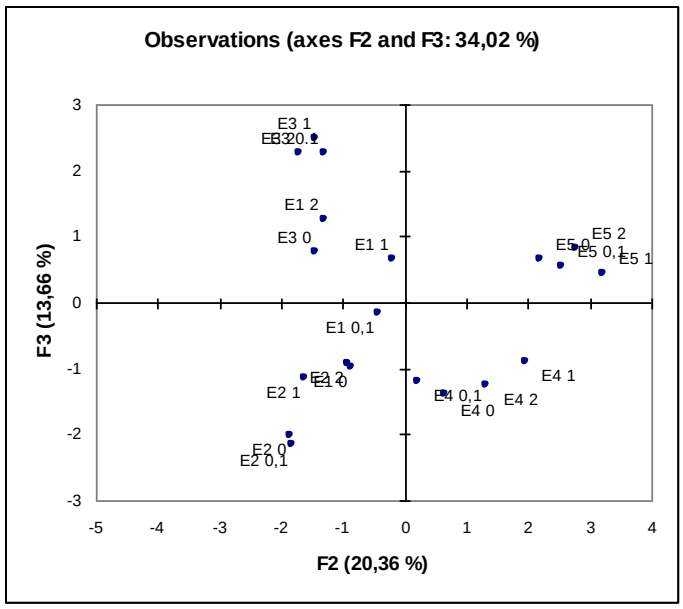
Observations (axes F2 and F3: 34,02 %)
F3 (13,66 %)
F2 (20,36 %)
E3 1
E1 2
E3 0
E1 1
E5 2
E5 0,1
E5 1
E1 0,1
E2 2
E2 1
E4 1
E4 0,1
E4 2
E4 0
E2 0
E2 0,1

b)

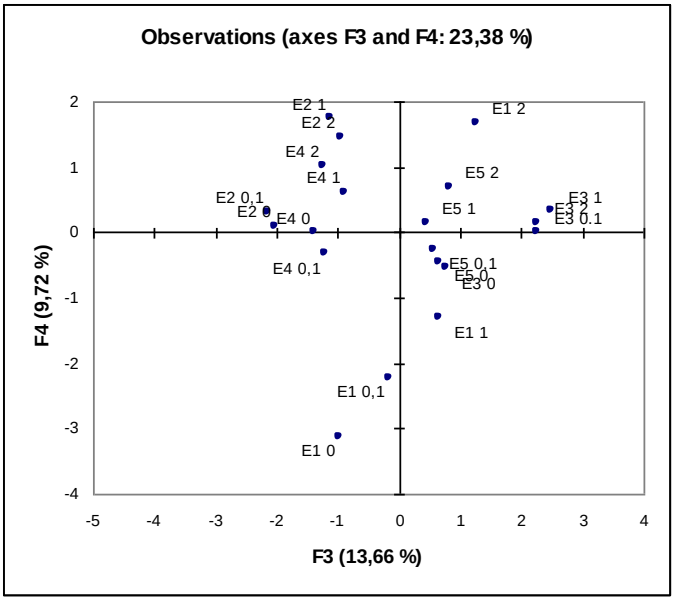

c)

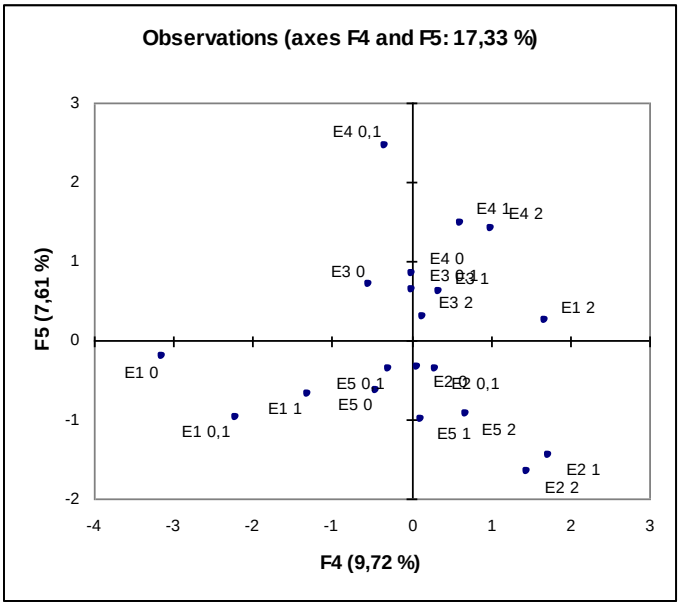

d)

Figure 2. Principal component score plots a) (F1 and F2), b) (F2 and F3), c) (F3 and F4), and d) (F4 and F5) of the studied plant samples based on the content of selected elements

From Figure 2a, it is visible that high content of potassium is present in the extract of apple peel samples on the right side of the plot and low on the left side of the plot. Also, it can be concluded that high content of magnesium is present in extracts of apple peel samples in the upper half of the plot and

low on the opposite side of the plot. Similarly, Figure 2b shows high content of magnesium on the right side of the plot, and low on the left side of the plot. High content of manganese is present in the extract of the apple peel samples in the upper half of the plot, and low on the opposite side of the plot. Figure 2c confirms the information of the low and high quantity of manganese, but it also shows the quantity of sodium; high content of sodium is present in the extracts of the apple peel samples in the upper half of the plot and low on the opposite side of the plot. High content of sodium is present in the extract of the apple peel samples on the right side of the plot and low on the left side of the plot (Figure 2d). High content of nickel is present in extract of the apple peel samples in the upper half of the plot and low on the opposite side of the plot (Figure 2d).

Conclusion

The mineral profiles of peel of five different apple cultivars were determined, and the examination of the efficiency of different HCl concentrations in methanol for their ultrasound-assisted extraction was performed. Principal component analysis (PCA) was applied to the results obtained from the ICP-OES analysis to characterize and differentiate the studied cultivars of apple. The contents of the 17 minerals were investigated in the apple peel extracts: macroelements (K, Mg, Na, P, Ca), essential trace elements (Mn, Ni, V, Zn, B, Cu, Fe), and toxic and potentially toxic elements (Sr, Al, Pb, As, Cd). Lead, arsenic, and cadmium were not detected. Reasonable grouping of apple samples was obtained using PCA.

Acknowledgment

The work was supported by the Ministry of Education, Science and Technological Development of the Republic of Serbia (contract number 451-03-68/2020-14/200124).

Conflict-of-Interest Statement

None.

References

Addinsoft, 2014. XLSTAT 2014: Data analysis and statistical solution for Microsoft Excel. Addinsoft, Paris.

Bakkali, K., Martos, N.R., Souhail, B., & Ballesteros, E. (2009). Characterization of trace metals in vegetables by graphite furnace atomic absorption spectrometry after closed vessel microwave digestion. Food Chemistry, 116, 590–594.

Beattie, J.K., & Quoc, T.N. (2000). Manganese in pineapplejuices. Food Chemistry, 68, 37-39.

Bo S., & Pisu E. (2008). Role of dietary magnesium in cardiovascular disease prevention, insulin sensitivity and diabetes. Current Opinion in Lipidology, 19, 50–56.

Carrera, C., Ruiz-Rodríguez, A., Palma, M. & Barroso, C.G. (2012). Ultrasound assisted extraction of phenolic compounds from grapes. Analytica Chimica Acta, 732, 100-104.

Dehelean, A., & Magdas, D.A. (2013). Analysis of mineral and heavy metal content of some commercial fruit juices by inductively coupled plasma mass spectrometry. The Scientific World Journal, http://dx.doi.org/10.1155/2013/215423

Ekinci, C., & Koklu, U. (2000). Determination of vanadium, manganese, silver and lead by graphite furnace atomic absorption spectrometry after preconcentration on silica-gel modified with 3-aminopropyltriethoxysilane. Spectrochimica Acta Part B, 55, 1491-1495.

Froes, R.E.S., Neto, W.B., Silva, N.O.C., Naveira, R.L.P., Nascentes, C.C., & Silva, J.B.B. (2009). Multivariate optimization by exploratory analysis applied to the determination of microelements in fruit juice by inductively coupled plasma optical emission spectrometry. Spectrochimica Acta Part B: Atomic Spectroscopy, 64, 619-622.

Hague, T., Petroczi, A., Andrew, P.L.R., Barker, J., & Naughton, D.P. (2008). Determination of metal ion content of beverages and estimation of target hazard quotients: a comparative study. Chemistry Central Journal, 2, 1–9.

Hall J.E. (2003). The kidney, hypertension, and obesity. Hypertension, 41, 625–633.

Horel, J. D. (1981). A rotated principal component analysis of the interannual variability of the northern hemisphere 500 mb height field. Monthly Weather Review, 109, 2080-2092.

Horel, J.D. (1984). Complex principal component analysis: theory and examples. Journal of Climate and Applied Meteorology, 23, 1660-1673.

Huskisson E., Maggini S., & Ruf M. (2007). The role of vitamins and minerals in energy metabolism and well-being. Journal of International Medical Research, 35, 277–289.

Kitanovic, S., Milenovic, D., &Veljkovic, V.B. (2008). Empirical kinetic models for the resinoid extraction from aerial parts of St John's Wort (*Hypericum perforatum* L.). Biochemical Engineering Journal, 41, 1–11

Ko, E.A., Han, J., Jung, I.D., & Park W.S. (2008). Physiological roles of K^+channels in vascular smooth muscle cells. Journal of Smooth Muscle Research, 44, 65–81.

Lambert, I.H., Hoffmann, E.K., & Pedersen S.F. (2008). Cell volume regulation: Physiology and pathophysiology. Acta Physiologica 194, 255–282.

López, F.F., Cabrera, C., Lorenzo, M.L., & López, M.C. (2002). Aluminium content of drinking waters, fruit juices and soft drinks: contribution to dietary intake. Science of the Total Environment, 292, 205-213.

Martinez-Ballesta, M.C., Dominguez-Perles, R., Moreno, D.A., Muries, B., Alcaraz-Lopez, C., Bastias, E., Garcia-Viguera, C., & Carvajal, M. (2010). Minerals in plant food: effect of agricultural practices and role in human health. A review. Agronomy for Sustainable Development, 30, 295–309.

Mićić, R.J., Dimitrijević, D.S., Kostić, D.A., Stojanović, G.S., Mitić, S.S., Mitić, M.N., Pavlović, A.N., & Ranđelović, S.S. (2013). Content of heavy metals in mulberry fruits and their extracts-correlation analysis. American Journal of Analytical Chemistry, 4, 674-682.

Milić, P.S., Rajković, K.M., Bekrić, D.M., Stamenković, O.S., & Veljković, V.B. (2014). The kinetic and thermodynamic analysis of ultrasound-extraction of minerals from aerial parts of white lady's bedstraw (*Galium mollugo* L.). Chemical Engineering Research and Design, 92, 1399–1409.

Mitić, S., Stojanović, B., Tošić, S., Pavlović, A., Kostić, D., & Mitić, M. (2019). Comparative study on minerals in peel and pulp of peach (*Prunus persica* L.) fruit. Revista de Chimie, 70, 2281-2285.

Mitic, S.S., Obradovic, M.V., Mitic, M.N., Kostic, D.A., Pavlovic, A.N., Tosic, S.B., & Stojkovic, M.D. (2012). Elemental composition of various sour cherry and table grape cultivars using inductively coupled plasma atomic emission spectrometry method (ICP-OES). Food Analytical Methods, 5, 279–286.

Morgan K.T. (2008). Nutritional determinants of bone health. Journal of Nutrition for the Elderly, 27, 3–27.

Pednekar, P.A., & Raman, B. (2013). Multielement determination in methanolic Soxhlet leaf extract of *Semecarpus anacardium* (Linn. F.) by ICP-AES technique. Asian Journal of Pharmaceutical and Clinical Research, 6, 132-137.

Petenatti, M.E., Petenatti, E.M., Del Vitto, L.A., Téves, M.R.T., Caffini, N.O.K., Marchevsky, E.J., & Pellerano, R.G. (2011). Evaluation of macro and microminerals in crude drugs and infusions of five herbs widely used as sedatives. Revista Brasileira de Farmacognosia Brazilian Journal of Pharmacognosy, 21, 1144-1149.

Renkema, K.Y., Alexander, R.T., Bindels, R.J., & Hoenderop, J.G. (2008). Calcium and phosphate homeostasis: Concerted interplay of newregulators. Annals of Medicine, 40, 82–91.

Savić, S.R., Petrović, S.M., Stamenković, J.J., & Petronijević, Ž.B. (2015). The presence of minerals in clear orange juices. Advanced technologies, 4, 71-78.

Sobotka L., Allison S., & Stanga, Z. (2008). Basics in clinical nutrition: Water and electrolytes in health and disease. e-SPEN, 3, 259–266.

Stojanović, B.T., Mitić, S.S., Mitić, M.N., Paunović, D.Đ., Arsić, B.B., & Stojanović, G.S. (2014). The multielement analysis of the apple peel using the ICP-OES method. Advanced technologies, 3, 96-104.

Stojanović, B.T., Mitić, S.S., Stojanović, G.S., Mitić, M.N., Kostić, D.A., Paunović, D.Đ., Arsić, B.B., & Pavlović, A.N. (2017). Phenolic profiles and metal ions analyses of pulp and peel of fruits and seeds of quince (*Cydonia oblonga* Mill.). Food Chemistry, 232, 466-475.

Szefer, P., & Grembecka M. (2007). Mineral components in food crops, beverages, luxury food, species, and dietary food, in: Szefer, P., Nriagu, J.O. (Eds.), Chemical and functional properties of food components series, CRC Press, Taylor and Francis Group, New York, USA, pp. 231–322.

Tormen, L., Torres, D.P., Dittert, I.M., Araujo, R.G.O., Frescura, V.L.A., & Curtius, A.J. (2011). Rapid assessment of metal contamination in commercial fruit juices by inductively coupled mass spectrometry after a simple dilution. Journal of Food Composition and Analysis, 24, 95–102.

Velimirović, D., Mitić, S., Tosić, S., Pavlović, A., & Stojković, M. (2013). Determination of the content of some trace elements in particular samples of grains, flours and breads by ICP-OES. Oxidation Communications, 35, 160 – 170.

Wang, L., & Weller, C.L. (2006). Recent advances in extraction of nutraceuticals from plants. Trends in Food Science & Technology, 17, 300–312.

Williams, F.H. (2008). Neuromuscular complications of nutritional deficiencies. Physical Medicine and Rehabilitation Clinics of North America, 19, 125–148.

Analiza više elemenata metanolskih ekstrakata kore jabuke induktivno spregnutom plazmom-optičkom emisionom spektrometrijom

Snežana S. Mitić[1], Branka T. Stojanović[1], Milan N. Mitić[1], Aleksandra N. Pavlović[1], Biljana Arsić[1], Vesna Stankov-Jovanović[1]

1- Univerzitet u Nišu, Prirodno-matematički fakultet, Departman za hemiju, Višegradska 33, 18000 Niš, Srbija

Sažetak

Jabuka spada u jedno od najpopularnijih voća u svetu. Bogate su fenolnim jedinjenjima, pektinom, šećerima, i ogromnim brojem neorganskih jedinjenja korisnih za ljudsko zdravlje. U ovom radu su proučavane varijacije u mineralnom sastavu između različitih metanolnih ekstrakata kore pet različitih sorti jabuka poreklom iz Srbije, korišćenjem induktivno spregnute plazme-optički emisione spektrometrije i analize glavne komponente (engl. PCA). K, Na, Ca i Mg su metali sa najvišim sadržajima. Među esencijalnim elementima, Fe je najzastupljeniji. Među toksičnim i potencijalno toksičnim elementima, jedino je utvrđeno prisustvo Al and Sr. Analizirani uzorci su klasifikovani u pet grupa korišćenjem PCA.

Ključne reči: makro-elementi, mikro-elementi, metanolni ekstrakt, sorte jabuka

Analyse multi-élément d'extraits de peau de pomme au méthanol par spectrométrie d'émission optique à plasma couplage inductif

Snežana S. Mitić[1], Branka T. Stojanović[1], Milan N. Mitić[1], Aleksandra N. Pavlović[1], Biljana Arsić[1], Vesna Stankov-Jovanović[1]

1-Université de Niš, Faculté des sciences naturelles et des mathématiques, Département de chimie, Višegradska 33, 18000 Niš, Serbie

RÉSUMÉ

Les pommes se trouvent parmi les fruits les plus appréciés au monde. Ils sont riches en composés phénoliques, en pectine, en sucres et en un grand nombre de substances inorganiques bénéfiques pour la santé humaine. Dans cette étude, les variations des teneurs en macro et micro éléments de cinq extraits de méthanol de la peau de cinq cultivars de pommes différents de Serbie ont été étudiées, en utilisant la spectrométrie d'émission optique plasma couplée inductivement et par le biais de l'analyse en composants principaux (ACP). En ce qui concerne les macro-éléments, K, Na, Ca et Mg sont les plus riches. L'élément essentiel le plus abondant est le Fe. Parmi les éléments toxiques et potentiellement toxiques, seule la présence d'Al et de Sr est enregistrée. Les échantillons analysés sont classés en cinq groupes par ACP.

Mots-clés : macroéléments, microéléments, extrait de méthanol, cultivars de pomme.

Многоэлементный анализ метанольных экстрактов кожуры яблони методом оптической эмиссионной спектрометрии с индуктивно связанной плазмой

Снежана С. Митич[1], Бранка Т. Стоянович[1], Милан Н. Митич[1], Александра Н. Павлович[1], Биляна Арсич[1], Весна Станков-Йованович[1]

1-Университет в Нише, Естественно-математический факультет, Кафедра химии, Вишеградска 33, 18000 Ниш, Сербия

АННОТАЦИЯ

Яблоки - одни из самых популярных фруктов в мире. Они богаты фенольными соединениями, пектином, сахарами и огромным количеством неорганических веществ, полезных для здоровья человека. В этом исследовании были рассмотрены вариации содержания макро и микроэлементов в метанольных экстрактах кожуры пяти различных сортов яблони из Сербии с использованием оптической эмиссионной спектрометрии с индуктивно связанной плазмой и анализа главных компонентов (PCA). Что касается макроэлементов, то наибольшее их содержание имеют K, Na, Ca и Mg. Самый распространенный незаменимый элемент - Fe. Среди токсичных и потенциально токсичных элементов регистрируется только присутствие Al и Sr. Анализируемые образцы разделены на пять групп с помощью PCA.

Ключевые слова: макроэлементы, микроэлементы, метанольный экстракт, сорта яблони.

Mehrelementanalyse von Methanol-Apfelschalenextrakten mittels induktiv gekoppelter Plasma - optischer Emissionsspektrometrie

Snežana S. Mitic[1], Branka T. Stojanovic[1], Milan N. Mitic[1], Aleksandra N. Pavlovic[1], Biljana Arsic[1], Vesna Stankov-Jovanovic[1]

1-Universität in Niš, Fakultät für Naturwissenschaften und Mathematik, Lehrstuhl für Chemie, Višegradska 33, 18000 Niš, Serbien

ABSTRACT

Äpfel gehören zu den beliebtesten Früchten der Welt. Sie sind reich an phenolischen Verbindungen, Pektin, Zucker und einer großen Anzahl von anorganischen Stoffen, die für die menschliche Gesundheit von Vorteil sind. In dieser Arbeit wurden die Variationen des Gehalts an Makro- und Mikroelementen in Methanolextrakten aus den Schalen von fünf verschiedenen Apfelsorten aus Serbien mit Hilfe von induktiv gekoppelter Plasma - optischer Emissionsspektrometrie und Hauptkomponentenanalyse (PCA) untersucht. Bei den Makroelementen sind K, Na, Ca und Mg mit den höchsten Gehalten vertreten. Das am häufigsten vorkommende essentielle Element ist Fe. Unter den toxischen und potenziell toxischen Elementen sind nur Al und Sr zu finden. Die analysierten Proben werden durch PCA in fünf Gruppen klassifiziert.

Schlüsselwörter: Makroelemente, Mikroelemente, Methanolextrakt, Apfelsorten

Chemia Naissensis, Vol 3, Issue 2, RESEARCH ARTICLE, 89-95

Comparative analysis of HPLC profiles and antioxidant activity of *Artemisia alba* Turra from two habitats in Serbia

Jovana D. Ickovski[1*], Milan N. Mitić[1], Milan B. Stojković[1], Gordana S. Stojanović[1]

1-Department of Chemistry, Faculty of Science and Mathematics, University of Niš, Višegradska 33, 18000 Niš, Serbia

Jovana D. Ickovski: jovana.ickovski@pmf.edu.rs
Milan N. Mitić: milan.mitic1@pmf.edu.rs
Milan B. Stojković: milan.stojkovic@pmf.edu.rs
Gordana S. Stojanović: gocast@pmf.ni.ac.rs

ABSTRACT

Artemisia alba Turra was collected at the blooming stage on two different locations in Serbia, Mojinci and Rosomač. Antioxidant activity and HPLC profiles of their methanolic extracts were determined and compared. Flavonoid compounds found in both samples were rutin, apigenin glucoside, quercetin, luteolin, kaempferol and apigenin, while detected phenolic acids were chlorogenic acid, *p*-coumaric acid, cynarine and rosmarinic acid. The only observed qualitative difference was related to the presence of vanillic acid. Extract of *A. alba* from Rosomač was richer in phenolic compounds and flavonoids than *A. alba* from Mojinci. The extract of *A. alba* from Rosomač also possessed higher antioxidant capacity than *A. alba* from Mojinci, which was especially noticed in the 2,2-diphenyl-1-picrylhydrazyl assay. Only the results for the ferric ion reducing antioxidant power assay were higher for extract of *A. alba* from Mojinci, than for the extract of *A. alba* from Rosomač.

Keywords: Artemisia alba, methanolic extract, HPLC, antioxidant activity

Introduction

The genus *Artemisia* L. is one of the largest and most widely distributed over all continents and includes more than 500 species (Bora and Sharma, 2011; Oberprieler et al., 2007). The majority of the *Artemisia* species have been used in folk medicine for the treatment of various diseases such as malaria (Willcox 2009), fever, helminthiasis, hepatitis, cancer, cardiac and digestive problems and neurodegenerative disorders (Bora and Sharma, 2011; Guarrera, 2005). Also, some of them showed antibacterial and antifungal activities (Vajs et al., 2004). *Artemisia alba* Turra (synonyms: *A. lobelii* All., *A. camphorata* Vill.) is an aromatic herb of the Asteraceae family, typical for the southern and south-eastern parts of Europe (Trendafilova et al., 2018). This plant was used in traditional medicine as a digestive, tonic, mineralising agent and decoction of leaves was used to heal burns and contusions (Peron et al., 2017). It was found that the essential oil of *A. alba* has antimicrobial activity (Stojanović et al., 2000). Phenolic compounds (phenolic acids and flavonoids) have antioxidant activity and possess the ability to reduce the risk of cancer and cardiovascular diseases (Fraisse et al., 2011; Zhishen et al., 1999).

There are significant differences in terpenoid profiles of *A. alba* essential oils depending on genetic factors, ecological factors (temperature, light, moisture) and type of soil (Radulović and Blagojević, 2010). Although the composition of methanolic extracts and antioxidant activities were the subject of numerous papers (Nikolova et al., 2014; Radović Jakovljević et al., 2020; Trendafilova et al., 2018), we considered that the enrichment of data is important to assess the impact of geographic factor on chemical composition and antioxidant activity. Therefore, this paper is focused on the comparison of antioxidant capacity and phenolic composition of *A. alba* methanolic extracts obtained from species originated from two different localities.

Experimental

Chemicals and reagents

Folin-Ciocalteu's phenol reagent, ABTS, 2,2-diphenyl-1-picrylhydrazyl, neocuproine were purchased from Sigma Co. (St. Louis, Missouri, USA). 6-Hydroxy-2,5,7,8-tetramethylchroman-2-carboxylic acid was purchased from Acros Organics (Morris Plains, New Jersey, USA). TPTZ (2,4,6-tripyridyl-*s*-triazine) was purchased from Merck (Darmstadt, Germany). All chemicals and reagents were of analytical purity.

Plant material and plant material extraction

The plant material (*Artemisia alba* Turra) was collected at blooming stage on August 2016 on two locations Mojinci (A1) and Rosomač (A2), Serbia; a voucher specimen 14323 and 14324, respectively, has been deposited in the Herbarium Moesiacum Niš (HMN), Department of Biology and Ecology, Faculty of Science and Mathematics, University of Niš, Serbia. The coordinates of the sites from which the plants were gathered are available in Table 1.

Table 1. Details of the localities from which *A. alba* was harvested

Plant material	Locality name	Longitude	Latitude	WRB soil type
A1	Put Vlkovija, Mojinci	22.90833333	43.08344444	Rendzic Leptosol
A2	Rosomač	22.84122222	43.1535	Rendzic Leptosol

* WRB soil type - World reference base for soil resources 2014

The aerial parts of the plants were used for the experiment. Fresh plant material was dried at room temperature, milled, packed in paper bags, and kept in dry and dark place. Dried plant material (10 g) was macerated with methanol (100 ml) and then was kept for 72 h in the dark, at room temperature, with occasional shaking. The resulting extracts were filtered and evaporated to dryness. The yield of A1 was 5.9%, while the yield of A2 was 9.6%. Dry extracts were dissolved in methanol (20 mg in 1 ml) and the obtained solutions were used for testing the antioxidant activity and HPLC analysis.

HPLC-DAD analysis

The concentration of individual phenolic compounds was determined by HPLC using a direct-injection method developed by Mitić (Mitić et al., 2013). Briefly, Agilent 1200 chromatographic system equipped with a quaternary pump, Agilent 1200 photodiode array detector, automatic injector, Agilent-Eclipse XDBC-18 4.6 × 150 mm column and ChemStation software was used. The column was thermostated at 30° C. Five μL of extract solution in methanol was injected. Two solvents were used for the gradient elution: A (5% formic acid in water) and B (80% acetonitrile + 5% formic acid in water). The elution program used was as follows: from 0 to 10 min 0% B, from 10 to 28 min gradually increases 0-25% B, from 28 to 30 min 25% B, from 30 to 35 min gradually increases 25-50% B, from 35 to 40 min gradually increases 50-80% B, and finally for the last 5 min gradually decreases 80-0% B. The detection wavelengths were 254, 280, 320, and 520 nm. Identification was performed by comparing retention indices and UV / VIS spectra of components with retention indices and UV / VIS spectra of standards. The contents of components in the extracts were quantified using standard curves and expressed as mg per g of dry extract (mg/g).

UV-VIS spectrophotometry

All spectrophotometric analyses of antioxidative potential of *A. alba* Turra extracts were performed on a UV-visible spectrophotometer Perkin Elmer lambda 15 (Massachusetts, USA). Experiments for all applied assays were performed in three independent repetitions and the mean values are presented.

Determination of total phenolic and total flavonoid content

The total phenolic content (**TPC**) of the extract was determined using Folin-Ciocalteu reagent according to the method of Singleton et al. (1999). The total phenolic content was expressed as gallic acid equivalent per milligram of dry extract weight (μg GAE/mg dw). Total flavonoid content (**TFC**) was assayed using the method described by Zhishen et al. (1999). Total flavonoid content was presented as quercetin equivalent (QE) per milligram of dry extract weight (μg QE/mg dw).

Determination of antioxidant activities

Free radical scavenging activity **(DPPH)** was determined using the stable 2,2-diphenyl-1-picrylhydrazyl (DPPH) radical according to the method of Hatano et al. (1988). The results were expressed as micrograms of Trolox equivalents per milligram of dry extract weight (μg TE/mg dw). The method used for determination of the antioxidant free radical capacity was the $ABTS^{\bullet+}$ (radical cation) decolorization assay **(ABTS),** described by Re et al. (1999). The radical scavenging capacity of extracts was expressed as micrograms of Trolox equivalents per milligram of dry extract weight (μg TE/mg dw). The ferric reducing antioxidant power (**FRAP**) assay was based on the methodology of Benzie and Strain (1996). FRAP values were presented as micromoles Fe^{2+} per mg of dry extract weight (μmol Fe/mg dw). Total reducing power test (**TRP**) represents the capacity of extract to reduce iron (III) to iron (II) and was assayed using the method described by Oyaizu (1986). The results were expressed as mg of ascorbic acid per mg of dry extract weight (mg AAE/mg dw). Cupric reducing antioxidant capacity analysis **(CUPRAC)** was used for the determination of antioxidants and hydroxyl radical scavengers, according to the method of Apak et al. (2004). The results of CUPRAC method were presented as Trolox equivalent per milligram of dry extract weight (mg TE/mg dw).

Results and Discussion

The yield of extract from Rosomač was higher (9.6%) than the yield of extract from Mojinci (5.9%), while in the cited papers yields were omitted. The number of identified components was eleven for A1 and ten for A2, as shown in Table 2.

Table 2. The components of methanolic extracts of *A. alba* identified by HPLC-DAD and their masses given in mg/g of dry extract weight

Component	A1, Mojinci	A2, Rosomač	A2/A1
Vanilllic acid	1.29	/	
Chlorogenic acid	2.66	18.6	**6.99**
p-Coumaric acid	0.51	4.28	**8.39**
Cynarine	2.08	16.9	**8.13**
Rutin	0.85	14.7	17.3
Apigenin glucoside	5.36	3.24	0.60
Rosmarinic acid	3.29	22.0	**6.69**
Quercetin	1.91	5.11	2.68
Luteolin	0.75	0.77	1.03
Kaempferol	0.82	0.66	0.80
Apigenin	0.60	1.17	1.95

Apigenin glucoside and rosmarinic acid were the most abundant phenolic constituents in A1 extract (5.36 and 3.29 mg/g of dry extract, respectively), while in A2 extract dominant compounds were rosmarinic acid and chlorogenic acid (22.0 and 18.6 mg/g of dry extract, respectively). Flavonoid compounds found in both samples were rutin, apigenin glucoside, quercetin, luteolin, kaempferol and apigenin, while detected phenolic acids were chlorogenic acid, *p*-coumaric acid, cynarine and rosmarinic acid. The only observed qualitative difference was related to the presence of vanillic acid. Vanillic acid was present only in A1 extract. The total amounts of flavonoids in A1 and A2 were 10.3 and 25.7 mg/g of dry extract, respectively. The contents of phenolic acids in those samples (A1 and A2) were 9.83 and 61.8 mg/g of dry extract,

respectively. Some regularity in the ratios of phenolic acids in these two samples A2/A1 can be noticed. The ratio between A2 and A1 for rosmarinic acid, chlorogenic acid, cynarine and *p*-coumaric acid was from 6.69 to 8.39. As we can see, A2 extract was richer in both flavonoid and phenolic acid constituents.

The phenolic profile of *A. alba* extract was previously published, and the significant similarity was noticed with our work. Research in North-East of Italy has shown that the phenolic compounds of the ethanolic extract of the plant from this territory were chlorogenic acid, rutin, kaempferol, that were also present in our samples, as well as quercetin 3-*O*-glucoside, isorhamnetin 3-*O*-rutinoside, kaempferol 3-*O*-glucopyranoside, isorhamnetin 3-*O*-glucopyranoside, quercetin dihexoside, isorhamnetin dihexoside, and isorhamnetin (Peron et al., 2017). Phenolic constituents of *A. alba* methanolic extract from Bulgaria, which were present in our samples, were chlorogenic acid, rutin, apigenin glucoside, luteolin and apigenin (Trendafilova et al., 2018). Chlorogenic acid, rutin, luteolin and apigenin were also found in the ethanolic extract of *A. alba* from Serbia (Đorđević et al., 2013).

Table 3. Total phenolic (TPC) and total flavonoid (TFC) contents and antioxidant activity (DPPH, ABTS, TRP, FRAP and CUPRAC assays) of *A. alba* methanolic extracts

Extract	TPC (μg GAE/mg)	TFC (μg QE/mg)	DPPH (μg TE/mg)	ABTS (μg TE/mg)	TRP (mg AAE/mg)	FRAP (μmol Fe/mg)	CUPRAC (mg TE/mg)
A1	117	35.5	29.1	83.1	38.1	39.2	152
A2	185	68.6	107	90.6	61.1	27.5	302

Two methanolic extracts of *A. alba* originated from different localities (A1 and A2) were analyzed for their total phenolic and flavonoid contents (Table 3). A2 was richer in phenolic compounds and flavonoids (185 μg GAE/mg; 68.6 mg μg QE/mg) than A1 (117 μg GAE/mg; 35.5 mg μg QE/mg). DPPH and ABTS tests were used for the estimation of antioxidant capacity of the extracts. As shown in Table 3, A2 extract possessed higher radical scavenging activity (107 and 90.6 μM TE/mg, respectively) than the A1 extract (29.1 and 83.1 μM TE/mg, respectively), especially in DPPH assay. Only the results from FRAP test are higher for A1 (39.2 μmol Fe/mg) than for A2 extract (27.5 μmol Fe/mg).

Conclusion

The presented results showed minor differences in the qualitative composition of the methanolic extracts (the only difference was related to the presence of vanillic acid), but significant differences in the quantitative composition, which caused different antioxidant activity. These results indicate that the impact of the site on the chemical composition of the methanolic extract is small if the same soil type is present on both sites.

Acknowledgment

The research was supported by Ministry of Education, Science and Technological Development of the Republic of Serbia (Project No. 451-03-68/2020-14/200124) and the Serbian Academy of Sciences and Art (SASA), Branch of SASA in Nis (Project No. 0-13-18).

References

Apak, R., Güçlü, K., Özyürek, M., & Karademir, S. E. (2004). Novel total antioxidant capacity index for dietary polyphenols and vitamins C and E, using their cupric ion reducing capability in the presence of neocuproine: CUPRAC method. Journal of Agricultural and Food Chemistry, 52, 7970-7981.

Benzie, I. F. F., & Strain, J. J. (1996). The ferric reducing ability of plasma (FRAP) as a measure of "Antioxidant Power": The FRAP assay. Analytical Biochemistry, 239, 70-76.

Bora, K. S., & Sharma, A. (2011). The genus *Artemisia*: A comprehensive review. Pharmaceutical Biology, 49, 101-109.

Đorđević, S., Stanisavljević, D., Ristić, M., Milenković, M., Veličković, D., Stojičević, S., & Zlatković, B. (2013). Chemical, antioxidant and antimicrobial analysis of the essential oil and extract of *Artemisia alba* Turra. Digest Journal of Nanomaterials & Biostructures, 8, 1377-1388.

Fraisse, D., Felgines, C., Texier, O., & Lamaison, J. L. (2011). Caffeoyl derivatives: major antioxidant compounds of some wild herbs of the Asteraceae family. Food and Nutrition Sciences, 2, 181-192.

Guarrera, P. M. (2005). Traditional phytotherapy in Central Italy (Marche, Abruzzo, and Latium). Fitoterapia, 76, 1-25.

Hatano, T., Kagawa, H., Yasuhara, T., & Okuda, T. (1988). Two new flavonoids and other constituents in licorice root: their relative astringency and radical scavenging effects. Chemical and Pharmaceutical Bulletin, 36, 2090-2097.

Mitić, M. N., Obradović, M. V., Mitić, S. S., Pavlović, A. N., Pavlović, J. LJ., & Stojanović, B. T. (2013). Free radical scavenging activity and phenolic profile of selected Serbian red fruit wines. Revista de Chimie, 64, 68-73.

Nikolova, M., Gussev, Ch., & Nguyen, T. (2010). Evaluation of the antioxidant action and flavonoid composition of *Artemisia* species extracts. Biotechnology & Biotechnological Equipment, 24, 101-103.

Oberprieler, C., Himmelreich, S., & Vogt, R. (2007). A new subtribal classification of the tribe Anthemideae (Compositae). Willdenowia, 37, 89-114.

Oyaizu, M. (1986). Studies on products of browning reaction. Antioxidative activities of products of browning reaction prepared from glucosamine. Japanese Journal of Nutrition, 44, 307-314.

Peron, G., Baldan, V., Sut, S., Faggian, M., Roccabruna, L., Zanini, D., Manzini, P., Maggi, F., & Dall'Acqua, S. (2017). Phytochemical investigations on *Artemisia alba* Turra growing in the North-East of Italy. Natural Product Research, 31, 1861-1868.

Radović Jakovljević, M., Grujičić, D., Tubić Vukajlović, J., Marković, A., Milutinović, M., Stanković, M., Vuković, N., Vukić, M., Milošević-Đorđević, O. (2020). *In vitro* study of genotoxic and cytotoxic activities

of methanol extracts of *Artemisia vulgaris* L. and *Artemisia alba* Turra. South African Journal of Botany, 132, 117-126.

Radulović, N., & Blagojević, P. (2010). Volatile profiles of *Artemisia alba* Turra from contrasting serpentine and calcareous habitats. Natural Product Communications, 5, 1117-1122.

Re, R., Pellegrini, N., Proreggente, A., Pannala, A., Yang, M., & Rice-Evans, C. (1999). Antioxidant activity applying an improved ABTS radical cation decolorization assay. Free Radical Biology and Medicine, 26, 1231-1237.

Singleton,V. L., Orthofer, R., & Lamuela-Raventós, R. M. (1999). Analysis of total phenols and other oxidation substrates and antioxidants by means of folin-ciocalteu reagent. Methods in Enzymology, 299, 152-178.

Stojanović, G., Palić, R., & Mitrović, J. (2000). Chemical composition and antimicrobial activity of the essential oil of *Artemisia lobelii* All. Journal of Essential Oil Research, 12, 621-624.

Trendafilova, A., Todorova, M., Genova, V., Peter, S., Wolfram, E., Danova, K., & Evstatieva, L. (2018). Phenolic profile of *Artemisia alba* Turra. Chemistry & Biodiversity, 15, 1872-1880.

Vajs, V., Trifunović, S., Janaćković, P., Soković, M., Milosavljević, S., & Tešević, V. (2004). Antifungal activity of davanone-type sesquiterpenes from *Artemisia lobelii* var. *conescens*. Journal of the Serbian Chemical Society, 69, 969-972.

Willcox, M. (2009). *Artemisia* species: from traditional medicines to modern antimalarial and back again. The Journal of Alternative and Complementary Medicine, 15, 101-109.

Zhishen, J., Mengecheng, T., & Jianming, W. (1999). The determination of flavonoid contents on mulberry and their scavenging effects on superoxide radical. Food Chemistry, 64, 555-559.

Uporedna analiza HPLC profila i antioksidativne aktivnosti Artemisia alba Turra sa dva staništa u Srbiji

Jovana D. Ickovski[1], Milan N. Mitić[1], Milan B. Stojković[1], Gordana S. Stojanović[1]

1- Univerzitet u Nišu, Prirodno-matematički fakultet, Departman za hemiju, Višegradska 33, 18000 Niš, Srbija

Sažetak

Artemisia alba Turra sakupljana je u fazi cvetanja na dve različite lokacije u Srbiji, Mojinci i Rosomač. Određeni su i upoređeni antioksidativna aktivnost i HPLC profili njihovih metanolnih ekstrakata. Flavonoidna jedinjenja pronađena u oba uzorka su rutin, apigenin-glukozid, kvercetin, luteolin, kempferol i apigenin, dok su identifikovane fenolne kiseline: hlorogena kiselina, *p*-kumarinska kiselina, cinarin i rozmarinska kiselina. Jedina uočena kvalitativna razlika odnosila se na prisustvo vanilinske kiseline. Metanolni ekstrakt *A. alba* iz Rosomača bio je bogatiji fenolnim jedinjenjima i flavonoidima od ekstrakta *A. albe* iz Mojinca. Ekstrakt *A. alba* iz Rosomača takođe je posedovao veći antioksidativni kapacitet od ekstrakta *A. alba* iz Mojinaca, posebno u pogledu 2,2-difenil-1-pikrilhidrazil testa. Samo su rezultati ispitivanja redukcionog antioksidativnog kapaciteta feri jona viši za ekstrakt *A. alba* iz Mojinaca, nego za ekstrakt *A. alba* iz Rosomača.

***Ključne reči**: Artemisia alba, metanolni ekstrakt, HPLC, antioksidativna aktivnost*

L'analyse comparative de profile HPLC et l'activité antioxydant de l'*Artemisia alba* Turra de deux habitats Serbes

Jovana D. Ickovski[1], Milan N. Mitić[1], Milan B. Stojković[1], Gordana S. Stojanović[1]

1-Université de Niš, Faculté des sciences naturelles et des mathématiques, Département de chimie, Višegradska 33, 18000 Niš, Serbie

RÉSUMÉ

Artemisia alba Turra a été collecté au stade de la floraison sur deux sites différents en Serbie, Mojinci et Rosomač. L'activité antioxydante et les profils HPLC de leurs extraits méthanoliques ont été déterminés et comparés. Les composés flavonoïdes trouvés dans les deux échantillons étaient les suivants : le rutin, l'apigénine-glucoside, la quercétine, la lutéoline, le kaempférol et l'apigénine, tandis que les acides phénoliques détectés étaient les suivants : l'acide chlorogénique, l'acide *p*-coumarique, la cynarine et l'acide rosmarinique. La seule différence qualitative observée était liée à la présence de l'acide vanillique. L'extrait d'*A. alba* de Rosomač était plus riche en composés phénoliques et en flavonoïdes que *A. alba* de Mojinci. L'extrait d'*A. alba* de Rosomač possédait également une capacité antioxydante plus élevée que *A. alba* de Mojinci, en particulier en ce qui concerne le test du 2,2-diphényl-1-picrylhydrazyle. Seuls les résultats du dosage du pouvoir antioxydant réducteur d'ions ferriques étaient plus élevés pour l'extrait d'*A. alba* de Mojinci que pour l'extrait d'*A. alba* de Rosomač.

Mots-clés : Artemisia alba, extrait méthanolique, HPLC, activité antioxydante.

Сравнительный анализ профилей ВЭЖХ и антиоксидантной активности *Artemisia alba* Turra из двух местообитаний в Сербии

Йована Д. Ицковски[1], Милан Н. Митич[1], Милан Б. Стойкович[1], Гордана С. Стоянович[1]

1-Университет в Нише, Естественно-математический факультет, Кафедра химии, Вышеградская 33, 18000 Ниш, Сербия

Аннотация

Artemisia alba Turra была собрана на стадии цветения в двух разных местах в Сербии, Мойинцы и Росомач. Определяли и сравнивали антиоксидантную активность и профили ВЭЖХ их метанольных экстрактов. Флавоноидные соединения, обнаруженные в обоих образцах, были рутин, апигенин-глюкозид, кверцетин, лютеолин, кемпферол и апигенин, в то время как обнаруженные фенольные кислоты были хлорогеновой кислотой, п-кумаровой кислотой, цинарином и розмариновой кислотой. Единственное наблюдаемое качественное различие было связано с присутствием ванилиновой кислоты. Экстракт *A. alba* из места Росомач был богаче фенольными соединениями и флавоноидами, чем A. alba из Мойинцы. Экстракт *A. alba* из места Росомач также обладал более высокой антиоксидантной способностью, чем *A. alba* из Мойинцы, особенно в отношении анализа 2,2-дифенил-1-пикрилгидразила. Только результаты анализа антиоксидантной способности восстановления ионов трехвалентного железа были выше для экстракта *A. alba* из Мойинцы, чем для экстракта *A. alba* из места Росомач.

Ключевые слова: *Artemisia alba, метанольный экстракт, ВЭЖХ, антиоксидантная активность.*

Vergleichende Analyse der HPLC-Profile und der antioxidativen Aktivität von *Artemisia alba* Turra an zwei Standorten in Serbien

Jovana D. Ickovski[1], Milan N. Mitić[1], Milan B. Stojković[1], Gordana S. Stojanović[1]

1- Universität Niš, Fakultät für Naturwissenschaften und Mathematik, Lehrstuhl für Chemie, Višegradska 33, 18000 Niš, Serbien

Artemisia alba Turra wurde im Blütestadium an zwei verschiedenen Standorten in Serbien, Mojinci und Rosomač, gesammelt. Die Antioxidationsaktivität und die HPLC-Profile ihrer methanolischen Extrakte wurden bestimmt und verglichen. Die in beiden Proben gefundenen Flavonoidverbindungen waren Rutin, Apigenin-Glucosid, Quercetin, Luteolin, Kaempferol und Apigenin, während die nachgewiesenen Phenolsäuren Chlorogensäure, p-Cumarsäure, Cynarin und Rosmarinsäure waren. Der einzige festgestellte qualitative Unterschied bezog sich auf das Vorhandensein von Vanillinsäure. Der methanolische Extrakt von *A. alba* aus Rosomač war reicher an Phenolverbindungen und Flavonoiden als der von *A. alba* aus Mojinci. Der Extrakt von *A. alba* aus Rosomač besaß auch eine höhere antioxidative Kapazität als *A. alba* aus Mojinci, insbesondere im Hinblick auf den 2,2-Diphenyl-1-picrylhydrazyl-Assay. Nur die Ergebnisse für den Eisenionen reduzierenden Antioxidationstest waren für den Extrakt von *A. alba* aus Mojinci höher als für den Extrakt von *A. alba* aus Rosomač.

Schlüsselwörter: Artemisia alba, methanolischer Extrakt, HPLC, antioxidative Aktivität

Essential oil profile of *Origanum vulgare* subsp. *vulgare* native population from Rtanj *via* chemometrics tools

Milica Aćimović[1]*, Lato Pezo[2], Stefan Ivanović[3], Katarina Simić[3], Jovana Ljujic[4]

1-Institute of Field and Vegetable Crops Novi Sad – National Institute of the Republic of Serbia, Maksima Gorkog 30, 21000 Novi Sad, Serbia

2-University of Belgrade, Institute of General and Physical Chemistry, Studentski trg 12, 11000 Belgrade, Serbia

3-University of Belgrade, Institute of Chemistry, Technology and Metallurgy – National Institute of the Republic of Serbia, Njegoševa 12, 11000 Belgrade, Serbia

4-University of Belgrade, Faculty of Chemistry, Department of Organic Chemistry, Studentski trg 12-16, 11000 Belgrade, Serbia

Milica Aćimović: milica.acimovic@ifvcns.ns.ac.rs
Lato Pezo: latopezo@yahoo.co.uk
Stefan Ivanović: stefan.ivanovic@ihtm.bg.ac.rs
Katarina Simić: katarina.simic@ihtm.bg.ac.rs
Jovana Ljujić: jovanalj@chem.bg.ac.rs

ABSTRACT

The aim of this study was to predict the retention indices of chemical compounds found in the aerial parts of *Origanum vulgare* subsp. *vulgare* essential oil, obtained by hydrodistillation and analyzed by GC-MS. A total number of 28 compounds were detected in the essential oil. The compounds with the highest relative concentrations were germacrene D (21.5%), 1,8-cineole (14.2%), sabinene (14.0%) and *trans*-caryophyllene (13.4%). The retention time was predicted by using the quantitative structure–retention relationship, using seven molecular descriptors chosen by factor analysis and genetic algorithm. The chosen descriptors were mutually uncorrelated, and they were used to develop an artificial neural network model. A total number of 28 experimentally obtained retention indices (log *RI*) were used to set up a predictive quantitative structure-retention relationship model. The coefficient of determination for the training cycle was 0.998, indicating that this model could be used for predicting retention indices for *O. vulgare* subsp. *vulgare* essential oil compounds.

Keywords: oregano, essential oil, hydrodistillation, GC-MS, QSSR, ANN

Introduction

Origanum is an important genus with multipurpose medicinal and spice plants. It belongs to the family Lamiaceae and is comprised of 42 species divided into 10 sections. Most *Origanum* species are locally distributed within the Mediterranean region where they grow in the mountainous areas on the islands, with high endemism rate (Lukas, 2010). However, among all sections in the genus, only section Origanum is monospecific, consisting of the species *O. vulgare*, but with the largest distribution area. Because of this, *O. vulgare* is an extremely variable species that includes six subspecies (subsp. *vulgare*, subsp. *glandulosum*, subsp. *gracile*, subsp. *hirtum*, subsp. *viridulum* and subsp. *virens*) which are characterized by a high morphological and chemical variability (Chishti et al., 2013; Kosakowska and Czupa, 2018). In general, differences in morphological and chemical features represent environmental adaptation. For example, sessile glands on leaves and the color of bracts and corollas are the main morphological traits (Kokkini et al., 1994). Furthermore, the yield and quality of the essential oil depends on genetics and is strongly affected by the environmental influences (Goliaris et al., 2002;Toncer et al., 2009).

O. vulgare subsp. *vulgare* is the most widespread species in Europe, and has longstanding use in traditional medicine for its carminative, stomachic, emmenagogue, and expectorant effects for treating cramps, flatulence, cough, or menstrual problems (Oniga et al., 2018). The main bioactive components of *O. vulgare* are essential oil and phenolic components, generated from cymyl- pathway such as *γ*-terpinene, *p*-cymene, carvacrol and thymol (Lukas, 2010;Stanojević et al., 2016). Their ratio represents the quality of the oil and indicates the aroma value (Morsy, 2017).

Quantitative structure retention relationship (QSRR) approach provides a deeper insight into the relation between the chemical compounds, their structure and the physicochemical or biological properties (Wolfender et al., 2015). Gas Chromatography coupled with Mass Spectrometry (GC-MS) extracts a huge amount of data, which could be compared and reproduced, and it also shows the exact retention time indices for large sets of compounds in different biological materials. The chemical compound structure is explained by the mathematical models, described by so-called molecular descriptors, which encode its data by the symbolic representation of a molecule into a numerical value (Héberger, 2007;Micić et al., 2019). Lately, various investigations were assigned to the QSRR coupled with GC-MS data analyses (Kaliszan, 2007;Khezeli et al., 2016;Marrero-Ponce et al., 2018; Wu et al., 2013). The relation between the molecular descriptors and the retention time can be established by using various mathematical tools, such as the artificial neural network (ANN), which was proven to be excellent in solving non-linear problems (Wolfender et al., 2015;Zisi et al., 2017), or by using machine learning algorithms (Tropsha and Golbraikh, 2007).

The aim of this study was to establish a new QSRR model for the prediction ofthe retention times of chemical compounds found in *O. vulgare* subsp. *vulgare* essential oil, obtained by hydrodistillation and analyzed by GC-MS using the coupled genetic algorithm (GA) and factor analysis (FA) variable selection method and the artificial neural network (ANN) model.

Experimental

Plant material

Origanum vulgare subsp. *vulgare* was collected on the 7th July 2018, on Mt. Rtanj. The plant species were at full flowering by this date. The plant aboveground parts were harvested manually at around 2-3 cm above the soil surface, and the biomass was placed in an air-dryer until constant weight at 35 °C to avoid essential oil losses. Voucher specimens were confirmed and deposited at the Herbarium BUNS, the University of Novi Sad, Faculty of Sciences, Department of Biology and Ecology, under the acquisition number 2-1450.

Essential oil isolation

Air-dried aerial parts of *O. vulgare* subsp. *vulgare* were submitted to hydrodistillation according to Ph. Eur. 5.0(Ph. Eur. 5.0) by using the Clevenger apparatus. The 30 g of the plant material was placed in round-bottomed flask of 1 L and 400 mL of distilled water was added. Then it was heated to the boiling point. The steam in combination with the essential oils was distilled into a graduated tube for 2h. After separation of essential oil from aqueous phase it was dried over anhydrous Na_2SO_4 and stored in a dark glass vial at 4 °C for further analysis. The essential oils yields were calculated on dry-weight basis, and average content of essential oil was 0.12%.

GC-MS analysis

GC-MS analysis was carried out using an HP 5890 gas chromatograph coupled to an HP 5973 MSD and fitted with a capillary column HP-5MS. The carrier gas was helium, and its inlet pressure was 25 kPa and linear velocity of 1 mL/min at 210 °C. The injector temperature was 250 °C, and analysis was conducted under splitless injection mode. Mass detection was carried out under source temperature conditions of 200 °C and interface temperature of 250 °C. The EI mode was set at electron energy, 70 eV with mass scan range of 40–350 amu. Temperature was programmed from 60 °C to 285 °C at a rate of 4.3 °C/min. The components were identified based on their linear retention index relative to C_8-C_{32}*n*-alkanes, by the comparison with data reported in the literature (Wiley and NIST databases). Quantification was done by external standard method using calibration curves generated by running GC analysis of representative authentic compounds.

Artificial neural network (ANN)

A multi-layer perceptron model (MLP) consisted of the three layers (input, hidden and output) was used in this paper, having in mind that it is well known and proven as being capable of approximating nonlinear functions (Aalizadeh et al., 2016). Broyden–Fletcher–Goldfarb–Shanno (BFGS) algorithm was used for ANN modelling. The experimental database was randomly divided into: train, testing and validation parts (60, 20 and 20%, respectively) for ANN modelling. A series of different neural network topologies was tested. The number of hidden neurons varied from 1 to 20 and 1,000,000 networks were tested, using random initial values of weights and biases. The weight coefficient was calculated during the training period, with the initial assumptions of parameters, which were adjusted using ANN structure and fitting (Kojic and Omorjan, 2018; Xuet al., 2015). The optimization process was performed on the basis of validation error minimization. Statistical investigation of the data has been performed mainly by the Statistica 10 software (Statistica, 2010).

Molecular descriptors

Coupled factor analysis and genetic algorithm were used to select the most relevant molecular descriptors for the representation of the retention indices (Goldberg, 1989; Tropsha, 2010), and a calculation was performed using Heuristic Lab (HeuristicLab, 3.3). The correlation between the obtained descriptors was examined and collinear descriptors were detected using factor analysis. GA was used to select the most appropriate molecular descriptors to develop a reliable model for the prediction of retention times of the compounds found in *O. vulgare* subsp. *vulgare* essential oil.

QSRR analysis

The molecular structure was introduced in the quantitative structure retention relationship (QSRR) calculation in the form of *.smi* files, which represented the structure of a molecule in a simplified molecular input line (Matyushin, et al. 2019). The calculation of the specified molecular descriptors for each chemical compound obtained in the GC-MS analysis was performed using PaDel-descriptor software (Dong et al., 2015; Yap, 2011). The PaDel-descriptor software was used

to calculate the 1875 molecular descriptors (1444 1D and 2D descriptors and 431 3D descriptors), which included: constitutional descriptors, topological descriptors, connectivity indices, information indices, 2D and 3D autocorrelations descriptors, Burden eigenvalues descriptors, eigenvalue-based indices, geometrical descriptors, WHIM descriptors, functional group counts, atom-centered fragments and molecular properties.

Global sensitivity analysis

Global sensitivity analysis was used to explore the relative influence of molecular descriptors on retention time (Yoon et al., 2017). This method was applied on the basis of the weight coefficients of the developed ANN.

Results and Discussion

Essential oil composition

A total number of 28 compounds were detected in the *O. vulgare* subsp. *vulgare* essential oil in this study, representing 99.5% of the total oil composition (Table 1). The compounds with the highest relative concentration in *O. vulgare* subsp. *vulgare* essential oil were germacrene D (21.5%), 1,8-cineole (14.2%), sabinene (14.0%) and *trans*-caryophyllene (13.4%). Out of these, 15 compounds had average relative concentrations over 1.0%. Monoterpene hydrocarbons (47.9%) and sesquiterpene hydrocarbons (42.9%) were the dominant classes. According to the obtained results, *O. vulgare* subsp. *vulgare* collected at Mt. Rtanj can be classified as germacrene D chemotype. This chemotype is already described (Mockute et al., 2001). Differences among the oregano accessions with respect to morphological traits and chemical constituents of essential oils, indicate the existence of intraspecific variations and chemical polymorphism (Aćimović et al., 2020; Radusiene et al., 2005). Subspecies which accumulate carvacrol and/or thymol and their precursors (*γ*-terpinene and *p*-cymene) contain low amounts of other monoterpenes (Kosakowska and Czupa, 2018).

Table 1. Chemical composition of *O. vulgare* subsp. *vulgare* essential oil from dry aerial parts.

No	Compound	RI[a]	RI[b]	%
1	*α*-Thujene	915	924	0.1
2	*α*-Pinene	926	932	1.5
3	Camphene	944	946	0.9
4	Sabinene	967	969	14.0
5	*β*-Pinene	971	974	3.9
6	*β*-Phellandrene	1026	1025	1.6
7	1,8-Cineole	1028	1026	14.2
8	*cis*-*β*-Ocimene	1033	1032	6.8
9	*trans*-*β*-Ocimene	1043	1044	4.5
10	*γ*-Terpinene	1052	1054	0.4
11	Borneol	1160	1165	1.2
12	Terpinen-4-ol	1172	1174	0.3

13	*α*-Terpineol	1187	1190	0.7
14	Bornyl acetate	1286	1287	0.1
15	*β*-Bourbonene	1384	1387	1.9
16	*trans*-Caryophyllene	1420	1408	13.4
17	*α*-Humulene	1454	1452	2.1
18	9-*epi*-*trans*-Caryophyllene	1461	1464	0.5
19	Germacrene D	1486	1484	21.5
20	Bicyclogermacrene	1497	1500	1.7
21	(*trans*,*trans*)-*α*-Farnesene	1509	1505	0.7
22	*δ*-Cadinene	1524	1513	1.1
23	Germacrene D-4-ol	1575	1574	0.8
24	Spathulenol	1577	1577	0.6
25	Caryophyllene oxide	1583	1582	3.9
26	Humulene epoxide II + *β*-Oplopenone	1606	1608	0.3
27	*epi*-*α*-Murrolol (=*tau*-muurolol)	1640	1640	0.4
28	*α*-Cadinol	1654	1652	0.9
	Monoterpene hydrocarbons			47.9
	Oxygenated monoterpenes			2.3
	Sesquiterpene hydrocarbons			42.9
	Oxygenated sesquiterpenes			6.9
	Total identified			99.5

RI[a] – Retention Index calculated; RI[b] – Retention Index from the NIST webbook database.

Artificial neural network (ANN)

Graphical representation of experimentally obtained retention time indices of *O. vulgare* subsp. *vulgare* essential oil composition (*RI*[a]), the retention time indices found in NIST database (*RI*[b]) and the retention time indices predicted by the ANN model ($RI_{pred.}$) were presented in Figure 1.

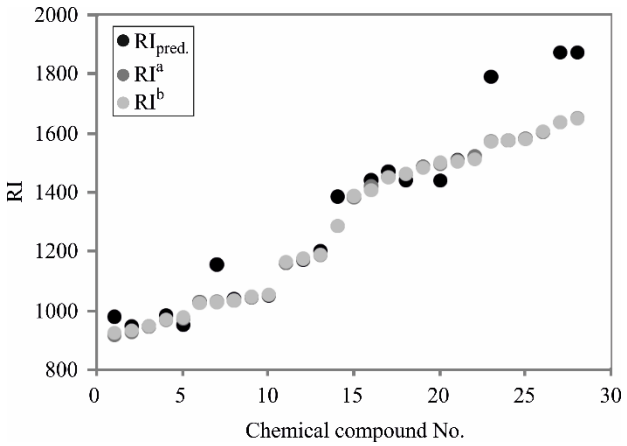

Figure 1. Retention time indices of the *O. vulgare* subsp. *vulgare* essential oil composition, from: experimentally obtained GC-MS data (RI[a]); NIST database (RI[b]) and predicted by the ANN (RI[pred.]).

The nonlinear relationship between *RI*s and the selected descriptors, applying the ANN technique was used in this paper. The statistical results of the MLP 7-12-1 network are shown in Table 2.

Table 2. ANN model summary (performance and errors), for training, testing and validation cycles

Net. name	Performance			Error			Train. algor.	Error funct.	Hidden activat.	Output activat.
	Train.	Test.	Valid.	Train.	Test.	Valid.				
MLP 7-12-1	0.998	0.958	0.999	53.764	2311.444	16294.67	BFGS 38	SOS	Tanh	Exponential

*Performance term represent the coefficients of determination, while error terms indicate a lack of data for the ANN model. ANN cycles: Train. – training, Test. – testing, Valid. – validation, algor. –algorithm, funct. – function, activat. – activation.

The better prediction of *RI*s was obtained in the training cycle, which was expected, because more chemical compounds retention time indices were used in the calculation compared with testing cycle. This is also obvious from Table 2, where the training set performance reached r^2 of 0.998, while the r^2 for testing set was lower. Also, better results for r^2 were obtained in training cycle, due to the fact that these data were used for the modelling of ANN, while the data in testing and verification cycles were used for testing purposes and to explore the quality of the ANN model created in training cycle. Obtained results reveal the reliability of the ANN models for predicting the *RI*s of compounds in *O. vulgare* subsp. *vulgare* essential oil determined by GC-MS.

Molecular descriptors

Seven molecular descriptors were chosen by FA and GA analyses for predictions of *RI* in the obtained ANN model.

- *Autocorrelation descriptors*

  1. ATSC3v - Centered Broto-Moreau autocorrelation - lag 3 / weighted by van der Waals volumes;
  2. AATSC5c - Average centered Broto-Moreau autocorrelation - lag 5 / weighted by charges;
  3. AATSC1v - Average centered Broto-Moreau autocorrelation - lag 1 / weighted by van der Waals volumes;
  4. AATSC1e -Average centered Broto-Moreau autocorrelation - lag 1 / weighted by Sanderson electronegativities;
  5. GATS5p - Geary autocorrelation - lag 5 / weighted by polarizabilities,

- *Information content descriptors:*

  6. BIC2 - Bond information content index (neighbourhood symmetry of 2-order);
  7. MIC0 - Modified information content index (neighbourhood symmetry of 0-order).

The above mentioned molecular descriptors encode different aspects of the molecular structure and they were used to develop a QSRR model for prediction of retention indices of

compounds found in *O. vulgare* subsp. *vulgare* essential oil. The values of the selected descriptors were displayed in Table 3.

Table 3. Molecular descriptors chosen by a genetic algorithm

Descriptors	Autocorrelation descriptors					Information content	
No	ATSC3v	AATSC5c	AATSC1v	AATSC1e	GATS5p	BIC2	MIC0
1	-881.860	1.2E-04	3.158	3.3E-04	0.563	0.768	6.797
2	-1182.918	-1.1E-04	3.158	3.3E-04	0.762	0.768	6.797
3	-1209.560	4.2E-04	3.158	3.3E-04	0.431	0.698	6.797
4	-868.539	3.1E-04	3.158	3.3E-04	0.594	0.742	6.797
5	-1169.597	-2.1E-04	3.158	3.3E-04	0.766	0.742	6.797
6	-694.032	2.5E-04	0.000	8.4E-17	0.798	0.790	6.797
7	-984.187	3.2E-05	1.156	2.1E-03	0.973	0.545	9.466
8	-823.247	2.7E-04	-3.410	-3.6E-04	0.717	0.686	6.797
9	-753.977	2.4E-04	0.000	8.4E-17	0.745	0.688	6.797
10	-1240.975	-2.0E-04	4.092	-2.6E-03	0.069	0.647	9.466
11	-901.854	9.7E-04	1.111	-2.8E-03	0.634	0.763	9.466
12	-1197.667	2.0E-04	0.865	1.0E-03	0.313	0.679	10.663
13	-1164.268	1.5E-04	4.159	4.4E-04	0.932	0.704	6.797
14	-1354.761	5.4E-05	2.131	2.2E-04	0.963	0.753	6.797
15	-1530.600	1.4E-04	0.000	8.4E-17	0.930	0.683	6.797
16	-1354.761	5.4E-05	2.131	2.2E-04	0.963	0.753	6.797
17	-739.324	1.4E-04	0.000	8.4E-17	0.941	0.772	6.797
18	-1398.721	4.3E-05	2.131	2.2E-04	0.960	0.711	6.797
19	-1124.305	2.2E-04	-2.244	-2.4E-04	0.810	0.673	6.797
20	-731.331	-4.4E-06	2.131	2.2E-04	0.970	0.711	6.797
21	-985.861	2.1E-04	0.779	-1.7E-03	0.972	0.735	8.851
22	-1352.199	9.3E-04	4.804	-1.6E-03	1.039	0.719	8.941
23	-1468.406	2.1E-04	2.708	1.7E-03	0.988	0.711	8.941
24	-667.006	-3.3E-05	2.042	1.2E-04	1.068	0.735	8.941
25	-986.239	-1.6E-04	2.828	-1.6E-03	0.984	0.737	8.851
26	-986.239	-1.6E-04	2.828	-1.6E-03	0.984	0.737	8.851

The most comprehensive explanation about the molecular descriptors could be found in the Handbook of Molecular Descriptors (Todeschini and Consonni, 2000). Table 4 represents the correlation matrix among these descriptors. There were no statistically significant correlation between selected molecular descriptors; therefore, they could be used for QSRR model building.

Table 4. The correlation coefficient matrix for the selected descriptors by GA

	AATSC5c	AATSC1v	AATSC1e	GATS5p	BIC2	MIC0
ATSC3v	0.000	-0.318	-0.108	0.003	0.188	-0.051
	p=0.999	p=0.113	p=0.599	p=0.988	p=0.359	p=0.804
AATSC5c		-0.097	-0.251	-0.040	0.100	0.135
		p=0.638	p=0.216	p=0.846	p=0.628	p=0.511
AATSC1v			-0.083	-0.062	0.157	0.177
			p=0.688	p=0.765	p=0.444	p=0.386
AATSC1e				0.179	-0.259	-0.277
				p=0.382	p=0.202	p=0.171
GATS5p					0.161	-0.166
					p=0.433	p=0.419
BIC2						-0.334
						p=0.096

QSRR model validation

The factor analysis was performed on the molecular descriptor data obtained from PaDel-descriptor software, in order to eliminate the descriptors with equal or almost equal factor values. Only one of the correlated descriptors remained in the GA calculation. GA was used to select the most appropriate set of molecular descriptors which were left in the calculation, while the selection of the most relevant set of descriptors was used in the evolution simulation(Mohammadhosseini, 2013; Nekoei et al., 2015). The number of elements was equal to the number of the molecular descriptors obtained in the PaDel-descriptor, and the population of the first generation in the GA calculation was selected randomly. The probability of generating zero for the element was set at least 60%. The operators used in the simulation were: crossover (90% probability) and mutation (0.5%). A population size of 100 elements was chosen for GA, and evolution was allowed for over 50 generations. The evolution of the generations was stopped when 90% of the generations took the same fitness.

The calibration and predictive capability of a QSRR model should be tested through the model validation. The most widely used squared correlation coefficient (r^2) can provide a reliable indication of the fitness of the model; thus, it was employed to validate the calibration capability of a QSRR model. The quality of the model fit was tested in Table 5, in which the lower reduced chi-square (χ^2), mean bias error (*MBE*), root mean square error (*RMSE*), mean percentage error (*MPE*) are presented (Arsenović et al., 2015).

Table 5. The "goodness of fit" tests for the developed ANN model

χ^2	*RMSE*	*MBE*	*MPE*
7519.609	85.032	-36.684	3.250

χ^2 - reduced chi-square, *MBE* - mean bias error, *RMSE* - root mean square error, *MPE* - mean percentage error.

The predicted *RI*s which were presented in Figure 2 confirmed the adequate prediction of the retention indices, for constructed ANN, by showing the relationship between the predicted and experimental retention values.

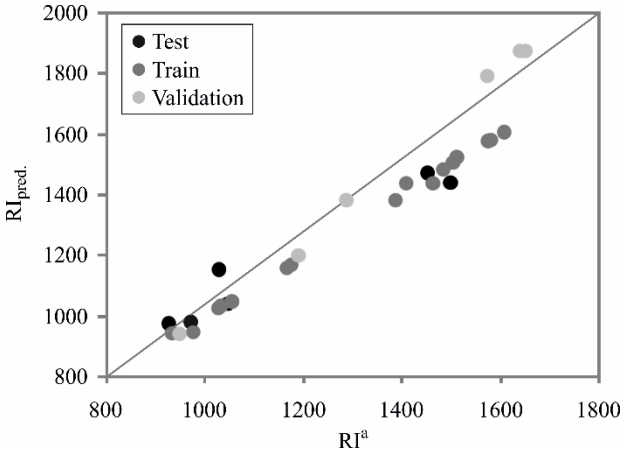

Figure 2. Comparison of experimentally obtained RIs with ANN predicted values

Global sensitivity analysis- Yoon's interpretation method

In this section the influence of seven the most important input variables, identified using genetic algorithm on *RI* was studied. According to the Figure 3, ATSC3v was the most influential parameter with approximately relative importance of 18.8%, while the influence of AATSC1v, AATSC1e, GATS5p and AATSC5c were 14.9, 14.6%, 13.6% and 13.3%, respectively. MIC0 and BIC2 were influential at levels 13.2% and 11.6%, respectively.

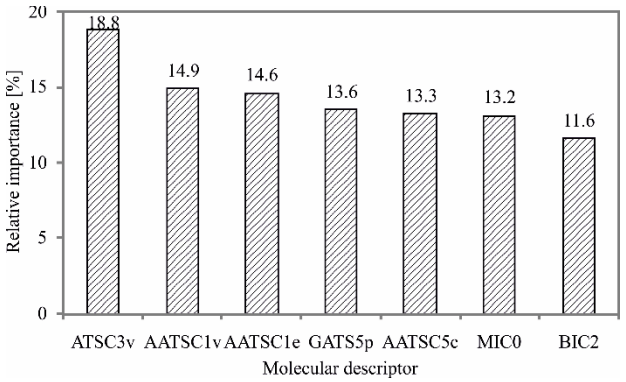

Figure 3 The relative importance of the molecular descriptors on RI, determined using Yoon interpretation method

Conclusion

The QSRR model for the estimation of retention times of *O. vulgare* subsp. *vulgare*essential oil compounds was developed for 28 compounds using the ANN modelling approach. The results demonstrated that the ANN model was adequate in predicting retention times

of found chemicalcompounds. A suitable model with high statistical quality and low prediction errors was derived.

The following five molecular descriptors were suggested by genetic algorithm: five 2D autocorrelation molecular descriptors (ATSC3v, AATSC1v, AATSC1e, AATSC5c and GATS5p) and two Information content descriptors (MIC0 and BIC2), that predicted retention times of the obtained compounds. Selected molecular descriptors were not mutually correlated and the obtained descriptors were suitable for QSRR model building. The results demonstrated that the ANN model was adequate to predict the *RIs* of the compounds in *O. vulgare* subsp. *vulgare*essential oil obtained by hydrodistillation and analysed by GC-MS. The coefficient of determination for training cycle was 0.998, which is a good indication that this model could be used for the prediction of retention time.

Acknowledgment

This work was supported by the Ministry of Education, Science and Technological Development of the Republic of Serbia, Contract No. 451-03-68/2020-14/200032.

Conflict-of-Interest Statement

Authors declare no conflict of interest.

References

Aalizadeh, R., Thomaidis, N.S., Bletsou, A.A.,& Gago-Ferrero, P. (2016). Quantitative structure–retention relationship models to support nontarget high-resolution mass spectrometric screening of emerging contaminants in environmental samples. Journal of Chemical Information and Modeling, 56, 1384-1398; https://doi.org/10.1021/acs.jcim.5b00752.

Aćimović, M., Zorić, M., Zheljazkov, V., Pezo, L., Čabarkapa, I., Stanković Jeremić, J.,& Cvetković, M. (2020). Chemical characterization and antibacterial activity of essential oil of medicinal plants from Eastern Serbia. Molecules, 25, 5482; DOI:10.3390/molecules25225482.

Arsenović, M., Pezo, L., Stanković, S.,& Radojević, Z. (2015). Factor space differentiation of brick clays according to mineral content: Prediction of final brick product quality. Applied Clay Science, 115, 108-114; https://doi.org/10.1016/j.clay.2015.07.030.

Chishti, S., Kaloo, Z.A.,& Sultan P. (2013). Medicinal importance of genus *Origanum*: A review. Journal of Pharmacognosy and Phytotherapy, 5, 170-177; DOI: 10.5897/JPP2013.0285

Council of Europe (2004). European Pharmacopoeia. 5 ed. Strasbourg, 1206-1208.

Dong, J., Cao, D.S., Miao, H.Y., Liu, S., Deng, B.C., Yun, Y.H., Wang, N.N., Lu, A.P., Zeng, W.B.,& Chen, A.F. (2015). ChemDes: an integrated web-based platform for molecular descriptor and fingerprint computation. Journal of Cheminformatics,7, 60. doi: 10.1186/s13321-015-0109-z.

Goldberg, D.E. (1989). Genetic algorithms in search, optimisation and machine learning. Addison-Wesley, Massachusetts, Boston, USA.

Goliaris A.H., Chatzopoulou P.S.,& Katsiotis S.T. (2002). Production of new Greek oregano clones and analysis of their essential oils. Journal of Herbs, Spices and Medicinal Plants, 10, 29-35; https://doi.org/10.1300/J044v10n01_04.

Héberger, K. (2007). Quantitative structure–(chromatographic) retention relationships. Journal of Chromatography A,1158, 273-305;https://doi.org/10.1016/j.chroma.2007.03.108.

HeuristicLab, 3.3 (Heuristic and Evolutionary Algorithms Laboratory, ver. 3.3.16) (Accessed 20 December 2020). https://dev.heuristiclab.com/trac.fcgi/

Hollas, B., Gutman, I.,& Trinajstić, N. (2005). On reducing correlations between topological indices. Croatica Chemica Acta, 78, 489-492.

Kaliszan, R. (2007). QSRR: Quantitative Structure - (Chromatographic) Retention Relationships. Chemical Reviews, 107, 3212-3246; https://doi.org/10.1021/cr068412z.

Khezeli, T., Daneshfar, A.,& Sahraei, R. (2016). A green ultrasonic-assisted liquid–liquid microextraction based on deep eutectic solvent for the HPLC-UV determination of ferulic, caffeic and cinnamic acid from olive, almond, sesame and cinnamon oil. Talanta, 150, 577-585; doi: 10.1016/j.talanta.2015.12.077.

Kojic, P.,& Omorjan, R. (2018). Predicting hydrodynamic parameters and volumetric gas–liquid mass transfer coefficient in an external-loop airlift reactor by support vector regression. ChemicalEngineering and Research and Design,125, 398-407; https://doi.org/10.1016/j.cherd.2017.07.029.

Kokkini S., Karousou R.,&Vokou D. (1994). Pattern of geographic variations of*Origanum vulgare* trichomes and essential oil content in Greece. Biochemical Systematics and Ecology, 22, 517-528; https://doi.org/10.1016/0305-1978(94)90046-9.

Kosakowska O.,& Czupa W. (2018). Morphological and chemical variability of common oregano (*Origanum vulgare* L. subsp. *vulgare*) occurring in eastern Poland. Herba Polonica, 64, 11-21; DOI: 10.2478/hepo-2018-0001

Lukas B. (2010). Molecular and phytochemical analyses of the genus *Origanum* L. (Lamiaceae). Doctoral Dissertation, Department of Botany and Biodiversity Research, Faculty of Life Sciences, Vienna University.

Marrero-Ponce, Y., Barigye, S.J., Jorge-Rodriguez, M.E.,& Tran-Thi-Thu, T. (2017). QSRR prediction of gas chromatography retention indices of essential oil components. Chemical Papers, 72, 57-69; https://doi.org/10.1007/s11696-017-0257-x.

Matyushin, D., Sholokhova, A.Y.,& Buryak, A.K. (2019). A deep convolutional neural network for the estimation of gaschromatographic retention indices. Journal of Chromatography A, 1607, 460395; https://doi.org/10.1016/j.chroma.2019.460395.

Micić, D., Ostojić, S., Pezo, L., Blagojević, S., Pavlić, B., Zeković, Z.,& Đurović, S. (2019). Essential oils of coriander and sage: Investigation of chemical profile, thermal properties and QSRR analysis. Industrial Crops and Products, 138, 111438; https://doi.org/10.1016/j.indcrop.2019.06.001.

Mockute, D., Bernotiene, G.,& Judzentiene A. (2001). The essential oil of *Origanum vulgare* L.ssp. *vulgare* growing wild in Vilnius district (Lithuania). Phytochemistry, 57, 65-69; https://doi.org/10.1016/S0031-9422(00)00474-X.

Mohammadhosseini, M. (2013). Novel PSO-MLR algorithm to predict the chromatographic retention behaviors of natural compounds. Analytical Chemistry Letters, 3, 226-248; https://doi.org/10.1080/22297928.2013.861164.

Moreau, G.,& Broto, P. (1980). The autocorrelation of a topological structure: A new molecular descriptor. Nouveau Journal De Chimie, 4, 359-360.

Morsy N.F.S. (2017). Chemical structure, quality indices and bioactivity of essential oil constituents. In: Active Ingredients from Aromatic and Medicinal Plants, Edited by: El-Shemy H. InTechOpen, London, UK.

Nekoei, M., Mohammadhosseini, M.,& Pourbasheer, E. (2015).QSAR study of VEGFR-2 inhibitors by using genetic algorithm-multiple linear regressions (GA-MLR) and genetic

algorithm-support vector machine (GA-SVM): a comparative approach. Medicinal Chemistry Research,24, 3037-3046; https://doi.org/10.1007/s00044-015-1354-4.

Oniga, I., Puscas, C., Silaghi-Dumitrescu, R., Olah, N.K., Sevastre, B., Marica, R., Marcus, I., Sevastre-Berghian, A.C., Benedec, D., Pop, C.E.,& Hanganu, D. (2018). *Origanum vulgare* ssp. *vulgare*: chemical composition and biological studies. Molecules, 23, 2077; doi:10.3390/molecules23082077

Radusiene, J., Ivanauskas, L., Janulis, V.,& Jakštas V. (2008) Composition and variability of phenolic compounds in*Origanum vulgare* from Lithuania. Biologija, 54, 45-49

Stanojević, Lj.P., Stanojević, J.S., Cvetković, D.J.,& Ilić, D.P. (2016). Antioxidant activity of oregano essential oil (*Origanum vulgare* L.). Biologica Nyssana, 7, 131-139.

Statistica 10 software (StatSoft, Inc. STATISTICA, ver. 10, data analysis software system) (Accessed 15 December 2018).

Todeschini, R.,& Consonni, V. (2000). Handbook of Molecular Descriptors, Methods and Principles in Medicinal Chemistry. Wiley-VCH Verlag GmbH, Weinheim, Germany.

Toncer, O., Karaman, S., Kizil, S.,& Diraz E. (2009). Changes in essential oil composition of oregano (*Origanum onites* L.) due to diurnal variations at different development stages. Notulae Botanicae Horti Agrobotanici Cluj-Napoca, 37, 177-181; https://doi.org/10.15835/nbha3723188.

Tropsha, A. (2010). Best practices for QSAR model development, validation, and exploitation.Molecular Informatics, 29, 476-488; https://doi.org/10.1002/minf.201000061.

Tropsha, A.,&Golbraikh, A. (2007). Predictive QSAR modeling workflow, model applicability domains, and virtual screening. Current Pharmaceutical Design, 13, 3494-3504; DOI:10.2174/138161207782794257

Wolfender, J.L., Martia, G., Thomas, A.,& Bertranda, S. (2015). Current approaches and challenges for the metabolite profiling of complex natural extracts. Journal of Chromatography A, 1382, 136-164; https://doi.org/10.1016/j.chroma.2014.10.091

Wu, L., Gong, P., Wu, Y., Liao, K., Shen, H., Qi, Q., Liu, H., Wang, G.,& Hao, H. (2013). An integral strategy toward the rapid identification of analogous nontarget compounds from complex mixtures. Journal of Chromatography A, 1303, 39-47; https://doi.org/10.1016/j.chroma.2013.06.041.

Xu, Q., Wei, C., Liu, R., Gu, S., &Xu, J. (2015). Quantitative structure–property relationship study of β-cyclodextrin complexation free energies of organic compounds. Chemometrics and Intelligent Laboratory Systems, 146, 313-321; https://doi.org/10.1016/j.chemolab.2015.06.001

Yap, C.W. (2011).PaDEL-descriptor: an open source software to calculate molecular descriptors and fingerprints. Journal of Computational Chemistry, 32, 1446-1474; doi: 10.1002/jcc.21707.

Yoon, Y., Swales, G., Margavio, T.M. (2017). A comparison of discriminant analysis versus artificial neural networks. Journal of the Operational Research Society, 44, 51-60; DOI: 10.2307/2584434

Zisi, C., Sampsonidis, I., Fasoula, S., Papachristos, K., Witting, M., Gika, H.G., Nikitas, P.,& Pappa-Louisi A. (2017). QSRR modeling for metabolite standards analyzed by two different chromatographic columns using multiple linear regression. Metabolites, 7, 7;https://doi.org/10.3390/metabo7010007.

Profil etarskog ulja prirodne populacije *Origanum vulgare* subsp. *vulgare* sa Rtnja primenom hemometrijskih alata

Milica Aćimović[1], Lato Pezo[2], Stefan Ivanović[3], Katarina Simić[3], Jovana Ljujić[4]

1-Institut za ratarstvo i povrtarstvo Novi Sad - Nacionalni institut Republike Srbije, Maksima Gorkog 30, 21000 Novi Sad, Srbija

2-Univerzitet u Beogradu, Institut za opštu i fizičku hemiju, Studentski trg 12, 11000 Beograd, Srbija

3-Univerzitet u Beogradu, Institut za hemiju, tehnologiju i metalurgiju - Nacionalni institut Republike Srbije, Njegoševa 12, 11000 Beograd, Srbija

4-Univerzitet u Beogradu, Hemijski fakultet, Odsek za organsku hemiju, Studentski trg 12-16, 11000 Beograd, Srbija

SAŽETAK

Cilj ovog istraživanja je bio predviđanje retencionih indeksa hemijskih jedinjenja nađenih u etarskom ulju nadzemnog dela biljke *Origanum vulgare* subsp. *vulgare*, dobijenom hidrodestilacijom i analiziranom korišćenjem GC-MS. Ukupno 28 jedinjenja je detektovano u etarskom ulju. Jedinjenja sa najvišim relativnim koncentracijama su germakren D (21.5%), 1,8-cineol (14.2%), sabinen (14.0%) i *trans*-kariofilen (13.4%). Retenciona vremena su predviđena kvantitativnom vezom struktura-retencija, korišćenjem sedam molekulskih deskriptora izabranih faktorskom analizom i genetskim algoritmom. Izabrani deskriptori nisu međusobno povezani i korišćeni su za razvijanje modela veštačke neuronske mreže. Ukupan broj od 28 eksperimentalno dobijenih retencionih indeksa (log *RI*) korišćen je za postavljanje prediktivno kvantitaivnog modela zavisnosti struktura-retencija. Koeficijent određivanja za trening ciklus je bio 0.998, označavajući da se ovaj model može koristiti za predviđanje retencionih indeksa jedinjenja iz etarskog ulja biljke *O. vulgare* subsp. *vulgare*.

Ključne reči: origano, etarsko ulje, hidrodestilacija, GC-MS, QSSR, ANN

Profil d'huiles essentielles d'*Origanum vulgare* subsp. *vulgare* population native de Rtanj via des outils de chimiométrie

Milica Acimovic[1], Lato Pezo[2], Stefan Ivanovic[3], Katarina Simic[3], Jovana Ljujic[4]

1- Institut des grandes cultures et des cultures maraîchères Novi Sad- Institut national de la République de Serbie, Maksima Gorkog 30, 21000 Novi Sad, Serbie
2- Université de Belgrade, Institut de chimie générale et physique, Studentski trg 12, 11000 Belgrade, Serbie
3- Université de Belgrade, Institut de chimie, technologie et métallurgie − Institut national de la République de Serbie, Njegoševa 12, 11000 Belgrade, Serbie
4- Université de Belgrade, Faculté de chimie, Département de chimie organique, Studentski trg 12-16, 11000 Belgrade, Serbie

RÉSUMÉ

Le but de cette étude était de prédire les indices de rétention des composés chimiques trouvés dans des parties aériennes d'*Origanum vulgare* subsp. *vulgare* huile essentielle de obtenue par hydrodistillation et analysée par GC-MS. Un nombre total de 28 composés ont été détectés dans l'huile essentielle. Les composés avec la concentration relative la plus élevée sont les suivants : le germacrène D (21,5%), le 1,8-cinéole (14,2%), le sabinène (14,0%) et le *trans*-caryophyllène (13,4%). Le temps de la rétention a été prédit en utilisant la relation quantitative structure-rétention, en utilisant sept descripteurs moléculaires choisis par l'analyse factorielle et l'algorithme génétique. Les descripteurs choisis ne sont pas corrélés les uns aux autres et ils ont été utilisés pour développer un modèle de réseau neuronal artificiel. Un nombre total de 28 indices de rétention obtenus expérimentalement (log *RI*) ont été utilisés pour mettre en place un modèle quantitatif prédictif de relation structure − rétention. Le coefficient de détermination pour le cycle de formation était de 0,998, ce qui indique que ce modèle pourrait être utilisé pour prédire les indices de rétention pour *O. vulgare* subsp. *vulgare* composés d'huiles essentielles.

Mots-clés : origan, huile essentielle, hydrodistillation, GC-MS, QSSR, ANN

Профиль эфирных масел *Origanum vulgare* subsp. *vulgare* коренное население из Ртани с помощью инструментов хемометрии

Милица Ачимович[1], Лато Пезо[2], Стефан Иванович[3], Катарина Шимич[3], Йована Люйич[4]

1-Институт полевых и овощных культур Нови-Сад - Национальный институт Республики Сербия, улица Максима Горького 30, 21000 Нови-Сад, Сербия

2-Университет в Белграде, Институт общей и физической химии, Студенческая площадь, 12, 11000 Белград, Сербия

3- Унивеситет в Белграде, Институт химии, технологии и металлургии - Национальный институт Республики Сербия, Негошева 12, 11000 Белград, Сербия

4- Унивеситет в Белграде, химический факультет, кафедра органической химии, Студенческая площадь, 12-16, 11000 Белград, Сербия

АННОТАЦИЯ

Целью данного исследования было прогнозирование индексов удерживания химических соединений, обнаруженных в надземных частях *Origanum vulgare* subsp. *vulgare* эфирного масла, полученное гидродистилляцией и проанализированное с помощью ГХ-МС. Всего в эфирном масле было обнаружено 28 соединений. Соединения с самой высокой относительной концентрацией представляют собой гермакрен D (21,5%), 1,8-цинеол (14,2%), сабинен (14,0%) и транс-кариофиллен (13,4%). Время удерживания было предсказано путем использования количественного отношения структура – удерживание, с использованием семи молекулярных дескрипторов, выбранных с помощью факторного анализа и генетического алгоритма. Выбранные дескрипторы не коррелируют друг с другом, и они были использованы для разработки модели искусственной нейронной сети. Всего 28 экспериментально полученных индексов удерживания (log RI) были использованы для создания прогнозирующей количественной модели взаимосвязи структура-удерживание. Коэффициент детерминации для цикла обучения составил 0,998, что указывает на то, что эту модель можно использовать для прогнозирования индексов удержания для *O. vulgare* subsp. *vulgare* соединения эфирных масел.

Ключевые слова: орегано, эфирное масло, гидродистилляция, ГХ-МС, QSSR, ANN

Das Profil des ätherischen Öls der einheimischen Population von *Origanum vulgare* subsp. *vulgare* aus dem Gebirge Rtanj mittels chemometrischer Werkzeuge

Milica Acimovic[1], Lato Pezo[2], Stefan Ivanovic[3], Katarina Simic[3], Jovana Ljujic[4]

1 - Institut für Acker- und Gemüsebau Novi Sad - Nationales Institut der Republik Serbien, Maksima Gorkog 30, 21000 Novi Sad, Serbien

2 - Universität Belgrad, Institut für Allgemeine und Physikalische Chemie, Studentski trg 12, 11000 Belgrad, Serbien

3 - Universität Belgrad, Institut für Chemie, Technologie und Metallurgie - Nationales Institut der Republik Serbien, Njegoševa 12, 11000 Belgrad, Serbien

4 - Universität Belgrad, Fakultät für Chemie, Abteilung für organische Chemie, Studentski trg 12-16, 11000 Belgrad, Serbien

ABSTRACT

Das Ziel dieser Arbeit war die Vorhersage der Retentionsindices von chemischen Verbindungen, die in dem ätherischen Öl der oberirdischen Pflanzenteile von *Origanum vulgare* subsp. *vulgare* gefunden wurden, das durch Hydrodestillation gewonnen und mittels GC-MS analysiert wurde. Insgesamt wurden 28 Verbindungen in dem ätherischen Öl nachgewiesen. Die Verbindungen mit der höchsten relativen Konzentration sind Germacrene D (21,5%), 1,8-Cineol (14,2%), Sabinen (14,0%) und trans-Caryophyllen (13,4%). Die Retentionszeiten wurden mit Hilfe der Quantitativen Struktur-Retentions-Beziehungen vorhergesagt, wobei sieben molekulare Deskriptoren verwendet wurden, die durch Faktorenanalyse und genetischen Algorithmus ausgewählt wurden. Die ausgewählten Deskriptoren sind untereinander unkorreliert und wurden zur Entwicklung eines künstlichen neuronalen Netzwerkmodells verwendet. Eine Gesamtzahl von 28 experimentell erhaltenen Retentionsindizes (log RI) wurde verwendet, um ein vorhersagendes Quantitatives Struktur-Retentions-Beziehungsmodell aufzustellen. Das Bestimmtheitsmaß für den Trainingszyklus betrug 0,998, was darauf hinweist, dass dieses Modell für die Vorhersage der Retentionsindices für ätherische Ölverbindungen von *O. vulgare* subsp. *vulgare* verwendet werden kann.

Schlüsselwörter: Oregano, ätherisches Öl, Hydrodestillation, GC-MS, QSSR, ANN

Chemia Naissensis, Vol 3, Issue 2, POPULAR SCIENTIFIC ARTICLE, 117-131

History of the Periodic System of the Elements

Danijela Kostić[1*], Nenad Krstić[1], Marina Blagojević[1]

1- University of Niš, Faculty of Sciences and Mathematics, Department of Chemistry,

Višegradska 33, 18000 Niš, Serbia

Danijela Kostić: danijelaaakostic@yahoo.com
Nenad Kostić: nenad.krstic84@yahoo.com
Marina Blagojević: marinablagojevic2631@gmail.com

ABSTRACT

There were several attempts to classify known elements before Mendeleev. Numerous scientists, such as John Newlands, Alexandre-Emile Beguyer de Chancourtois and Julius Lothar Mayer, have contributed to the discovery of the periodic table.

Mendeleev was not the first to try to arrange the elements according to their properties, but he was the first to recognize and leave empty positions for the elements to be discovered. Many of his predictions came true and time confirmed the periodic law and the accuracy of the periodic table of elements.

Keywords: Periodic Table, Mendeleev, history, standard form, alternative form

Introduction

What is the quality of a great scientist? When we hear anecdotes about scientists who have dealt with important scientific issues, they often seem harmonious, peaceful, and interesting. However, in themselves there is a period of struggle and confusion that ends when alone genius sees the light, perhaps in a dream. Then everything falls into place, the paradigm changes and nothing is the same anymore. That, however, sounds more noble than the stories of numerous desperate attempts to solve a scientific problem, right? (Philip Ball, 2019)

Great scientists discover new facts, find meaning in it and connect it with other already known facts and resolve important issues. They also give their explanations, which other scientists accept as correct, although sometimes not immediately. Nevertheless, a good scientist goes further and predicts the consequences of his ideas that can be tested. This courage is a characteristic of great scientists. One of them was a Russian chemist Dmitry Mendeleev - the creator of the Periodic Table of the Elements.

He was not the first to try to arrange the elements according to their properties, but he was the first to recognize and leave gaps that must match elements that have not yet been discovered. Many of his predictions came true and thus strengthened his legacy (Joshua Howgego, 2021).

Others, such as John Newlands, Alexandre-Emile Beguyer de Chancourtois and Julius Lothar Meyer, contributed to the first Periodic Table of the Elements, but the greatest contribution goes to Mendeleev.

Historical development

Chemists studied each chemical element separately. Connection between them was observed, although some were very similar to each other, and some were quite different in physical and chemical properties. They could not even guess how many elements there are. It was a real question which property of the elements to take as a criterion in their classification (Mandić et al., 2011).

Chemists have always searched ways to arrange the elements according to their properties. The formation of the Periodic Table is something that is routinely attributed to Mendeleev; however, the periodization and systematization of the elements has a much longer history. Certainly, Mendeleev was the first to publish the version of the system that we accept today, but do all the merits belong to him? Other chemists before Mendeleev also studied the properties of elements that were known at their

time, searching for appropriate patterns. As in many other scientific discoveries, other scientists have come close to the same.

Figure 1. Dalton's symbols (Stack Exchange Inc., 2021).

Although the structure of the atom was not known at that time, the idea of the modern Periodic Table was well established and used to predict the properties of undiscovered elements long before the concept of atomic number was developed (Royal Society of Chemistry, 2021).

As early as the 17th century, more precisely in 1661, Robert Boyle ranked 13 known elements by increasing relative atomic masses. During the 18th century, some new elements were discovered and marked with geometric, astronomy and astrology symbols (Figure 1).

This system was expanded by Antoine-Laurent de Lavoisier with 11 elements. In 1789, Lavoisier made the first modern list of elements-33 of them, including light, warm, unextracted radicals and some oxides. He grouped them based on their properties into gases, not metals, metals and earths (Figure 2) (Royal Society of Chemistry, 2021).

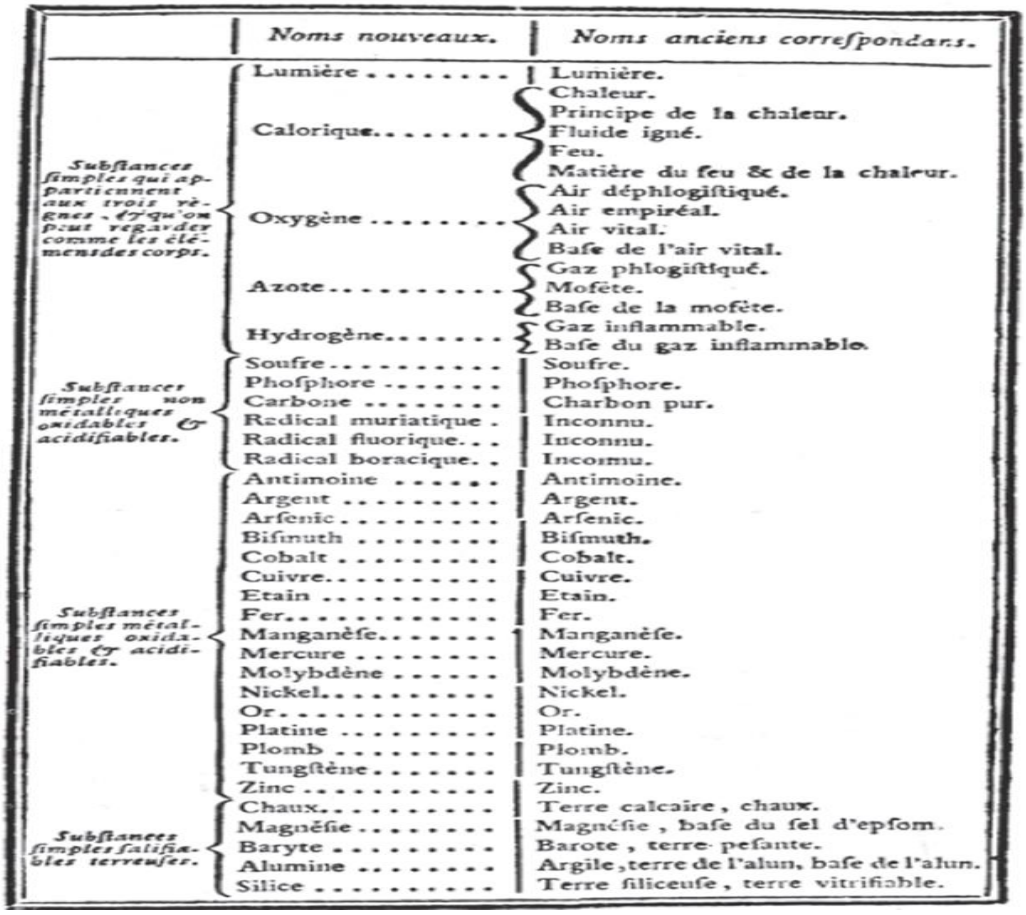

	Noms nouveaux.	Noms anciens correſpondans.
Subſtances ſimples qui appartiennent aux trois règnes, & qu'on peut regarder comme les élémens des corps.	Lumière	Lumière.
	Calorique	Chaleur. Principe de la chaleur. Fluide igné. Feu. Matière du feu & de la chaleur.
	Oxygène	Air déphlogiſtiqué. Air empiréal. Air vital. Baſe de l'air vital.
	Azote	Gaz phlogiſtiqué. Moſète. Baſe de la moſète.
	Hydrogène	Gaz inflammable. Baſe du gaz inflammable.
Subſtances ſimples non métalliques oxidables & acidifiables.	Soufre	Soufre.
	Phoſphore	Phoſphore.
	Carbone	Charbon pur.
	Radical muriatique	Inconnu.
	Radical fluorique	Inconnu.
	Radical boracique	Inconnu.
Subſtances ſimples métalliques oxidables & acidifiables.	Antimoine	Antimoine.
	Argent	Argent.
	Arſenic	Arſenic.
	Biſmuth	Biſmuth.
	Cobalt	Cobalt.
	Cuivre	Cuivre.
	Etain	Etain.
	Fer	Fer.
	Manganèſe	Manganèſe.
	Mercure	Mercure.
	Molybdène	Molybdène.
	Nickel	Nickel.
	Or	Or.
	Platine	Platine.
	Plomb	Plomb.
	Tungſtène	Tungſtène.
	Zinc	Zinc.
Subſtances ſimples ſalifiables terreuſes.	Chaux	Terre calcaire, chaux.
	Magnéſie	Magnéſie, baſe du ſel d'epſom.
	Baryte	Barote, terre peſante.
	Alumine	Argile, terre de l'alun, baſe de l'alun.
	Silice	Terre ſiliceuſe, terre vitrifiable.

Figure 2. Lavoisier's periodic system (HolidayMapQ.com, 2020)

He also redefined the term chemical element. It was found that water is made of hydrogen and oxygen, air of oxygen and nitrogen, so they realized that water and air cannot be elements. He, therefore, concluded that substances that decompose into simpler ingredients are not elements (Anonymous, 2014-2020). By then, any metal except mercury was not considered element. Lavoisier helped to build the metric system, wrote the first list of elements, and established the basis of chemical nomenclature. He predicted the existence of silicon (1787) and he established sulfur as an element (1777) and not a compound. He found that although matter can change shape or state, its mass always remains the same — the Law of Conservation of Mass (Anonymous, 2014-2020).

Through the entire XX century there was a search for a more precise classification scheme. During this period, significant discoveries in the field of chemistry and physics enabled the discovery of new elements. This was the reason to classify the growing number of known elements.

In 1803, John Dalton proposed his principles of atomic theory (he introduced the concept of atomic weight or, more precisely, relative mass, taking the hydrogen atom as the standard, because it is

the lightest and attributed atomic mass to it 1), suggesting that all elements composed of tiny, indestructible particles, called atoms. Atoms of the same element are equal and have the same mass. Atoms of an element can enter or leave new molecules during a chemical reaction, but their total mass remains unchanged (Wikipedia, John Dalton, 2021).

The first common chemical characteristics of the elements were noticed by the German chemist Johann Wolfgang Döbereiner. In 1829, he noticed that the properties of bromine lay somewhere in between the properties of chlorine and iodine. The same could be applied to the following three elements: calcium, strontium, barium as well as sulfur, selenium and tellurium. Lithium, sodium, and potassium, for example, are grouped together in a trinity as soft reactive metals, and it has been shown that the properties of the middle element can be predicted from the properties of the other two. Since the elements are gathered into groups of three elements, this Döbereiner's classification attempt is called the Law of Triads (Figure 3). This was certainly a good start, but Döbereiner abandoned his idea so it was understood only as a mere coincidence and was quickly forgotten (Kepić, 2013).

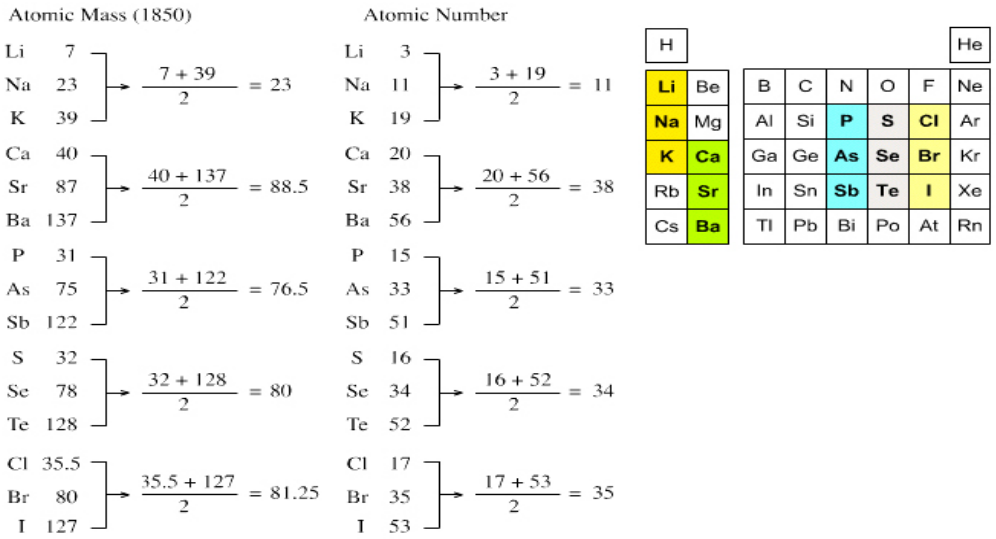

Figure 3. Döbereiner's periodic system (hemija.biologijakp.com, 2021)

The German chemist, Leopold Gmelin was using the mentioned law in his work and by 1843 he had identified ten trinities, three groups of four elements, and one group of five elements (Figure 4) (Wikipedia, Leopold Gmelin, 2019).

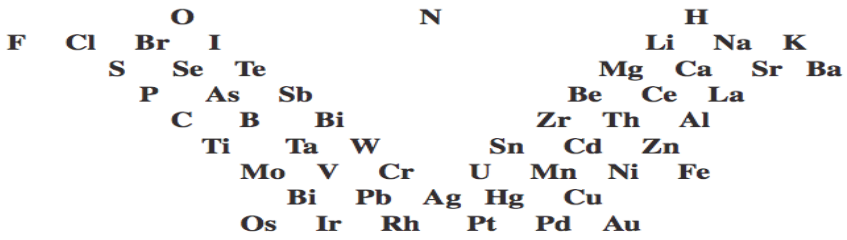

Figure 4. Gmelin's periodic system

(The Chemogenesis Web Book, The Internet database of periodic tables, 2021)

In 1857, Jean-Baptiste Dumas published a paper in which he described the relations between different groups of metals. Although many chemists were able to identify relationships between small groups of elements, it was still necessary to create a single scheme that would include all the elements (Wikipedia, Jean-Baptiste Dumas, 2021).

The German chemist August Kekulé, observing carbon, realized that this element usually has four other atoms attached to it. Methane, for example, has one carbon atom and four hydrogen atoms. This concept eventually became known as a valence; different elements bind to different numbers of atoms (Wikipedia, August Kekule, 2021).

The first attempt of chemical periodicity was announced by the French geologist Alexandre-Emile Beguyer de Chancourtois. In 1862, he published the first three-dimensional forms of the Periodic Table and called it a telluric helix. De Chancourtois was the first scientist who noticed the periodicity of the elements. He showed that elements with similar properties mostly appear at regular intervals, by arranging the elements spirally on the cylinder, according to the increasing atomic weight. His diagram also contained some ions and compounds in addition to the elements. This work did not rise much interest (Wikipedia, Alexandre-Emile Beguyer de Chancourtois, 2020).

In the United States, the Danish emigrant, Gustavus Detlef Hinrichs, also realized that all elements could be included within a single coherent system, as did the German chemist Lothar Meyer.

Gustavus Detlef Hinrichs, in 1867, published a spiral periodic system based on atomic spectra, weights, and chemical similarities. His work was characterized as "idiosyncratic, ostentatious and labyrinthine", which negatively contributed to the recognition and acceptance of the same (Wikipedia, Gustavus Detlef Hinrichs, 2020).

Julius Lothar Meyer, a German chemist, in 1864 published a periodic table with 44 elements arranged according to valence (Wikipedia, Lothar Meyer, 2020).

The table shows that elements with similar properties usually have the same valence. Meyer never came up with the idea to predict the discovery of new elements and to correct atomic masses. Just a few months after Mendeleev's system, Meyer released a virtually identical system. Some people consider Mendeleev and Meyer to be the co-creators of the Periodical System (Opusteno.rs, 2016).

This was followed by the discoveries of two London chemists, John Newlands and William Odling, who came to their basic periodic systems while working completely independently.

Certainly, the most serious move towards today's Periodic Table, before Mendeleev, was given by John Newlands, an English chemist, who made a series of projects in the period from 1863 to 1866. He discovered that when elements are arranged according to the increasing value of their atomic weights, similar physical and chemical properties begin to be repeated in the interval number eight. He compared this periodicity to octaves in music and called it the Law of Octaves (Wikipedia, John Newlands (chemist), 2020). If you have one proton, it is hydrogen. If you have 12 protons, that's carbon. As you add protons, you will find that similar properties appear after every 8 elements. Lithium, for example, with atomic number 3, is a reactive metal - just like sodium (element number 11) and potassium (number 19) (Figure 5). A good way is to imagine running your fingers over the piano keys. The notes resonate at higher and higher pitches as the hand moves to the right. By pressing the eighth key, something beautiful happens - a note is heard in the air that has something from the first one. As a sign of respect for this musical analogy, this law justified its name (Joshua Howgego, 2021). In vertical columns, the elements were arranged in ascending order of atomic relative mass, while horizontal species were conditioned by similarity in properties. Newlands was too consistent in arranging the elements by increasing atomic mass and he overlooked the fact that many elements had not yet been discovered, so his table had many shortcomings (Kepić, 2013). This so-called Octave Law, however, was ridiculed by most Newlands' contemporaries, and the Chemical Society refused to publish his work, noting that it would certainly find some legitimacy if he arranged the elements in the alphabetical order. Despite this, Newlands managed to create a system of elements and use it to predict the existence of missing elements, as is the case with germanium. The Chemical Society acknowledged the importance of his discoveries only five years after the credit went to Mendeleev (Wikipedia, John Newlands (chemist), 2020).

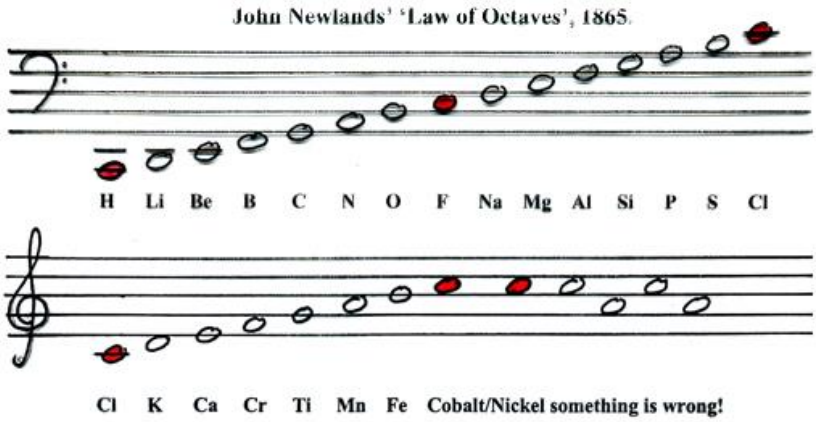

Figure 5. Newlands' periodic table (SlidePlayer.com Inc., 2021)

William Odling, an English chemist, published his system with 57 elements arranged according to their atomic weights. With a few irregularities and omissions, he noticed among the elements something resembling the periodicity of atomic weights and this was consistent with "their mostly acquired groupings" (Figure 6). Odling was close to the discovery of the periodic law, but he failed to conduct the research to the end. Subsequently, in 1870, he proposed the classification of elements based on their valence (Wikipedia, William Odling, 2020).

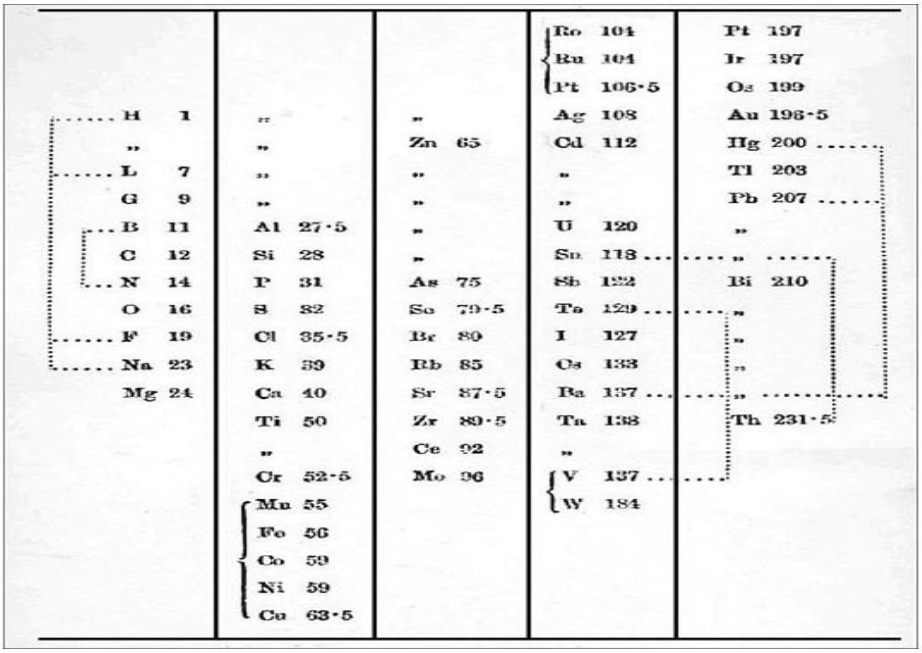

Figure 6. Odling's periodic table

(The Chemogenesis Web Book, Odling's table of elements, 2021**)**

None of these scientists was able to predict new elements that could be discovered, or to emphasize the value of the Periodic Table, as Mendeleev did.

Year of discovery (1869)

All these ideas, however, remained in the field of experimentation and were only an overture to following discoveries (Kepić, 2013).

The first "mosaic" that contained all 63 elements known until then, was assembled by the Russian chemist Dmitri Ivanovich Mendeleev. In 1869, he made the Periodic Table of chemical elements as a graphical representation of the periodic law. According to that law, the properties of elements are periodically repeated, because they depend on their atomic masses. He attributed the connection between the elements to their atomic masses (Mandić et al., 2011).

Mendeleev realized that there were not enough quality books on chemistry and decided to write a book on his own, a capital book for that time: Principles of Chemistry in Two Volumes (1868-1870). While writing this book, he came to the discovery that was his greatest achievement (Edukacija, 2014-2020). He tried to classify chemical elements according to their chemical properties, which he observed in regular repetitive patterns, which led him to compile his Periodic Table (Wikipedija, Dmitrij Mendeljejev, 2021). Mendeleev gradually formed a file, where each chemical element known until then had its own card with the name, basic properties, and the most important compounds. Comparing the cards, Dmitry Ivanovich noticed regularities. When he placed the chemical elements in order of increasing relative atomic masses, he saw that they periodically repeated the chemical properties (Antonijević Ivana, 2013). He made the following table (Table 1):

Table 1. Mendeleev's cards with elements

Cl 25.5	K 39	About 40
Br 80	Rb 85	We 88
I 127	Cs 133	Ba 137

In creating the Periodic Table, he strictly adhered to the periodic repetition of these properties and at the cost of minor deviations from the order of the elements as the atomic mass increased, which shows that he intuitively understood the essence. By adding other elements and following this scheme, Dmitri developed an expanded version of his Periodic Table (Antonijević Ivana, 2013).

All the elements known until then found their place in the table, and those that were subsequently discovered were placed in the empty spaces left for them. Mendeleev then classified known elements

according to a similar principle as Newlands, he placed related elements one below the other (Kepić, 2013).

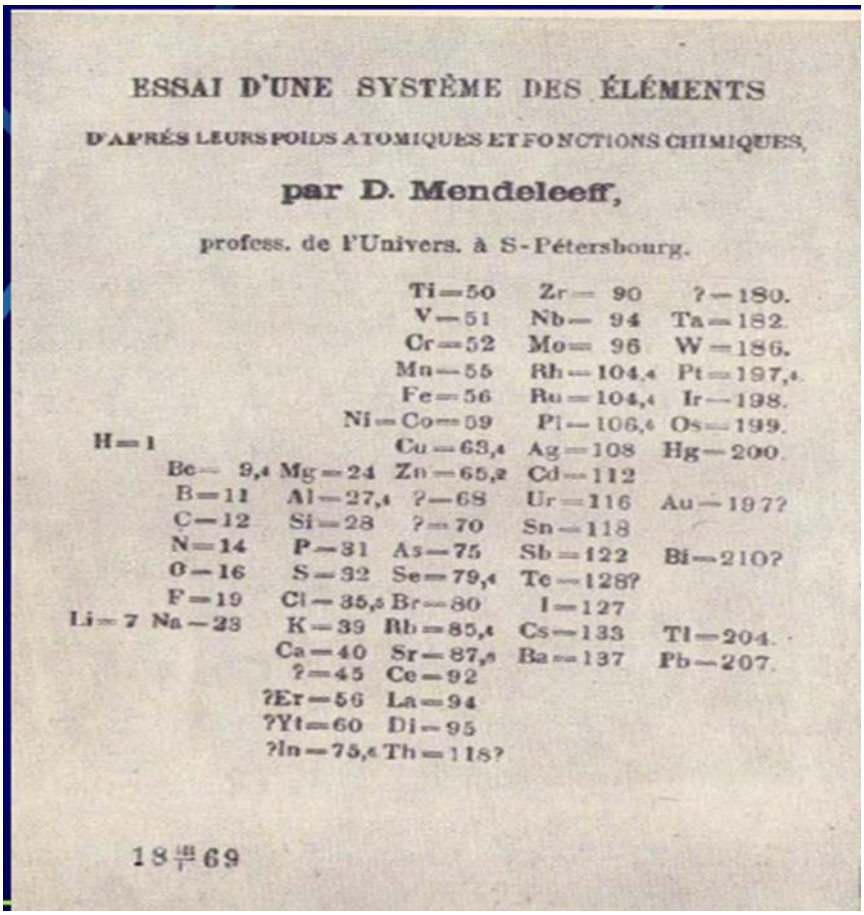

ESSAI D'UNE SYSTÈME DES ÉLÉMENTS

D'APRÉS LEURS POIDS ATOMIQUES ET FONCTIONS CHIMIQUES,

par D. Mendeleeff,

profess. de l'Univers. à S-Pétersbourg.

			Ti=50	Zr=90	?=180.
			V=51	Nb=94	Ta=182.
			Cr=52	Mo=96	W=186.
			Mn=55	Rh=104,4	Pt=197,4.
			Fe=56	Ru=104,4	Ir=198.
			Ni=Co=59	Pl=106,6	Os=199.
H=1			Cu=63,4	Ag=108	Hg=200.
	Be=9,4	Mg=24	Zn=65,2	Cd=112	
	B=11	Al=27,4	?=68	Ur=116	Au=197?
	C=12	Si=28	?=70	Sn=118	
	N=14	P=31	As=75	Sb=122	Bi=210?
	O=16	S=32	Se=79,4	Te=128?	
	F=19	Cl=35,5	Br=80	I=127	
Li=7	Na=23	K=39	Rb=85,4	Cs=133	Tl=204.
		Ca=40	Sr=87,6	Ba=137	Pb=207.
		?=45	Ce=92		
		?Er=56	La=94		
		?Yt=60	Di=95		
		?In=75,6	Th=118?		

18 $\frac{III}{I}$ 69

Figure 7. Mendeleev's Periodic Table (Moreno/Lyons productions LLC, 2015)

He arranged the elements into vertical and horizontal rows. There were elements of similar physical and chemical properties in the vertical arrays and they were called groups. In the horizontal rows, there were elements whose properties gradually changed, and the atomic masses increased; these were periods (Mandić et al., 2011). However, unlike the Newlands, Mendeleev did not blindly adhere to series of equal lengths, so that his first period had only two members, the second seven, and the third seventeen (Kepić, 2013). In periods, the gradual change of properties is abruptly interrupted, because the next element has properties that coincide with the properties of the first element in the previous period (Figure 7) (Mandić et al., 2011).

Mendeleev's ideas were presented to the Russian Physical and Chemical Society. Professor Menshutkin introduced them because Mendeleev was ill. His ideas were subsequently published in one of the most widely read chemical journals of the time, the Zeitschrift für Chemie.

Mendeleev was far-sighted enough to predict the existence of undiscovered elements, and he left empty spaces for them. Based on the chemical properties of neighboring elements, he was able to assume their properties. Mendeleev was not the first chemist to do so, but he was the first who recognized the possibility to predict the properties of those elements that were undiscovered. He gave these hypothetical elements names with the prefix *eka*, which means one in Sanskrit, and they were *eka*-boron, *eka*-aluminum and *eka* -silicon, which corresponds to today's elements scandium, gallium and germanium (Figure 8) (Kepić, 2013).

Predictions		Determinations
Eka*) - aluminium		Gallium
		(discovered in 1875 by Lecoq de Boisbaudran)
at. w.	68	69.9
sp. w.	6.0	5.96
at. vol.	11.5	11.7
Ekaboron		Scandium
		(discovered in 1879 by Nilson)
at. w.	44	43.79
oxide	Eb_2O_3 sp. w. 3.5	Sc_2O_3 sp. w. 3.864
sulphate	$Eb_2(SO_4)_3$	$Sc_2(SO_4)_3$
bisulphate	not isomorphous with alum	small narrow columns
Ekasilicon		Germanium
		(discovered in 1886 by Winkler)
at. w.	72	72.3
sp. w.	5.5	5.469
at. vol.	13	13.2
oxide	EsO_2	GeO_2
sp. w. oxide	4.7	4.703
chloride	$EsCl_4$	$GeCl_4$
boil. pnt. chloride	$< 100^\circ$	86°
density chloride	1.9	1.887
fluoride	EsF_4	$GeF_4.3H_2O$
not gaseous		white solid mass
ethyl compound	$EsAe_4$	$Ge(C_2H_5O)_4$
boil. pnt. ethyl compound	160°	160°
sp. w. ethyl compound	0.96	a little < 1

*) Eka = Prefix being the Sanskrit numeral one

Eka-aluminium	Gallium
Eka-boron	Scandium
Eka-silicon	Germanium
Eka-manganese	Technetium
Tri-manganese	Rhenium
Dvi-tellurium	Polonium
Dvi-caesium	Francium
Eka-tantalum	Protactinium

Figure 8. Mendeleev's postulated elements

(The Chemogenesis Web Book, Mendeleev's predicted elements, 2021)

The first of these elements was gallium, named after a part of France, the homeland of its inventor, Paul-Emile Lecoq de Boisbaudran. Gallium was discovered by de Boisbaudran examining an ore from the Pyrenees and noticing a purple line in the spectrum. He concluded that it originated from a new element and directed his work towards its isolation. The work was extremely difficult because the new element was reluctant to separate from zinc, but at the end he got about 0.1 grams of

gallium. Examining its properties, he saw the resemblance to Mendeleev *eka* –aluminum. This was just the beginning of the confirmation of the Periodic Table of the Elements (Kepić, 2013).

In 1879, another postulated element, the *eka*- boron, was discovered. It is called scandium. When the Swedish chemist Nilson (Lars Fredrik Nilson) realized that he was dealing with a new element, he saw that its properties coincided with *eka*-boron, which accelerated its confirmation (Kepić, 2013).

The third postulated element was *eka*-silicon, germanium. German chemist Clemens Alexander Winkler sent a silver mineral for analysis. He soon realized that there was a certain amount of an unknown element in the mineral, so he tried to identify it by spectroscopic methods. However, it failed, because germanium has wavelengths in the ultraviolet part of the spectrum. He then turned to classical methods, first converting the element to oxide, and then reducing it. At first, they wanted the element to be called neptunium, because its existence was predicted before the discovery, as in the case of the planet Neptune. In the end, he called it germanium, part of his country (Kepić, 2013).

The later discovered elements, such as technetium, rhenium, polonium, astatine, francium, and radium, fitted very easily into the table formed in this way. This was especially facilitated by the fact that their properties could be assumed, which means that the researchers could focus their efforts on the targeted discovery of an element (Kepić, 2013).

Another important thing that Mendeleev did was to correct incorrectly determined atomic masses. At that time, the relative atomic mass (then called atomic weight) was measured using the following formula:

atomic weight = equivalent weight x valence

Equivalent weights were usually correct, but sometimes the element would be assigned the wrong valence. To preserve the rule that chemically similar elements come one below the other, he had to correct the atomic mass of beryllium from 13.5 to 9, because it was given a valence of 3, due to its chemical similarity to aluminum. With the correction, beryllium came above magnesium, to the place that really belongs to. In two more cases he corrected the atomic masses and put tellurium in front of iodine and cobalt in front of nickel. Although he was wrong this time as far as atomic masses are concerned, these four elements took their places in the Periodic Table of the Elements. This anomaly was explained when the existence of different isotopes of one element was detected (Kepić, 2013).

Sima Lozanić, famous Serbian chemist, was among the first in the world to accept Mendeleev's system (Wikipedija, Sima Lozanić, 2021).

Of course, Mendeleev continued to correct the shortcomings of the Periodic Table, to publish his Periodic Table in a new form, with groups of similar elements arranged in columns rather than rows. These columns were marked with Roman numerals (from I to VIII), which corresponded to the oxidation state of each element. He also made detailed predictions regarding the properties of the

elements, which he previously pointed out as undiscovered, but which should exist. He presented his achievements to the foreign scientific public and published his work in the German journal Liebigs Annalen in 1871 (Wikipedija, Dmitrij Mendeljejev, 2021).

The significance of atomic numbers for the organization of the Periodic Table was not considered important until the existence and properties of protons and neutrons were understood. Atomic weight was used in predicting the properties of undiscovered elements more accurately than any other method known at the time (Wikipedia, Dmitrij Mendeljejev, 2021).

Later, in 1913, the English physicist Henry Moseley determined the experimental values of the nuclear charge *i.e.,* the atomic number of individual elements. These results confirmed that Mendeleev's distribution of elements is according to atomic numbers (Wikipedia, Henry Moseley, 2021).

As the discovery of the structure of the atom followed many years after the Periodic Table, Mendeleev's effect is even more impressive (Editorial, 2019).

One thing that Mendeleev did not foresee was the discovery of a whole group of elements, noble gases, which were found in the last decade of the 19th century by the Scot William Ramsay together with his colleagues. Mendeleev was disappointed at first. He initially rejected Ramsay's discovery of argon, which nevertheless further improved periodic laws, so chemists finally realized that argon was part of a completely new group of chemical elements (Opusteno.rs, 2018). The existence of elements with zero valence between two groups of valences exactly coincided with Mendeleev's previously rejected idea that the valences of groups of elements are alternately even and odd numbers (Kostić, 2010). Before he died in 1907, Mendeleev realized that Ramsay's findings did not contradict the system, but further proved it. Ramsay received the Nobel Prize for discovering five elements. Mendeleev never received that honor. Maybe because his discovery took root so quickly in the world of science, which, due to its simplicity, seems to have always been there. Nevertheless, one element with atomic number 101 is named after him - Mendelevium. The creator of the Periodic Table of the Elements certainly deserved something like that (Opusteno.rs, 2018).

If we say that Lavoisier initiated the first revolution in chemistry by putting it on the right track, Mendeleev is certainly responsible for the second revolution which confirmed the correctness of movement on that track (Kepić, 2013).

Acknowledgment

Authors want to thank Dr Biljana Arsić, Department of Chemistry, Faculty of Sciences and Mathematics, University of Nis, Republic of Serbia for language corrections.

Conflict-of-Interest Statement

None.

References

Anonymous. Periodic Table day. (2014-2020).

Antonijević Ivana. Čovek koji je složio kockice. (2013).

Editorial. Anniversary celebrations are due for Mendeleev's periodic table. (2019)

Edukacija. Dmitrij Ivanovič Mendeljejev. (2014-2020).

Gunjić, D. (1996). Chemistry and I, Belgrade.

hemija.biologijakp.com. Periodni sistem elemenata. (2021).

HolidayMapQ.com. Periodic table list. (2020).

Joshua Howgego. The periodic table: A beautiful way to organize the building blocks of everything around us. (2021).

Kepić, D. (2013). History hem otherwise, Belgrade.

Kostic, D. (2010). Nobel Prizes in Chemistry, Nis.

Mandić, Lj., Korolija J., & Danilović D. (2011). Chemistry for the 7th grade of primary school, Belgrade.

Moreno/Lyons Productions LLC. The periodic table. (2015).

Opusteno.rs. Biografija: naučnik Dmitrij Ivanovič Mendeljejev. (2016).

Opusteno.rs. Kako je nastao Periodni sistem elemenata. (2018).

Philip Ball. The true story of the birth of the periodic table, 150 years ago. (2019).

Royal Society of Chemistry. Periodic table. (2021).

SlidePlayer.com Inc. (2021).

Stack Exchange Inc. Chemistry. (2021).

The Chemogenesis Web Book. Mendeleev's predicted elements. (2021).

The Chemogenesis Web Book. Odling's table of elements. (2021).

The Chemogenesis Web Book. The Internet database of periodic tables. (2021).

Wikipedia. Alexandre-Emile Beguyer de Chancourtois. (2020a).

Wikipedia. August Kekule. (2021).

Wikipedia. Gustavus Detlef Hinrichs. (2020).

Wikipedia. Henry Moseley. (2021).

Wikipedia. Jean-Baptiste Dumas. (2021).

Wikipedia. John Dalton. (2021).

Wikipedia. John Newlands (chemist). (2020).

Wikipedia. Leopold Gmelin. (2019).

Wikipedia. Lothar Meyer. (2020).

Wikipedia. William Odling. (2020).

Wikipedija. Dmitrij Mendeljejev. (2021).

Wikipedija. Sima Lozanić. (2021).

Istorija Periodnog sistema elemenata

Danijela Kostić[1*], Nenad Krstić[1], Marina Blagojević[1]

1- Univerzitet u Nišu, Prirodno-matematički fakultet, Departman za hemiju, Višegradska 33, 18000 Niš, Srbija

SAŽETAK

Postojalo je nekoliko pokušaja klasifikacije poznatih elementa pre Mendeljejeva, ali on je bio prvi koji je izvršio sistematizaciju, i predvideo osobine elemenata koji će biti otkriveni. Najozbiljniji pokušaj pre Mendeljejeva je izvršio Džon Njulend. Trenutni standardni oblik Periodnog Sistema elemenata se sastoji od elemenata razvrstanih u 18 kolona i 7 redova, sa dva reda ispod tablice: lantanoida i aktinoida, i prvi ga je napravio Horas Grouv Deming. Alternativni periodni sistemi su najčešće napravljeni da bi istakli različite hemijske i fizičke osobine elemenata. Nauka je uvek u dinamičnom kretanju, tako da se možda mogu očekivati novi aspekti u pogledu Periodnog sistema u budućnosti.

Ključne reči: Periodni sistem, Mendeljejev, istorija, standardni oblik, alternativni oblici

Histoire du système périodique des éléments

Danijela Kostic[1], Nenad Krstic[1], Marina Blagojevic[1]

1- Université de Niš, Faculté des sciences naturelles et des mathématiques, Département de chimie, Višegradska 33, 18000 Niš, Serbie

RÉSUMÉ

Il y a eu plusieurs tentatives pour classer les éléments connus avant Mendeleev, mais il a été le premier à faire la systématisation et il a prédit les propriétés des éléments à découvrir. La tentative la plus sérieuse avant Mendeleev a été faite par John Newland. La forme standard actuelle du tableau périodique des éléments est composée d'éléments disposés en 18 colonnes et 7 rangées, avec deux rangées d'éléments en dessous de ce tableau : lanthanides et actinides, fait par Horace Groves Deming. Des systèmes périodiques alternatifs sont le plus souvent développés pour souligner les différentes propriétés chimiques et physiques des éléments. La science est toujours dans un mouvement dynamique, alors peut-être pouvons-nous nous attendre à l'avenir aux nouveaux aspects concernant le tableau périodique également.

Mots-clés : Tableau périodique, Mendeleïev, histoire, forme standard, formes alternatives.

История Периодической системы элементов

Даниела Костич[1], Ненад Крстич[1], Марина Благоевич[1]

1-Университет в Нише, Естественно-математический факультет, Кафедра химии, Вишеградска 33, 18000 Ниш, Сербия

АННОТАЦИЯ

До Менделеева было несколько попыток классифицировать известные элементы, но он был первым, кто произвел систематизацию и предсказал свойства элементов, которые должны быть обнаружены. Самую серьезную попытку до Менделеева предпринял Джон Ньюленд. Текущая стандартная форма Периодической таблицы химических элементов состоит из элементов, расположенных в 18 столбцов и 7 строк, с двумя рядами элементов отдельно внизу таблицы (лантаноиды и актиниды) и была создана Горацием Г. Демингом. Альтернативные периодические системы чаще всего разрабатывают, чтобы подчеркнуть различные химические и физические свойства элементов. Наука всегда находится в динамичном движении, поэтому можно ожидать, что в будущем появятся новые аспекты Периодической таблицы.

Ключевые слова: периодическая таблица, Менделеев, история, стандартная форма, альтернативные формы.

Die Geschichte des Periodensystems der Elemente

Danijela Kostic[1], Nenad Krstic[1], Marina Blagojevic[1]

1-Universität in Niš, Fakultät für Naturwissenschaften und Mathematik, Lehrstuhl für Chemie, Višegradska 33, 18000 Niš, Serbien

ABSTRACT

Es gab mehrere Versuche, die bekannten Elemente vor Mendelejew zu klassifizieren, aber er war der erste dem es gelang, die Systematisierung der Elemente durchzuführen und die Eigenschaften der zu entdeckenden Elemente vorauszusagen. Der ernsthafteste Versuch vor Mendelejew wurde von John Newland unternommen. Die aktuelle Standardform des Periodensystems der Elemente besteht aus Elementen, die in 18 Spalten und 7 Reihen angeordnet sind, mit zwei Reihen von Elementen unterhalb dieser Tabelle: Lanthaniden und Actiniden, und ist Horace Groves Deming zuzuschreiben. Alternative Periodensysteme werden meist entwickelt, um die unterschiedlichen chemischen und physikalischen Eigenschaften der Elemente zu betonen. Die Wissenschaft ist immer in einer dynamischen Bewegung, so dass wir vielleicht auch in Zukunft neue Aspekte bezüglich des Periodensystems erwarten können.

Schlüsselwörter: Periodensystem, Mendelejew, Geschichte, Standardform, alternative Formen